Ecological evolution ~~of ungulates in northern Iberia (SW Europe) during the Late Pleistocene~~ in northern Iberia during the Late Pleistocene through stable isotopic analysis o~~f~~n ungulate ~~ungulate~~ teeth

Mónica Fernández-García[1,2,3] (*)**, Sarah Pederzani**[2,34]**, Kate Britton**[35]**, Lucía Agudo-Pérez**[1]**,**
Andrea Cicero[1]**, Jeanne Marie Geiling**[1]**, Joan Daura**[64]**, Montserrat Sanz**[46]**, Ana B.**
Marín-Arroyo[1](*)

1 Grupo de I+D+i EVOADAPTA (Evolución Humana y Adaptaciones durante la Prehistoria), Departamento de Ciencias Históricas, Universidad de Cantabria, 44. 39005 Santander, Spain

2 Departament de Prehistòria, Arqueologia i Història Antiga, Universitat de València, Av. Blasco Ibañez 28, 46010 Valencia, Spain.

3 Institut Català de Paleoecologia Humana i Evolució Social (IPHES-CERCA), zona Educacional 4 Edifici W3, Campus Sescelades URV, 43007 Tarragona, Spain.

~~2 3~~ 4 Archaeological Micromorphology and Biomarkers Laboratory (AMBI Lab), Instituto Universitario de Bio-Orgánica "Antonio González", Universidad de La Laguna, 38206 San Cristóbal de La Laguna, Tenerife, Spain

5 Department of Archaeology, University of Aberdeen, Aberdeen AB24 3UF, United Kingdom

~~6~~4 Grup de Recerca del Quaternari (GRQ-SERP), Department of History and Archaeology, Universitat de Barcelona, ~~Grup de Recerca del Quaternari (GRQ SERP),~~ C/Montalegre 6-8, 08001 Barcelona ~~08001~~, Spain.

(*) Corresponding authors: anabelen.marin@unican.es,

Abstract

During the Late Pleistocene, stadial and interstadial fluctuations affected vegetation, fauna, and human groups that were forced to cope with these pronounced spatial ~~and~~ temporal climatic and environmental changes ~~in time and space~~. These changes were especially abrupt during the Marine Isotopic Stage (MIS) 3. ~~However, little is still known about the local and regional climatic conditions experienced by hominins in Europe.~~ Here, we reconstruct the climatic trends in northern Iberia considering the stable isotopic composition of ungulate skeletal tissues found in archaeological deposits dated between 80 to 15 ka,~~000~~ cal BP. The carbon and oxygen isotopic composition preserved in the carbonate fraction of tooth enamel provides a reliable and high-resolution proxy of the food and water consumed by these animals, which is indirectly related to the local vegetation, environment, and climate, allowing us to estimate paleotemperatures and rainfall ~~data~~intensity. This study presents new isotope data from 44 bovine, equid, and cervid teeth from five archaeological sites in the Vasco-Cantabrian region (El Castillo, ~~El Otero,~~ Axlor, Labeko Koba, Aitzbitarte III interior and El Otero,) and one in ~~the Mediterranean area~~northeastern Iberia (Canyars), where human evidence is attested from the Mousterian to the Magdalenian. The carbon isotope values reflect animals feeding on diverse C3 plants ~~with a mix-feeder diet mainly developed~~ in open environments, and point to. ~~However, carbon isotope value ranges point to~~ differentiated ecological niches for equids and bovines, especially during the Aurignacian in the Vasco-Cantabrian region. Temperature estimations based on oxygen isotopic compositions and rainfall obtained from carbon isotopic compositions indicate colder and more arid conditions than nowadays from the Late Mousterian to the Aurignacian. The contemporary ~~Mediterranean~~ northeastern Iberia site shows slightly lower temperatures related to an arid period when animals mainly graze in open landscapes. In the Vasco-Cantabrian region, during the MIS2, the Gravettian data reflect a landscape opening, whereas the Magdalenian point~~s~~ to warmer ~~conditions (~~but still arid) conditions.

Keywords: Middle and Upper Palaeolithic; Neanderthal; Homo sapiens, palaeoecology; geochemistry

1. Introduction

Understanding ~~the~~ local and regional climatic ~~evolution~~ variability during the Late Pleistocene in southern Europe is crucial for assessing the potential impact of climate on the adaptation and decline of Neanderthals~~,~~ ~~as well as~~and the subsequent expansion and resilience of Anatomically Modern Humans during the Upper Paleolithic (e.g., D'Errico and Sánchez Goñi, 2003; Finlayson and Carrión, 2007; Sepulchre et al., 2007; Staubwasser et al., 2018). During the Late Pleistocene, the climatic records demonstrate stadial and interstadial continuous fluctuations during the Marine Isotope Stage 3 (MIS 3, ca. 60-27 ka) and MIS 2 (ca. 27-11 ka). Human groups had to face those episodes, which affected ~~different~~ vegetation and fauna to different extents, depending on the region. Northern Iberia is a key study area due to the abundance of well-preserved archaeological caves and rock shelters where, in the last decade, an updated and multidisciplinary approach has been applied to disentangle how changing environmental conditions affected the subsistence dynamics of Middle and Upper Paleolithic hominins. Recent chronological, technological, ~~and~~ subsistence studies and ecological reconstructions are revealing a ~~wider regional circumstance~~ more complex regional panorama than previously known (e.g., ~~(~~Sánchez Goñi, 2020; Vidal-Cordasco et al., 2022; 2023; Timmermann, 2020; Klein et al., 2023).

The Vasco-Cantabrian region, located in northwest~~ern~~ Iberia, is subject to the influence of Atlantic climatic conditions~~,~~ and has~~where~~ ~~been widely~~ recently has been evaluated ~~debated as a region that was significantly~~the impact~~ed~~ ~~of~~ by the glacial-interglacial oscillations during ~~the~~ MIS3 (Vidal-Cordasco et al., 2022). Modelling of traditional environmental proxies (small vertebrates and pollen) from archaeo-paleontological deposits show a progressive shift in the climatic conditions with decreasing temperatures and rainfall levels detected during the late Mousterian (Fernández-García et al., 2023). Ecological alterations have been observed in large mammals, such as niche partitioning between horses and cervids (Jones et al., 2018), a decrease in the available biomass for secondary consumers, and consequently, a ~~decrease~~ reduction in the ungulate ~~herbivores~~ carrying capacity ~~with regards to ungulates (~~(Jones et al., 2018; Vidal-Cordasco et al., 2022). Cold and arid conditions are maintained during the Aurignacian and the Gravettian until the onset of MIS2. Afterwards, during the Last Glacial Maximum (LGM, 23-19 ka), the global climatic deterioration associated with this glacial phase results in colder and more arid conditions in the region, with a predominance of open landscapes. However, this region still provided resources for human ~~exploitation~~ survival acting as a refugia ~~area~~ with more humid conditions in comparison to the Mediterranean area (Cascalheira et al., 2021; Garcia-Ibaibarriaga et al., 2019a; Lécuyer et al., 2021; Fernández-García et al., 2023; Fagoaga, 2014; Posth et al., 2023). By the end of the LGM, a climate amelioration and a moderate expansion of the deciduous forest are documented from the late Solutrean through the Magdalenian (Jones et al., 2021; Garcia-Ibaibarriaga et al., 2019a).

In contrast, northeastern Iberia is influenced by the Mediterranean climate. During MIS 3, ~~this period in~~ temperatures in this region ~~has frequently been described as~~is often~~were~~ ~~characterised as being~~ cooler~~by colder temperatures~~ and with~~,~~ ~~and with~~ higher rainfall, ~~, higher rainfall~~ compared to the present, but ~~and less~~with climatic fluctuations ~~described as being~~ less pronounced ~~climatic fluctuations when~~ compared to the Vasco-Cantabrian region ~~in the same period~~ (López-García et al., 2014; Fernández-García et al., 2020; Vidal-Cordasco et al., 2022). Archaeobotanical and small vertebrate evidence ~~Small vertebrate communities and archaeobotanical evidence~~ indicate relatively stable climatic conditions, but also suggest the persistence of open forests during the Middle to Upper Paleolithic transition, as found in northwestern Iberia (Allué et al., 2018; Ochando et al., 2021). However, certain records indicate specific climatic ~~excursions~~episodes, such as increased aridity and landscape opening during Heinrich Events 4 and 5 (e.g., Álvarez-Lao et al., 2017; Daura et al., 2013; López-García et al., 2022; Rufí et al., 2018).

These multi-proxy studies have significantly expanded our understanding of the environmental evolution in Iberia, alongside proxies derived from marine core records in Iberia margins (Naughton et al., 2007; Roucoux et al., 2001; Sánchez-Goñi et al., 1999, 2009; Martrat et al., 2004; Fourcade et al., 2022) and other regional paleoclimatic records sourced from local natural deposits (e.g., Pérez-Mejías et al., 2019; Moreno et al., 2010, 2012; González-Sampériz et al., 2020; Ballesteros et al., 2020)~~, thereby providing a valuable~~

93 ~~framework for understanding environmental evolution~~. However, the availability of proxies enabling the
94 ~~establishment of~~ direct connections between these environmental shifts and human activities remains
95 limited.

96

97 ~~These While multi-proxy studies have significantly expanded our understanding of the environment in Iberia.~~
98 ~~However,, there is still limited availability of high-resolution proxies directly linked~~ directly to human activity.
99 In this study, we ~~propose to~~ investigate the palaeoecolog~~ical~~y and palaeoenvironmental dynamics ~~of past~~
100 ~~ungulates of this region~~ in northern Iberia during the late Middle and Upper Paleolithic by measuring the
101 carbon and oxygen isotopic composition ~~(δ¹³C, δ¹⁸O)~~ of bioapatite carbonates $(δ^{13}C_{carb}/δ^{18}O_{carb})$ preserved
102 in archaeological mammal teeth. These analyses provide high-resolution snapshots of ecological
103 information from animals accumulated during human occupations at the ca~~v~~sites. Tooth enamel forms
104 incrementally and does not biologically remodel (Passey and Cerling, 2002; Kohn, 2004), in contrast to other
105 bod~~ily~~y tissues such as bone, which implies that the isotope values measured on them reflect the animal
106 diet and water sources consumed during its mineralisation, around one to two years of ~~animal life in our~~
107 ~~study species~~life for the species included in our study (bovids, equids, cervids)(e.g., Hoppe et al., 2004;
108 Pederzani and Britton, 2019; Ambrose and Norr, 1993; Luz et al., 1984). ~~The preserved carbon and oxygen~~
109 ~~isotope composition in the carbonate fraction of tooth enamel offers a high resolution record of the dietary~~
110 ~~choices of the plants and water animals consume, which indirectly reflects the vegetation, environmental~~
111 ~~conditions, and climate.~~The preserved carbon isotope composition rel~~y on dietary choices of animals~~
112 ~~reflecting mainly the type of plant consumed (C3/C4), exposition to ligh and levels of humidity~~ies on animal
113 dietary choices reflecting mainly the type of plant consumed (C3/C4), exposition to light and humidity levels.
114 Otherwise, the oxygen isotope composition reflects mainly the environmental water consumed by animals,
115 directly by dr~~in~~king or through diet, which reflects isotopic information derived from water sources as well as
116 changes in climatic conditions. Both indirectly provide information on the vegetation and climate that ~~This~~
117 allows ~~us to~~ estimat~~ing~~e past temperatures, rainfall, and moisture ~~levels~~ on a sub-annual scale, returning
118 isotopic ~~information~~ data of the foraging areas where animals were feeding during ~~tooth~~ teeth formation.

119 By analysing the stable isotopic composition of 44 ungulate teeth obtained from 15 archaeological levels
120 directly associated with human occupation, including El Castillo, ~~El Otero,~~ Axlor, Labeko Koba, Aitzbitarte
121 III interior and El Otero in northwestern Iberia, and Terrasses de la Riera dels Canyars in northeastern Iberia,
122 this study presents novel insights into local and regional environmental and climatic trends during the Late
123 Pleistocene (Fig.1; Fig.2; Appendix A). Specifically, it focuses on the Middle to Upper Paleolithic transition
124 in both areas and the post-LGM period in the Vasco-Cantabrian region.

125 The main objectives of this work are: 1) to assess how regional environmental conditions, including changes
126 in moisture and vegetation cover, but also temperatures and rainfall, are recorded ~~in tooth enamel~~ in the
127 stable isotopic composition of tooth enamel; 2) to ~~approach~~ characterize animal diet and their ecological
128 niches; 3) to obtain quantitative temperature data to compare with available proxies; 4) to characterise
129 seasonal patterns of animals found in the archaeological sites by identifying winter and summer fluctuations.
130 The chronological ~~resolution~~ information ~~in~~ associated to the ~~study~~ studied ~~areas~~ levels ~~for this period~~ allows
131 us to ~~cor~~relate regional paleoenvironmental changes with global records.

132
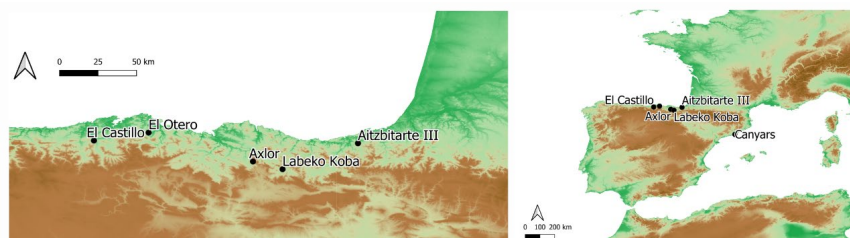
Figure 1. Location of the archaeological sites included in this ~~work~~study. From west to east, in the autonomous community of Cantabria, El Castillo, and El Otero; in the Basque Country, Axlor and Aitzbitarte III interior; in Catalonia, Canyars.
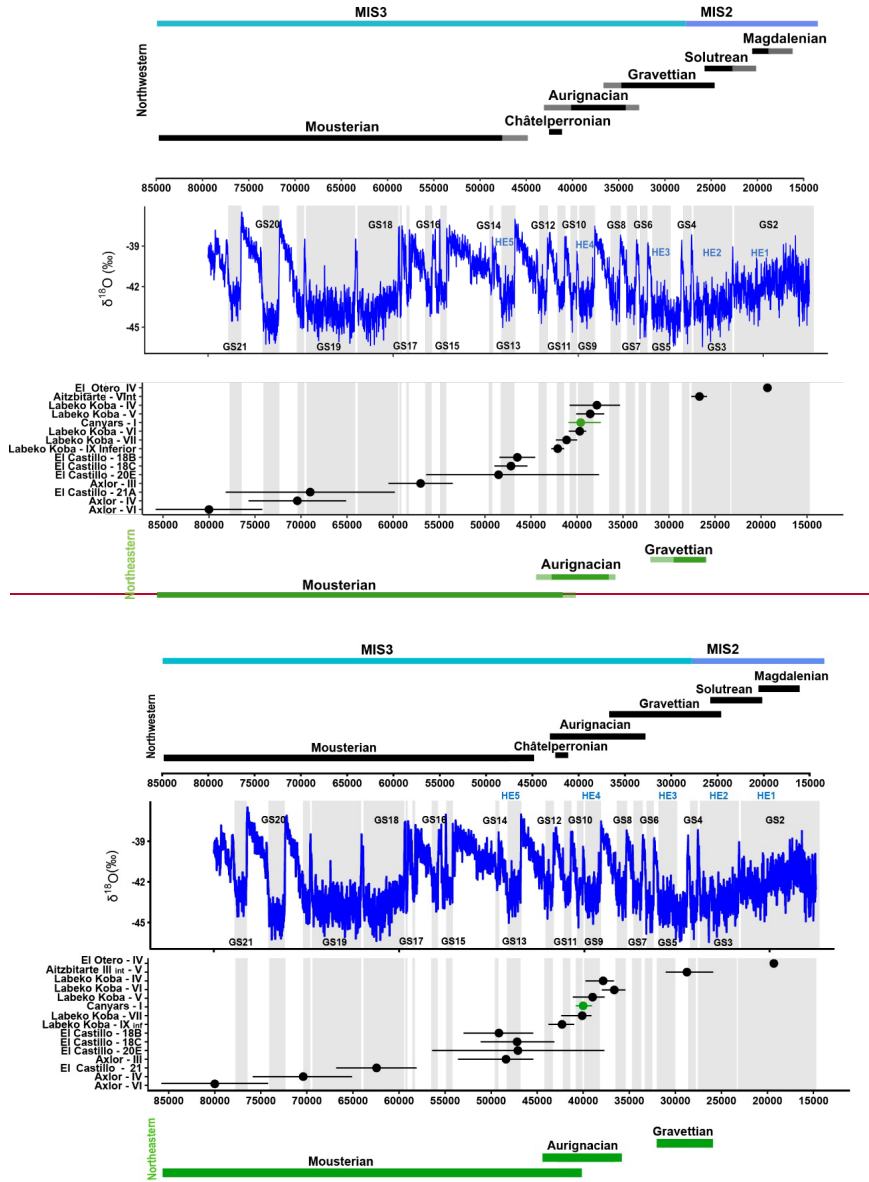
Figure 2. Representation of the ~~The temporal position of the a~~Mm~~ean~~edian chronological ~~dates f~~ro~~mor~~ each ~~a~~rchaeological level~~s~~ (bars represent 95% confidence intervals) ~~included in the study is~~ are shown ~~to the occurrence~~in relation ~~related~~ to ~~of~~ different techno-complexes in both ~~northwestern~~north-western (in black) and ~~northeastern~~north-eastern Iberia (in green). ~~Additionally~~ and ~~the.~~ ~~, as well as the~~δ~~d~~[18]O record from the NGRIP ~~ice core~~ (North Greenland Ice Core Project members, 2004; Rasmussen et al.,

142 2014). Grey bands indicate Greenland Stadials (GS). Detailed ~~chronological~~ information on ESR and ^{14}C dates, along with ,[14]C

143 calibration, are shown~~is presented~~ in Appendix B.

2. Archaeological sites and sampled material

This study selected a total of 44 ungulate teeth including 25 bovines (*Bos primigenius, Bison priscus, Bos/Bison* sp.), 14 equids (*Equus* sp. and *Equus ferus*), and five~~5~~ cervids (*Cervus elaphus*) ~~found in~~originating from five archaeological sites in the Vasco-Cantabrian region (El Castillo, El Otero, Axlor, Labeko Koba, Aitzbitarte III interior) and one in the Mediterranean area (Terrasses de la Riera dels Canyars, henceforth Canyars). These teeth were recovered from 15 archaeological levels attributed to the following technocomplexes: Mousterian (n=14), Transitional Aurignacian (n=10), Châtelperronian (n=2), Aurignacian (n=12), Gravettian (n=1) and Magdalenian (n=5) (Table 1 and 2~~; Appendix B~~). Archaeozoological studies of the archaeological sites are available (synthesis in Marín-Arroyo and Sanz-Royo, 2022; Daura et al., 2013) and most prove that faunal remains were accumulated by human acquisition during the different cultural phases. ~~The isotopic results of equids from El Castillo~~ The isotopic results of equids teeth and other ungulates bone collagen from El Castillo were previously published by Jones et al. (2019) in combination with the ~~bone collagen~~ stable isotopes of~~n~~ ungulate ~~prey capture at~~s from the site, as well as the combined ~~bioapatite~~ carbonate and phosphate analyses of bovines from Axlor (Pederzani et al., 2023). Single radiocarbon dates for each site were calibrated using OxCal4.4 software (Ramsey, 2009), considering the INTCAL20 calibration curve (Reimer et al., 2020). Dates provided represent an approximate age for each level where ungulate remains were recovered, incorporating either multiple dates or a single date. For sites with ~~multiple~~various dates, Bayesian chronology modeling was performed using OxCal4.4. A comprehensive description of each archaeological site is provided in Appendix A, while further details on dating methods and selected dates for each level can be found in Appendix B.

3. Methods

3.1 Tooth sampling

All teeth included were sequentially sampled to reconstruct the complete $\delta^{18}O_{carb}$ and $\delta^{13}C_{carb}$ intratooth profiles based on enamel carbonate bioapatite. Intratooth sequential sampling was applied to the second and third molars and third and fourth premolars. Bovine and horse teeth sampled exceeded 3-4 cm of crown height to ensure that at least a one-year isotopic record of animal life was obtained (Hoppe et al., 2004; Britton et al., 2019). Samples were taken perpendicular to the growth axis on the tooth where the enamel was best preserved, avoiding, whenever possible taphonomic alterations such as cracks or postdepositional damages. Samples were performed in the ~~labial~~ buccal face for the lower teeth and the lingual part for the upper ones. The outermost enamel surface was abraded to remove the superficial enamel, calculus, cementum, or concretions adhering to the surface to avoid contaminations. The sequential sampling consisted of straight strips (ca. 8 x 1.5 x 1 mm) covering the width of the selected lobe, approximately every 2-3 mm, from the crown to the Enamel-Root-Junction (ERJ). The sample depth covered around 75% of the enamel depth, and dentine inclusion was avoided. A low-revolution variable-speed manual drill was used, equipped with 1 mm diamond-coated drill bits of conical and cylindrical shape. About 10-15mg of enamel powder was collected in each subsample, generating 693 subsamples for IRMS measurements~~s~~ (see complete intratooth profiles in Appendix C).

Site	Level - Cultural period	Bovines	Horses	Red deer	Teeth	Subsamples
Axlor	VI - Mousterian	2			2	32
	IV - Mousterian	1			1	12
	III - Mousterian	4			4	62
El Castillo	21 A - Mousterian	2	1		3	47
	20 E - Mousterian	2	2		4	56
	18C - Trans. Aurignacian	4			4	66
	18B - Trans. Aurignacian	3	2	1	6	93
Labeko Koba	IX - Châtelperronian		1	1	2	24
	VII - ProtoAurignacian	3			3	68
	VI - Aurignacian		1		1	16
	V - Aurignacian	1	1		2	39
	IV - Aurignacian		1		1	16
Canyars	I - Aurignacian	2	3		5	76
Aitzbitarte III	V - Gravettian	1			1	18
El Otero	IV - Magdalenian		2	3	5	68
TOTAL		25	14	5	44	693

Site	Level - Cultural period	Bovines	Horses	Red deer	Teeth	Subsamples
Axlor	VI - Mousterian	2			2	32
	IV - Mousterian	1			1	12
	III - Mousterian	4			4	62
El Castillo	21A - Mousterian	2	1		3	47
	20E - Mousterian	2	2		4	56
	18C - Trans. Aurignacian	4			4	66
	18B - Trans. Aurignacian	3	2	1	6	93
Labeko Koba	IX inf - Châtelperronian		1	1	2	24
	VII - ProtoAurignacian	3			3	68
	VI - Aurignacian		1		1	16
	V - Aurignacian	1	1		2	39
	IV - Aurignacian		1		1	16
Canyars	I - Aurignacian	2	3		5	76
Aitzbitarte III interior	V - Gravettian	1			1	18
El Otero	IV - Magdalenian		2	3	5	68
TOTAL		25	14	5	44	693

Table 1. Number of teeth sampled by species, archaeological sites and cultural periods.

3.2 Sample treatment and stable isotope mass spectrometry

Several authors have debated the necessity of chemical pre-treatments to remove organic matter and secondary carbonates from bioapatite carbonates before stable isotopic analysis. Some chemical treatments can introduce secondary carbonates, increase carbonate content, and alter the original isotopic signal (Snoeck and Pellegrini, 2015; Pellegrini and Snoeck, 2016). The "side effects" of these pre-treatments can compromise the final isotopic signal measured. For this reason, in this work, most of the samples were not pretreated, except for the equids and cervids samples from Labeko Koba, and Aitzbitarte III interior, and the cervids and equids from El Otero and El Castillo that were sampled and pretreated in the context of the initial project in an earlier phase of the project. The absence of pretreatment can elevate the risk of secondary carbonates (France et al., 2020; Chesson et al., 2021). Nonetheless, any pretreatment method cannot guarantee their complete removal, and the 'side effects' may compromise the final isotopic signal to a greater extent. While variations in pretreatment methods exist among samples in this study, the lack of a universally accepted protocol necessitates careful consideration of any potential isotopic effects resulting from these differences.

Pretreatment was followed for above-mentioned samples of this work from fourteen teeth was established by Balasse et al. (2002), where around 7 mg of powdered enamel was prepared and pretreated with 3% of

sodium hypochlorite (NaOCl) at room temperature for 24 h (0.1 ml/mg sample), and thoroughly rinsed with deionised water, before a reaction with 0.1M acetic acid for 4 h (0.1 ml/mg sample) (Balasse et al., 2002; equivalent protocol in Jones et al., 2019). Samples were then thoroughly rinsed, frozen, and freeze-dried. NaOCl is one of the most common agents used for pretreating carbonates and works as a base that removes organic matter by oxidation. Although it is considered one of the most efficient agents for removing organic matter, it can induce the absorption of exogenous carbonates, such as atmospheric CO_2 and secondary carbonates (Snoeck and Pellegrini, 2015; Pellegrini and Snoeck, 2016). It is argued that using acetic acid after NaOCl pretreatment can remove exogenous carbonates absorbed during NaOCl application. However, it is unclear if all newly introduced carbonates are finally released and which effect they produce on the original isotopic composition. While variations in pretreatment methods exist among samples in this study, the lack of a universally accepted protocol necessitates careful consideration of any potential isotopic effects resulting from these differences. These samples were analysed in the Godwin Laboratory (Department of Earth Sciences, University of Cambridge). Enamel powder samples were reacted with 100% orthophosphoric acid for 2 h at 70°C in individual vessels in an automated Gasbench interfaced with a Thermo Finnigan MAT253 isotope ratio mass spectrometer. Results were reported in reference to the international standard VPDB and calibrated using the NBS-19 standard (limestone, $\delta^{13}C$ = +1.95‰ and $\delta^{18}O$ = -2.2‰; Coplen, 2011) for which the precision is better than 0.08‰ for $\delta^{13}C$ and 0.11‰ for $\delta^{18}O$.

For the non-pre-treated samples, carbon and oxygen stable isotopic ratios were measured using continuous flow-isotope ratio mass spectrometry, specifically a Europa Scientific 20-20 IRMS coupled to a chromatograph, at the Iso-Analytical laboratory in Cheshire, UK. The samples were weighed into clean exetainer tubes after being flushed with 99.995% helium. Phosphoric acid was then added to the samples, and they were allowed to react overnight to ensure the complete conversion of carbonate to CO_2, following the method outlined by Coplen et al. (1983). The reference materials used for VPDB calibration and quality control of the analysis included: IA-R022 (calcium carbonate, $\delta^{13}C$ = -28.63‰, $\delta^{18}O$ = -22.69‰), NBS-18 (carbonatite, $\delta^{13}C$ = -5.01‰, $\delta^{18}O$ = -23.2‰), IA-R066 (chalk, $\delta^{13}C$ = +2.33‰; $\delta^{18}O$ = -1.52). The accepted values of the in-house standards IA-R022 and IA-R066 were obtained by calibrating against IAEA international reference materials, NBS-18 and NBS-19, and NBS-18 and IAEA-CO-1 (Carrara marble, $\delta^{13}C$ = 2.5‰, and $\delta^{18}O$ = -2.4‰), respectively. Additionally, in-house standards long-term measured were used: ILC1 (calcite, $\delta^{13}C$ = 2.13, $\delta^{18}O$ = -3.99‰), and Y-02 (calcite, $\delta^{13}C$ = 1.48, $\delta^{18}O$ = -9.59‰). The analytical precision of quality control standard replicates was better than 0.09‰ for $\delta^{13}C$ and better than 0.12‰ for $\delta^{18}O$. The calcium carbonate content test on of these samples, ranging between 3.9% to and 8.9%, does not indicate a substantial presence of secondary carbonates, considering (Chesson et al. (, 2021). Additionally, phosphate results on samples from Axlor showed $\delta^{18}O_{carb}$-$\delta^{18}O_{phos}$ offsets within the expected range for well-preserved samples (Pederzani et al., 2023).

3.3 Carbon stable isotopic compositions as environmental and ecological tracers

To unravel animal diet and to compare the different species, in standardised terms, it is necessary to consider the fractionation enrichment factor (ϵ^*) between $\delta^{13}C$ obtained by the animal on its diet ($\delta^{13}C_{diet}$) and $\delta^{13}C$ recorded on enamel carbonates ($\delta^{13}C_{carb}$) (Bocherens, 2003; Cerling and Harris, 1999). The ϵ^* estimated for large ruminant mammals results in an offset of around 14.1‰ between diet and dental enamel, which is commonly applied generally commonly applied to medium-sized herbivores. However, it is well-known that this offset varies between species, considering animals' different physiological parameters. Recently, a formal model to predict species-specific diet-consumer isotopic offsets has been proposed, which uses body mass (BM) and digestive physiology as the main factors that regulating regulate the ϵ^* (Tejada-Lara et al., 2018). This model proposes the following prediction equations for ruminant or foregut fermenters (Equation 1: Eq.1) and hindgut fermenters (Eq. 2):

245   (Eq. 1) ε* = 2.34+0.05 (BM)   [r^2=0.78; p-value=0.008]

246   (Eq. 2) ε* = 2.42+0.032 (BM)   [r^2=0.74; p-value=0.003]

247 In this work, we compareThis work compares species with different digestive physiology, ruminants for
248 bovines and cervids, and non-ruminants for equids. The ε* value was adjusted to for each animal to avoid
249 bias from digestive physiology when comparing these species. The following fractionation enrichment
250 factors have been used: 14.6‰ for *Bos taurus* (Passey et al., 2005a), 13.7‰ for *Equus caballus* (Cerling
251 and Harris, 1999), and 13.2‰ for *Cervus elaphus* (Merceron et al. (2021) following (Eq. 1) for ruminants
252 with a mean body mass of 125 kg.

253 In body tissues, cCarbon isotopic composition in body tissues is considered a combination of diet
254 (understood as consumed food), environment openness (and associated exposure to light), and the amount
255 of precipitation. Assuming that δ^{13}C of past vegetation is close to δ^{13}C$_{diet}$ of ungulates, Having the
256 precipitation in mind, Lécuyer et al. (2021) proposed to estimate Mean Annual Precipitations (MAP) from
257 δ^{13}C$_{carb}$ preserved in enamel carbonates, derived from diets based on C3 plants. After transforming δ^{13}C
258 from enamel carbonate (δ^{13}C$_{carb}$) to δ^{13}C of the diet (δ^{13}C$_{diet}$) using the fractionation enrichment factors
259 established above, this work suggested transforming this value to δ^{13}C from vegetation (δ^{13}C$_{leaf}$). However,
260 the isotopic composition of animals' diet may not directly reflected vegetation cover, but rather the food
261 preference of the animal and this approach should be discussed alongside other environmental data.

262 The MAP estimation is based on least square regression developed by Rey et al. (2013) and based on Kohn
263 (2010) dataset (Eq.4), which requires first to estimate the δ^{13}C$_{leaf}$ (Eq. 3). The δ^{13}C values of atmospheric
264 CO$_2$ (δ^{13}C$_{atm}$) are fixed in -7‰ (Lécuyer et al., 2021; Leuenberger et al., 1992; Schmitt et al., 2012).
265 Atmospheric CO$_2$ levels have varied throughout the Late Pleistocene, with δ^{13}C$_{atm}$ range between -7 to -
266 6.4‰ (Eggleston et al., 2016), favouring an age-specific correction approach. However, maintaining general
267 corrections is preferred considering the chronological uncertainty of the studied levels.

268   (Eq.3) δ^{13}C$_{leaf}$ (VPDB) = (δ^{13}C$_{atm}$ - δ^{13}C$_{diet}$) / [1+(δ^{13}C$_{diet}$ / 1000)]

269

270   (Eq.4) Log1(MAP+300) = 0.092(±0.004) x δ^{13}C$_{leaf}$ + 1.148(±0.074)

271

272 Additionally, The Lécuyer et al. (2021) equation also incorporatesaccounts for the consideration of the pCO$_2$
273 effect on δ^{13}C$_{leaf}$ estimation, which is expected to result in an offset of +1‰ from current levels (considering
274 that pCO$_2$ was 180 ppm during the LGM, which is lower than thate 300ppm experienced during the post
275 post after the deglaciation period around 15 ka). If this correction was not applied, MAP results will could
276 be underestimated by -150mm. In agreement with Lécuyer et al. (2021) appreciation, these MAP estimations
277 are a preliminary approximation and should be cross-validated with other environmental proxies. The
278 associated uncertainties range from ±100 to 200 mm, influencing the interpretation of the final values.

279

280

281 **3.4 Oxygen stable isotope compositions as environmental tracers**

282 Intratooth profiles are known to provide a time-averaged signal compared to the input isotopic signal (δ^{13}C/
283 δ^{18}O$_{carb}$) during enamel formation (Passey et al., 2005b). This signal attenuation is caused both by time-
284 averaging effects incurred through the extended nature of amelogenesis and tooth formation, and through
285 the sampling strategy. During mineralisation, the maturation zone, which is time-averaged, often affects a
286 large portion of the crown height and might affect the temporal resolution of the input signal of the sample
287 taken. To obtain climatically informative seasonal information on the analysed teeth, the application of the

> **Formatted:** Subscript

inverse modelling method proposed by (Passey et al. (2005b) is, therefore, required~~applied in this work~~. This method allows us to computationally estimate the time-averaging effects of sampling and tooth formation to obtain more accurately the original amplitude of the isotopic input signal, thus~~the original amplitude of the isotopic input signal more accurately, thus,~~ to summer and winter extremes (Appendix D). This method considers parameters based on the amelogenesis trends of each species and sampling geometry, which are critical for a meaningful interpretation of intratooth isotope profiles. To evaluate the data's reproducibility and precision, the model also estimates the error derived from the uncertainty of the sampling and the mass spectrometer measurements~~he model also estimates the error derived from the sampling uncertainty and the mass spectrometer measurements to evaluate the data's reproducibility and precision~~. This method was initially developed for continuously growing teeth, taking into account a constant growth rate within a linear maturation model, which ~~with~~ a progressive time average increment as sampling advances along the teeth profile. The species studied in this research exhibit non-linear tooth enamel formation, particularly in later-forming molars (Bendrey et al., 2015; Zazzo et al., 2012; Passey and Cerling, 2002; Kohn, 2004; Blumenthal et al., 2014). Although the aforementioned model~~model mentioned above~~ is not ideal, as it does not account for non linear enamel formation and certain growth parameters for the species included are unknown, it is the best estimation based on the current state of the field and remains widely used (Pederzani et al., 2023, 2021a, b). Flat and less sinusoidal profiles are less suitable for the application of the model, given its inherent assumption of an approximately sinusoidal form. Therefore, we chose not to apply this methodology in the analysis of intratooth $\delta^{13}C$ profiles, and it is recommended to approach the interpretation of model outcomes for non-sinusoidal $\delta^{18}O$ curves with caution. Further details on the application of this method can be found in Appendix D.

Stable oxygen isotopes from meteoric water (mainly derived from rainfall) ~~have a strong relationship~~strongly correlate with mean air temperatures in mid to high latitudes (Rozanski et al., 1992; Dansgaard, 1964) on a regional-to-local scale. Obligate drinkers, ~~such as~~like bovines and horses, acquire this water and record its isotopic composition in their teeth and bones with a fixed~~,~~ but species-specific offset (Pederzani and Britton, 2019). Considering this two-step relationship, past climatic conditions can be estimated. However, most of the temperature reconstructions based on $\delta^{18}O$ have considered the $\delta^{18}O$ from the phosphate fraction of bioapatite enamel ($\delta^{18}O_{phos}$) to build linear correlations between tooth enamel and drinking water $\delta^{18}O$ and obtain climatic information. For this reason, the $\delta^{18}O_{carb}$ ~~from carbonates~~ values obtained in this work (~~$\delta^{18}O_{carb}$~~) were converted into $\delta^{18}O_{phos}$ ~~from phosphates ($\delta^{18}O_{phos}$)~~. To do so, first, to express in VSMOW notation, the $\delta^{18}O_{carb}$ was corrected using the following correlation (Coplen et al., 1983; Brand et al., 2014):

(Eq.5) $\delta^{18}O_{carb}$ (VSMOW)= 1.0309 x $\delta^{18}O_{carb}$ (VPDB) + 30.91

Second, considering the relationship existent in tooth enamel between the carbonate and phosphate fraction (Iacumin et al., 1996; Pellegrini et al., 2011), from a compilation of the existent bibliography of modern animals measurements (Trayler and Kohn, 2017; Pellegrini et al., 2011; Bryant et al., 1996), Pederzani et al. (2023) proposed the following correlation:

(Eq.6) $\delta^{18}O_{phos}$ (VSMOW) = 0.941 x ~~$\delta^{18}O_{carb}$~~ c (VSMOW) - 7.16

Once the isotopic information is expressed in $\delta^{18}O_{phos}$ (VSMOW), we can estimate the $\delta^{18}O$ on meteoric waters ($\delta^{18}O_{mw}$). It is known that different physiological factors will condition how oxygen isotope composition is fixed in each mammalian group. Thus, ~~usually,~~ the correlations ~~–~~are usually species-specific and developed considering the ~~particular~~ physiology of each animal group. The correlation employed by this work relies on recent data compilations (Pederzani et al., 2021b, 2023). In the case of horses (Eq. 7), it has been considered the data combination of Blumenthal et al. (2019); Chillón et al. (1994); Bryant et al., 1994; Delgado Huertas et al., 1995), whereas for bovines (Eq. 8) the data from D'Angela and Longinelli (1990)

332 and Hoppe (2006) have been put together in Eq. 4. To estimate $\delta^{18}O_{mw}$ from red deer remains, we selected
333 D'Angela and Longinelli (1990) correlation (Eq. 9):

334   (Eq.7) $\delta^{18}O_{mw}$ (VSMOW)= ($\delta^{18}O_{phos}$ (VSMOW) - 22.14) / 0.6287

335   (Eq.8) $\delta^{18}O_{mw}$ (VSMOW)= ($\delta^{18}O_{phos}$ (VSMOW) - 22.136) / 0.785

336   (Eq.9) $\delta^{18}O_{mw}$ (VSMOW)= ($\delta^{18}O_{phos}$ (VSMOW) - 24.39) / 0.91

337 Finally, paleotemperatures estimations from $\delta^{18}O_{mw}$ are typically approached using a geographically
338 adjusted linear regression, which can vary from precise adjustments (aimed at reducing errors) to broader
339 geographical adjustments that encompass more variability and but also introduce greatermore significant
340 uncertaintybut are less precise (e.g., Pryor et al., 2014; Skrzypek et al., 2011; Tütken et al., 2007). the mean
341 annual temperatures (MAT) were calculated from $\delta^{18}O_{mw}$, In this work, temperatures were calculated
342 considering the linear regression model relating $\delta^{18}O_{mw}$ and air temperatures from Iberia proposed by
343 Pederzani et al. (2021). Fernández-García et al. (2019). This correlation is based on monthly climatic
344 records (monthly mean $\delta^{18}O_{mw}$ and monthly mean air temperatures), from Western, Southern and Central
345 Europe all Iberian stations from the Global Network of Isotopes in Precipitation, operated by the International
346 Atomic Energy Association and the World Meteorological Organization (IAEA/ WMO, 20182020).
347 Considering current IAEA data sets from northern Iberia, there is a strong positive relationship between
348 δ18Omw and annual or monthly temperatures (Moreno et al., 2021). However, it is known that Iberia is
349 under a mixed influence between Atlantic and Mediterranean moisture sources that affects the isotopic
350 composition of rainfall (Moreno et al., 2021; Araguas-Araguas and Diaz Teijeiro, 2005; García-Alix et al.,
351 2021). Given uncertainties in past atmospheric circulation patterns and the limited availability of reference
352 stations, it was deemed most appropriate to select an equation that extends beyond the borders of Iberia
353 and incorporates higher variability. Different correlations were for mean annual temperature (Eq. 10),
354 summer (Eq. 11), and winter (Eq. 12) temperatures (T):

355   (Eq.10) $\delta^{18}O_{mw}$ (VSMOW)= (0.50 x T) - 13.64

356   (Eq.11) $\delta^{18}O_{mw}$ (VSMOW) = (0.46 x T) - 14.70

357   (Eq.12) $\delta^{18}O_{mw}$ (VSMOW)= (0.52 x T) - 11.26

358 (Eq. 10) MAT (°C) = 2.38(± 0.10) × $\delta^{18}O_{mw}$ + 28.19(± 0.58)

359   [r^2= 0.65; n=304; p value ><0.0001]

360 Nonetheless, oscillations between glacial and interglacial conditions in the past have influenced global ice
361 volume and sea level fluctuations (Dansgaard, 1964; Shackleton, 1987), impacting seawater oxygen isotope
362 composition and the surface hydrological cycle on a globalworldwide scale, including $\delta^{18}O_{mw}$ (Schrag et al.,
363 2002). Prior studies have used sea level information to correct $\delta^{18}O_{mw}$ (e.g., Fernández-García et al., 2019;
364 Schrag et al., 2002). Given the chronological uncertainty in the studied levels, a general correction was
365 applyied to $\delta^{18}O_{mw}$ before temperatures estimations, following Fernández-García et al. (2020) approach.
366 Considering the mean sea level descent for the MIS3 period (50 meters below present-day sea
367 level)(Chappell and Shackleton, 1986), this may have contributed to a potential increase in the global $\delta^{18}O_{mw}$
368 value by ≈0.56‰, inferring a bias in calculated air temperatures of ≈1°C.

369 Following (Pederzani et al., (2021b), mean annual temperatures (MAT) wereas deduced from the $\delta^{18}O$ mean
370 average of $\delta^{18}O_{carb}$ values between summer and winter detected in original sinusoidal intratooth profiles
371 (Appendix C) in each tooth before modeling to reduce associated error and maximise number of usable data
372 records. This work shows that comparable results can be obtained before and after model application, but
373 doing it beforehand avoids the associated errors induced by the inverse model. Summer and winter

374 ~~estimations were extracted from the obtained δ18O values after inverse modeling application, to identify~~
375 ~~seasonal variation. o maximize data, in non-sinusoidal teeth profiles, MAT was deduced from the average~~
376 ~~of all points within a tooth. However, this approach is less reliable when complete annual cycles are not~~
377 ~~recorded. When possible, summer and winter estimations were derived from the obtained δ18O~~carb~~ values~~
378 ~~after inverse modelling application, aiming to identify the seasonal amplitude, which is dampened in the~~
379 ~~original δ18O~~carb~~ signal.~~

380 Due to the uncertainties incurred from converting stable isotope measurements to palaeotemperature, the
381 final estimations in this work should be considered exploratory and as a method of standardisation to make
382 results comparable ~~with~~ among different sites, ~~data from different~~ species, and other non-isotopic
383 palaeoclimatic records. In these estimations, the associated error from converting $\delta^{18}O_{phos}$ to MAT is
384 enlarged by the uncertainty derived from the transformation of $\delta^{18}O_{carb}$ (VPDB) to $\delta^{18}O_{phos}$ (VSMOW) (see
385 Pryor et al., 2014; Skrzypek et al., 2016 for further discussion). However, Pryor et al. (2014) and Pederzani
386 et al. (2023) concluded that the impact of this conversion is negligible compared to the error propagation in
387 subsequent calibrations used for temperature estimations from $\delta^{18}O_{phos}$. These associated errors were
388 quantified following the methodology outlined by Pryor et al. (2014).

389 ### 3.5 Inverse modelling applied to intratooth profiles

390 Intratooth profiles frequently provide a time-averaged signal compared to the input isotopic signal ($\delta^{13}C/$
391 $\delta^{18}O_{carb}$) during enamel formation (Passey et al., 2005b). This signal attenuation is caused by time-averaging
392 effects incurred through the extended nature of amelogenesis and tooth formation, and through the sampling
393 strategy. During mineralisation, the maturation zone, which is time-averaged, often affects a large portion of
394 the crown height and might affect the temporal resolution of the input signal of the sample taken. To obtain
395 climatically informative seasonal information on the analysed teeth, the ~~the~~ inverse modelling method
396 proposed by (Passey et al. (2005b) is applied in this work. This method computationally estimates the time-
397 averaging effects of sampling and tooth formation to obtain the original amplitude of the isotopic input signal
398 more accurately, thus, to summer and winter extremes (Appendix D). This method considers parameters
399 based on the amelogenesis trends of each species and sampling geometry, which are critical for a
400 meaningful interpretation of intratooth isotope profiles. The model also estimates the error derived from the
401 sampling uncertainty and the mass spectrometer measurements to evaluate the data's reproducibility and
402 precision. This method was initially developed for continuously growing teeth, taking into account a constant
403 growth rate within a linear maturation model, with a progressive time-average increment as sampling
404 advances along the teeth profile. The species studied in this research exhibit non-linear tooth enamel
405 formation, particularly in later-forming molars (Bendrey et al., 2015; Zazzo et al., 2012; Passey and Cerling,
406 2002; Kohn, 2004; Blumenthal et al., 2014). Although the model mentioned above is not ideal, as it does not
407 take into account ~~for~~ non-linear enamel formation and ~~certain~~specific growth parameters for the species
408 included are unknown, it is the best estimation based on the current state of the field and remains widely
409 used (Pederzani et al., 2023, 2021a, b). Flat and less sinusoidal profiles are less suitable for the application
410 of the model, given its inherent assumption of an approximately sinusoidal form. Therefore, we chose not to
411 apply this methodology in the analysis of intratooth $\delta^{13}C$ profiles, and it is recommended to approach the
412 interpretation of model outcomes for non-sinusoidal $\delta^{18}O$ curves with caution. Further details on the
413 application of this method can be found in Appendix D.

414 Following Pederzani et al. (2021b), mean annual temperatures (MAT) were deduced from the average of
415 $\delta^{18}O_{carb}$ values between summer and winter detected in original sinusoidal intratooth profiles (Appendix C).
416 This work shows that comparable results for annual means can be obtained before and after model
417 application, but doing it beforehand avoids the associated errors induced by the inverse model. To maximize
418 data, in non-sinusoidal teeth profiles, MAT was deduced from the average of all points within a tooth.
419 However, this approach is less reliable when complete annual cycles are not recorded. When possible,

420 summer and winter temperature estimations were derived from the obtained $\delta^{18}O_{carb}$ values after inverse
421 modelling application, aiming to identify the corrected seasonal amplitude, which is dampened in the original
422 $\delta^{18}O_{carb}$ signal.

423

424 **3.64 Present-day isotopic and climatic data**

425 Present-day climatic conditions surrounding each site have been considered, allowing an inter-site
426 comparison, essential for compare our this study but also a regional to a with other regional and global
427 perspectivedata. Considering current MATs and MAPs, estimated climatic data is expressed in relative
428 terms as MAT and MAP anomalies. Present-day summer and winter temperatures were also considered.
429 Present-day temperatures and precipitation values were obtained from the WorldClim Dataset v2 (Fick and
430 Hijmans, 2017) (Appendix B). This dataset includes the average of bioclimatic variables between 1970-2000
431 in a set of raster files with a spatial resolution every 2.5 minutes. The exact location of the selected archeo-
432 palaeontological sites was used, using geographical coordinates in the projection on modern climatic maps
433 with QGIS software.

434 Present-day $\delta^{18}O_{mw}$ values from the analysed sites' areas were obtained using the Online Isotopes in
435 Precipitation Calculator (OIPC Version 3.1 (4/2017); Bowen, 2022) based on datasets collected by the
436 Global Network for Isotopes in Precipitation from the IAEA/WMO (Appendix B).

Site	Level	Culture	Species	Tooth type	Code	CCE (%)	n	δ13Ccarb VPDB (‰)	min	max	SD	Range	δ18Ocarb VPDB (‰)	min	max	SD	Range
Axlor	III	Mousterian	*Bos/Bison* sp.	LRM3	AXL59	5.6	14	-8.9	-9.6	-8.2	1.4	0.4	-6.0	-7.3	-5.2	0.7	2.1
Axlor	III	Mousterian	*Bos/Bison* sp.	LRM2	AXL60	5.5	18	-9.7	-10.0	-8.9	1.1	0.3	-5.7	-6.8	-4.6	0.7	2.2
Axlor	III	Mousterian	*Bos/Bison* sp.	LRM3	AXL65	6.2	13	-8.9	-9.3	-8.1	1.2	0.4	-6.0	-7.2	-4.6	0.8	2.6
Axlor	III	Mousterian	*Bos/Bison* sp.	LRM2	AXL66	5.6	16	-8.9	-9.8	-8.3	1.5	0.5	-4.8	-6.1	-3.8	0.7	2.3
Axlor	IV	Mousterian	*Bos/Bison* sp.	LRM2	AXL70	5.7	12	-9.1	-9.4	-8.6	0.7	0.3	-5.3	-7.3	-3.9	1.2	3.4
Axlor	VI	Mousterian	*Bos/Bison* sp.	LLM3	AXL77	5.9	14	-9.7	-10.2	-9.2	1.0	0.4	-6.2	-7.9	-5.0	0.9	2.9
Axlor	VI	Mousterian	*Bos/Bison* sp.	LLM3	AXL86	5.5	18	-9.9	-10.2	-9.3	0.9	0.3	-5.4	-6.5	-3.8	0.7	2.6
El Castillo	20E	Mousterian	*Equus* sp.	LRP3/LRP4	CAS60		14	-11.9	-12.5	-11.5	1.0	0.3	-3.3	-4.1	-2.4	0.4	1.6
El Castillo	20E	Mousterian	*Equus* sp.	LRP3/LRP4	CAS61		14	-12.2	-12.4	-12.1	0.3	0.1	-4.9	-5.8	-4.3	0.4	1.5
El Castillo	20E	Mousterian	*Bos/Bison* sp.	LLM2	CAS139	6.7	16	-11.6	-12.2	-11.2	0.9	0.3	-5.6	-6.3	-4.9	0.5	1.4
El Castillo	20E	Mousterian	*Bos/Bison* sp.	LLM2	CAS140	5.7	12	-11.5	-11.9	-11.1	0.8	0.3	-5.5	-6.3	-4.6	0.6	1.7
El Castillo	21A	Mousterian	*Bos/Bison* sp.	LLM3	CAS141	5.7	15	-11.2	-11.5	-10.9	0.6	0.2	-5.4	-6.5	-4.3	0.6	2.2
El Castillo	21A	Mousterian	*Bison priscus*	LLM3	CAS142	6.1	15	-11.2	-11.7	-10.9	0.7	0.2	-5.0	-5.7	-4.4	0.4	1.3
El Castillo	21A	Mousterian	*Equus* sp.	LLM3	CAS143	6.5	17	-12.6	-12.9	-12.5	0.4	0.1	-6.2	-7.2	-5.4	0.5	1.8
El Castillo	18B	Transitional Aurignacian	*Bos/Bison* sp.	ULM2	CAS132	6.2	13	-11.3	-11.5	-10.9	0.6	0.2	-6.2	-7.4	-4.9	0.7	2.6
El Castillo	18B	Transitional Aurignacian	*Bos/Bison* sp.	ULM2	CAS133	6.8	18	-10.9	-11.6	-10.5	1.1	0.3	-5.4	-6.5	-4.2	0.7	2.2
El Castillo	18B	Transitional Aurignacian	*Bos/Bison* sp.	ULM2	CAS134	6.6	18	-12.4	-12.8	-11.6	1.2	0.3	-5.4	-6.3	-4.5	0.5	1.8
El Castillo	18C	Transitional Aurignacian	*Bos/Bison* sp.	LLM3	CAS135	6	17	-11.3	-11.5	-11.0	0.5	0.2	-6.1	-6.6	-5.5	0.3	1.1
El Castillo	18C	Transitional Aurignacian	*Bos/Bison* sp.	LLM3	CAS136	5.8	17	-12.0	-12.5	-11.7	0.9	0.2	-5.8	-6.7	-5.0	0.6	1.7
El Castillo	18C	Transitional Aurignacian	*Bos/Bison* sp.	LLM3	CAS137	6.6	14	-10.2	-10.6	-9.9	0.7	0.2	-5.8	-6.5	-4.1	0.7	2.4
El Castillo	18C	Transitional Aurignacian	*Bos/Bison* sp.	LLM3	CAS138	6.1	18	-11.6	-11.8	-11.4	0.4	0.1	-5.3	-5.9	-4.8	0.3	1.2
El Castillo	18B	Transitional Aurignacian	*Cervus elaphus*	ULM2+ULM3	CAS8		11	-13.0	-14.9	-12.1	2.8	1.0	-6.8	-10.4	-4.1	2.1	6.3
El Castillo	18B	Transitional Aurignacian	*Equus* sp.	ULP3/ULP4	CAS58		19	-11.7	-11.8	-11.5	0.3	0.1	-6.6	-7.5	-5.6	0.5	1.8
El Castillo	18B	Transitional Aurignacian	*Equus* sp.	LLP3/LLP3	CAS59		14	-11.5	-11.7	-11.0	0.7	0.2	-4.0	-4.7	-3.5	0.4	1.2
Labeko Koba	IX inf	Chatelperronian	*Equus* sp.	URM3	LAB38		17	-12.0	-12.2	-11.9	0.3	0.1	-6.6	-7.7	-5.9	0.5	1.9
Labeko Koba	IX inf	Chatelperronian	*Cervus elaphus*	LLM2	LAB02		7	-12.3	-12.4	-12.1	0.3	0.1	-4.7	-6.0	-3.7	1.0	2.3
Labeko Koba	VI	Aurignacian	*Equus* sp.	URM2	LAB20		16	-12.0	-12.2	-11.8	0.4	0.1	-6.1	-6.4	-5.3	0.4	1.7
Labeko Koba	V	Aurignacian	*Equus* sp.	LRM3	LAB42		17	-11.9	-12.3	-11.5	0.2	0.7	-5.7	-6.6	-5.0	0.5	1.6
Labeko Koba	IV	Aurignacian	*Equus* sp.	LRM2	LAB36		17	-11.6	-11.8	-11.3	0.6	0.2	-5.9	-6.2	-5.5	0.2	0.7
Canyars	I	Aurignacian	*Equus* sp.	URM3	CAN01	7.8	12	-10.0	-10.4	-9.5	0.9	0.3	-4.8	-5.3	-4.3	0.3	1.1
Canyars	I	Aurignacian	*Equus ferus*	URM3	CAN02	6.2	17	-10.5	-10.7	-10.3	0.4	0.1	-4.4	-5.0	-3.6	0.5	1.4
Canyars	I	Aurignacian	*Equus ferus*	URP3/URP4	CAN03	6.4	17	-10.7	-11.2	-10.4	0.8	0.2	-4.8	-5.3	-4.0	0.4	1.4
Labeko Koba	VII	Aurignacian	*Bos primigenius*	LRM3	LAB53	5.2	23	-9.5	-10.1	-8.7	1.4	0.3	-5.7	-7.0	-4.2	0.9	2.8
Labeko Koba	VII	Aurignacian	*Bos primigenius*	LRM3	LAB55	5.6	23	-10.4	-11.5	-9.8	1.6	0.3	-5.1	-7.0	-2.7	1.2	4.3
Labeko Koba	VII	Aurignacian	*Bos/Bison* sp.	LRM3	LAB62	6.5	21	-9.7	-10.2	-9.1	1.2	0.3	-7.2	-8.1	-6.2	0.6	2.0
Labeko Koba	V	Aurignacian	*Bos primigenius*	LRM3	LAB69	5.5	21	-9.3	-10.3	-7.3	3.0	0.9	-7.2	-8.8	-5.5	0.9	3.3
Canyars	I	Aurignacian	Bos primigenius	ULM3	CAN04	6.8	14	-9.3	-9.8	-8.7	1.1	0.3	-3.6	-4.2	-2.6	0.5	1.6
Canyars	I	Aurignacian	Bos primigenius	ULM3	CAN05	6.6	14	-9.0	-9.5	-8.5	0.9	0.3	-5.5	-6.2	-5.0	0.4	1.2
Aitzbitarte III	V (int)	Gravettian	*Bos/Bison* sp.	LLM3	AITI10	5.5	17	-9.2	-9.6	-8.7	0.9	0.3	-5.5	-6.5	-4.3	0.5	2.2
El Otero	IV	Magdalenian	*Cervus elaphus*	LLM2+LLM3	OTE1		11	-11.4	-11.6	-11.2	0.4	0.1	-4.4	-5.8	-2.9	1.0	2.9
El Otero	IV	Magdalenian	*Cervus elaphus*	LLM2+LLM3	OTE5		10	-11.3	-11.5	-11.0	0.5	0.2	-5.1	-5.7	-3.8	0.6	1.9
El Otero	IV	Magdalenian	*Cervus elaphus*	LLM2+LLM3	OTE6		14	-11.4	-11.8	-10.6	1.2	0.3	-4.6	-5.4	-4.0	0.4	1.4
El Otero	IV	Magdalenian	*Equus* sp.	LLP3/LLP4	OTE11		17	-11.6	-11.8	-11.4	0.5	0.1	-5.0	-6.3	-3.9	0.7	2.4
El Otero	IV	Magdalenian	*Equus* sp.	LLP3/LLP4	OTE12		16	-11.3	-11.5	-10.9	0.6	0.1	-3.9	-4.9	-3.3	0.6	1.6

437

Site	Level	Culture	Species	Tooth type	Code	n	δ13Ccarb VPDB (‰)	min	max	SD	Range	δ18Ocarb VPDB (‰)	min	max	SD	Range
Axlor	III	Mousterian	*Bos/Bison* sp.	LRM3	AXL59	14	-8.9	-9.6	-8.2	1.4	0.4	-6.0	-7.3	-5.2	0.7	2.1
Axlor	III	Mousterian	*Bos/Bison* sp.	LRM2	AXL60	18	-9.7	-10.0	-8.9	1.1	0.3	-5.7	-6.8	-4.6	0.7	2.2
Axlor	III	Mousterian	*Bos/Bison* sp.	LRM3	AXL65	13	-8.9	-9.3	-8.1	1.2	0.4	-6.0	-7.2	-4.6	0.8	2.6
Axlor	III	Mousterian	*Bos/Bison* sp.	LRM2	AXL66	16	-8.9	-9.8	-8.3	1.5	0.5	-4.8	-6.1	-3.8	0.7	2.3
Axlor	IV	Mousterian	*Bos/Bison* sp.	LRM2	AXL70	12	-9.1	-9.4	-8.6	0.7	0.3	-5.3	-7.3	-3.9	1.2	3.4
Axlor	VI	Mousterian	*Bos/Bison* sp.	LLM3	AXL77	14	-9.7	-10.2	-9.2	1.0	0.4	-6.2	-7.9	-5.0	0.9	2.9
Axlor	VI	Mousterian	*Bos/Bison* sp.	LLM3	AXL86	18	-9.9	-10.2	-9.3	0.9	0.3	-5.4	-6.5	-3.8	0.7	2.6
El Castillo	20E	Mousterian	*Equus* sp.	LRP3/LRP4	CAS60	14	-11.9	-12.5	-11.5	1.0	0.3	-3.3	-4.1	-2.4	0.4	1.6
El Castillo	20E	Mousterian	*Equus* sp.	LRP3/LRP4	CAS61	14	-12.2	-12.4	-12.1	0.3	0.1	-4.9	-5.8	-4.3	0.4	1.5
El Castillo	20E	Mousterian	*Bos/Bison* sp.	LLM2	CAS139	16	-11.6	-12.2	-11.2	0.9	0.3	-5.6	-6.3	-4.9	0.5	1.4
El Castillo	20E	Mousterian	*Bos/Bison* sp.	LLM2	CAS140	12	-11.5	-11.9	-11.1	0.8	0.3	-5.5	-6.3	-4.6	0.6	1.7
El Castillo	21A	Mousterian	*Bos/Bison* sp.	LLM3	CAS141	15	-11.2	-11.5	-10.9	0.6	0.2	-5.4	-6.5	-4.3	0.6	2.2
El Castillo	21A	Mousterian	*Bison priscus*	LLM3	CAS142	15	-11.2	-11.7	-10.9	0.7	0.2	-5.0	-5.7	-4.4	0.4	1.3
El Castillo	21A	Mousterian	*Equus* sp.	LLM3	CAS143	17	-12.6	-12.9	-12.5	0.4	0.1	-6.2	-7.2	-5.4	0.5	1.8
El Castillo	18B	Transitional Aurignacian	*Bos/Bison* sp.	ULM2	CAS132	13	-11.3	-11.5	-10.9	0.6	0.2	-6.2	-7.4	-4.9	0.7	2.6
El Castillo	18B	Transitional Aurignacian	*Bos/Bison* sp.	ULM2	CAS133	18	-10.9	-11.6	-10.5	1.1	0.3	-5.4	-6.5	-4.2	0.7	2.2
El Castillo	18B	Transitional Aurignacian	*Bos/Bison* sp.	ULM2	CAS134	18	-12.4	-12.8	-11.6	1.2	0.3	-5.4	-6.3	-4.5	0.5	1.8
El Castillo	18C	Transitional Aurignacian	*Bos/Bison* sp.	LLM3	CAS135	17	-11.3	-11.5	-11.0	0.5	0.2	-6.1	-6.6	-5.5	0.3	1.1
El Castillo	18C	Transitional Aurignacian	*Bos/Bison* sp.	LLM3	CAS136	17	-12.0	-12.5	-11.7	0.9	0.2	-5.8	-6.7	-5.0	0.6	1.7
El Castillo	18C	Transitional Aurignacian	*Bos/Bison* sp.	LLM3	CAS137	14	-10.2	-10.6	-9.9	0.7	0.2	-5.8	-6.5	-4.1	0.7	2.4
El Castillo	18C	Transitional Aurignacian	*Bos/Bison* sp.	LLM3	CAS138	18	-11.6	-11.8	-11.4	0.4	0.1	-5.3	-5.9	-4.8	0.3	1.2
El Castillo	18B	Transitional Aurignacian	*Cervus elaphus*	ULM2+ULM3	CAS8	11	-13.0	-14.9	-12.1	2.8	1.0	-6.8	-10.4	-4.1	2.1	6.3
El Castillo	18B	Transitional Aurignacian	*Equus* sp.	ULP3/ULP4	CAS58	19	-11.7	-11.8	-11.5	0.3	0.1	-6.6	-7.5	-5.6	0.5	1.8
El Castillo	18B	Transitional Aurignacian	*Equus* sp.	LLP3/LLP3	CAS59	14	-11.5	-11.7	-11.0	0.7	0.2	-4.0	-4.7	-3.5	0.4	1.2
Labeko Koba	IX inf	Chatelperronian	*Equus* sp.	URM3	LAB38	17	-12.0	-12.2	-11.9	0.3	0.1	-6.6	-7.7	-5.9	0.5	1.9
Labeko Koba	IX inf	Chatelperronian	*Cervus elaphus*	LLM2	LAB02	7	-12.3	-12.4	-12.1	0.3	0.1	-4.7	-6.0	-3.7	1.0	2.3
Labeko Koba	VI	Aurignacian	*Equus* sp.	URM2	LAB20	16	-12.0	-12.2	-11.8	0.4	0.1	-5.3	-6.1	-4.4	0.6	1.7
Labeko Koba	V	Aurignacian	*Equus* sp.	LRM3	LAB42	17	-11.9	-12.3	-11.5	0.2	0.7	-5.7	-6.6	-5.0	0.5	1.6
Labeko Koba	IV	Aurignacian	*Equus* sp.	LRM2	LAB36	17	-11.6	-11.8	-11.3	0.6	0.2	-5.9	-6.2	-5.5	0.2	0.7
Canyars	I	Aurignacian	*Equus* sp.	URM3	CAN01	12	-10.0	-10.4	-9.5	0.9	0.3	-4.8	-5.3	-4.3	0.3	1.1
Canyars	I	Aurignacian	*Equus ferus*	URM3	CAN02	17	-10.5	-10.7	-10.3	0.4	0.1	-4.4	-5.0	-3.6	0.5	1.4
Canyars	I	Aurignacian	*Equus ferus*	URP3/URP4	CAN03	17	-10.7	-11.2	-10.4	0.8	0.2	-4.8	-5.3	-4.0	0.4	1.4
Labeko Koba	VII	Aurignacian	*Bos primigenius*	LRM3	LAB53	23	-9.5	-10.1	-8.7	1.4	0.3	-5.7	-7.0	-4.2	0.9	2.8
Labeko Koba	VII	Aurignacian	*Bos primigenius*	LRM3	LAB55	23	-10.4	-11.5	-9.8	1.6	0.3	-5.1	-7.0	-2.7	1.2	4.3
Labeko Koba	VII	Aurignacian	*Bos/Bison* sp.	LRM3	LAB62	21	-9.7	-10.2	-9.1	1.2	0.3	-7.2	-8.1	-6.2	0.6	2.0
Labeko Koba	V	Aurignacian	*Bos primigenius*	LRM3	LAB69	21	-9.3	-10.3	-7.3	3.0	0.9	-7.2	-8.8	-5.5	0.9	3.3
Canyars	I	Aurignacian	*Bos primigenius*	ULM3	CAN04	14	-9.3	-9.8	-8.7	1.1	0.3	-3.6	-4.2	-2.6	0.5	1.6
Canyars	I	Aurignacian	Bos primigenius	ULM3	CAN05	14	-9.0	-9.5	-8.5	0.9	0.3	-5.5	-6.2	-5.0	0.4	1.2
Aitzbitarte III	V (int)	Gravettian	*Bos/Bison* sp.	LLM3	AITI10	17	-9.2	-9.6	-8.7	0.9	0.3	-5.5	-6.5	-4.3	0.5	2.2
El Otero	IV	Magdalenian	*Cervus elaphus*	LLM2+LLM3	OTE1	11	-11.4	-11.6	-11.2	0.4	0.1	-4.4	-5.8	-2.9	1.0	2.9
El Otero	IV	Magdalenian	*Cervus elaphus*	LLM2+LLM3	OTE5	10	-11.3	-11.5	-11.0	0.5	0.2	-5.1	-5.7	-3.8	0.6	1.9
El Otero	IV	Magdalenian	*Cervus elaphus*	LLM2+LLM3	OTE6	14	-11.4	-11.8	-10.6	1.2	0.3	-4.6	-5.4	-4.0	0.4	1.4
El Otero	IV	Magdalenian	*Equus* sp.	LLP3/LLP4	OTE11	17	-11.6	-11.8	-11.4	0.5	0.1	-5.0	-6.3	-3.9	0.7	2.4
El Otero	IV	Magdalenian	*Equus* sp.	LLP3/LLP4	OTE12	16	-11.3	-11.5	-10.9	0.6	0.1	-3.9	-4.9	-3.3	0.6	1.6

Table 2. Mean, maximum value (Max), minimum value (Min), and standard deviation (SD) of δ13C and δ18O values per archaeological site and level organised by cultural periods. CCE, calcium carbonate equivalent; n, = number of intratooth subsamples measured. In tooth type: position (U, upper; L, lower); laterality (R, right; L, left); tooth (M, molar; P, premolar).

4. Results

In northwestern Iberia, specifically in the Vasco-Cantabrian region, the mean δ13Ccarb values range from -13~~8.9~~‰ to -~~8.9~~13‰, with a mean value of -11‰ (SD = 1.2‰) (Table 2; Table 3). Considering species' different ~~fractionation~~ enrichment factors, the δ13Ccarb were transformed in δ13Cdiet, resulting in mean values that extend from -27~~23.5~~‰ to -23.5~~27~~‰ (Fig. 4). It must be considered that average values may reflect slightly different periods or be affected by seasonal bias because different teeth encompass ~~different~~ diverse periods, but it has been verified in our teeth that the variations are limited when the seasonal information of the sequential sampling is incorporated (±0.2; Appendix B). The carbon isotopic composition varies between species. The bovines have generally higher mean δ13Ccarb (from -12.4~~8.9~~‰ to -~~8.9~~12.4‰) than the horses (from -12.6~~11.3~~‰ to -11.3~~12.6~~‰), whereas the red deer ~~samples~~ fall within the horses' range (from -11~~.3~~‰ to -11.3‰). Average values of δ18Ocarb in all Vasco-Cantabrian individuals extend between -7.2~~3.3~~‰ and -3.3~~7.2~~‰ (mean = -5.5‰; SD = 0.8‰). When transformed to δ18O expected from meteoric waters (δ18Omw), with species-adapted correlations, the δ18Omw values range from -10.6~~3.9~~‰ to -5.5~~9.9~~‰. Less clear patterns in δ18Ocarb are observed between bovines and horses, with mean values of -5.7‰ and -5.2‰, respectively. In the Mediterranean area, the site of Canyars, both species have relatively high δ18Ocarb values that fall inside the range of variation observed in the Cantabria region, between -5.5~~3.6~~‰ and -3.6~~5.5~~‰ in bovines and between -4.8~~4~~‰ and -4.4~~8~~‰ in ~~case of~~ horses.

		Vasco-Cantabrian region (NW Iberia)				Mediterranean region (NE Iberia)			
		δ13Ccarb VPDB (‰)	δ13Cdiet VPDB (‰)	δ18Ocarb VPDB (‰)	d18Omw VSMOW (‰)	δ13Ccarb VPDB (‰)	δ13Cdiet VPDB (‰)	δ18Ocarb VPDB (‰)	d18Omw VSMOW (‰)
	Mean	-11.0	-25.1	-5.5	-6.7	-9.9	-24.0	-4.6	-5.4
	Max	-8.9	-23.5	-3.3	-3.9	-9.0	-23.6	-3.6	-4.3
	Min	-13.0	-27.0	-7.2	-9.9	-10.7	-24.4	-5.5	-6.5
	Range	4.1	3.5	3.9	6.0	1.7	0.8	1.9	2.2
	SD	1.2	0.9	0.8	1.1	0.8	0.3	0.7	0.8
	Mean	-10.4	-25.0	-5.7	-6.8	-9.1	-23.7	-4.5	-5.4
	Max	-8.9	-23.5	-4.8	-5.7	-9.0	-23.6	-3.6	-4.3
	Min	-12.4	-27.0	-7.2	-8.5	-9.3	-23.9	-5.5	-6.5
	Range	3.5	3.5	2.4	2.7	0.3	0.3	1.9	2.2
	SD	1.1	1.1	0.6	0.7	0.2	0.2	1.4	1.6
	Mean	-11.8	-25.5	-5.2	-6.0	-10.4	-24.1	-4.7	-5.4
	Max	-11.3	-25.0	-3.3	-3.9	-10.0	-23.7	-4.4	-5.1
	Min	-12.6	-26.3	-6.6	-7.6	-10.7	-24.4	-4.8	-5.6
	Range	1.4	1.4	3.3	3.7	0.7	0.7	0.5	0.5
	SD	0.4	0.4	1.1	1.2	0.3	0.3	0.3	0.3

		Vasco-Cantabrian region (NW Iberia)				Northeastern Iberia			
		δ13Ccarb VPDB (‰)	δ13Cdiet VPDB (‰)	δ18Ocarb VPDB (‰)	δ18Omw VSMOW (‰)	δ13Ccarb VPDB (‰)	δ13Cdiet VPDB (‰)	δ18Ocarb VPDB (‰)	δ18Omw VSMOW (‰)
Total	Mean	-11.0	-25.1	-5.5	-8.0	-9.9	-24.0	-4.6	-7.1
	Max	-8.9	-23.5	-3.3	-5.5	-9.0	-23.6	-3.6	-5.0
	Min	-13.0	-27.0	-7.2	-10.6	-10.7	-24.4	-5.5	-7.9
	Range	4.1	3.5	3.9	5.1	1.7	0.8	1.9	2.9
	SD	1.2	0.9	0.8	1.2	0.8	0.3	0.7	1.2
Bovines	Mean	-10.4	-25.0	-5.7	-7.7	-9.1	-23.7	-4.5	-6.2
	Max	-8.9	-23.5	-4.8	-6.5	-9.0	-23.6	-3.6	-5.0
	Min	-12.4	-27.0	-7.2	-9.5	-9.3	-23.9	-5.5	-7.4
	Range	3.5	3.5	2.4	3.0	0.3	0.3	1.9	2.4
	SD	1.1	1.1	0.6	0.7	0.2	0.2	1.4	1.7
Horses	Mean	-11.8	-25.5	-5.2	-8.5	-10.4	-24.1	-4.7	-7.6
	Max	-11.3	-25.0	-3.3	-5.5	-10.0	-23.7	-4.4	-7.2
	Min	-12.6	-26.3	-6.6	-10.6	-10.7	-24.4	-4.8	-7.9
	Range	1.4	1.4	3.3	5.1	0.7	0.7	0.5	0.7
	SD	0.4	0.4	1.1	1.8	0.3	0.3	0.3	0.4

Table 3. Mean δ13C from enamel carbonate ($\delta^{13}C_{carb}$) and diet ($\delta^{13}C_{diet}$), and δ18O from enamel carbonate ($\delta^{18}O_{carb}$) and meteoric waters ($\delta^{18}O_{mw}$), by species on the Vasco-Cantabrian and ~~Mediterranean~~ northeastern Iberia areas. Max: maximum value; Min: minimum value; SD: standard deviation.

4.1 Axlor (ca. 80 ka BP - ~~50~~45 ka cal BP)

A total of seven bovine teeth were included from levels III (n = 4), IV (n = 1), and VI (n = 2) of Axlor cave (Pederzani et al., 2023). The mean $\delta^{13}C_{carb}$ range from -9~~8~~.9‰ to -8~~9~~.9‰ ($\delta^{13}C_{diet}$= -24~~3~~.5‰ to -24~~3~~.5‰); whereas mean $\delta^{18}O_{carb}$ values are between ~~-6.2~~-4.8‰ and -4.8~~6.2~~‰ ($\delta^{18}O_{mw}$ = -8.3~~5~~.7‰ and -6.5~~7.3~~‰), indicating a range of variation around 1‰ and 1.4‰, respectively (Fig. 3; 4). Considering isotopic compositions by levels, mean $\delta^{13}C_{carb}$ decreases from level III to level IV, whereas mean $\delta^{18}O_{carb}$ remains stable through the sequence (Table 2; Appendix B). A range between 0.3‰ and 0.5‰ is observed in $\delta^{13}C_{carb}$ variation within tooth profiles. Individuals show clear $\delta^{18}O$ sinusoidal profiles, with peaks and troughs, and intratooth ranges from 2.1‰ to 3.4‰. The $\delta^{18}O_{mw}$ after inverse modelling intratooth profiles range from -9.1~~5~~‰ to -7.3~~6.5~~‰ (Appendix C; D). Mean Annual Temperatures (MATs)~~, estimated from mean $\delta^{18}O_{mw}$ values, with seasonal control,~~ oscillated between 10~~9~~.1ºC and 12.6~~4~~ºC (MATAs = -3.1/+0.4~~+1.8/-2.1~~ºC) (Table 4). From sinusoidal profiles, summer temperatures were extracted from peaks, ~~which are estimated to extend~~resulting from 15.4ºC to 23.7ºC, and winter temperatures from troughs provided values ranging from -7ºC to 10.8ºC. Mean Annual Precipitation (MAPs), extracted from $\delta^{13}C_{carb}$, extend between 204mm and 326mm (MAPAs = -843~~721~~/-721~~843~~mm). Based on these estimations, a non-clear climatic trend is observed through these levels.

4.2 El Castillo (ca. 75 ka BP – 4~~2.9~~7 ka cal BP)

From El Castillo, this work includes bovines (n = 11), horses (n = 5), and red deer (n = 1) teeth from the Mousterian (21 and 20E) and the Transitional Aurignacian levels (18B and 18C). The mean $\delta^{13}C_{carb}$ values are lower for horses, bovines, and red deer (-13‰ to -10.2‰) than other sites. Between -12.4‰ and -10.2‰ for bovines ($\delta^{13}C_{diet}$ = -24.6‰ to -25.8‰) and between -12.6‰ and -11.5‰ for horses ($\delta^{13}C_{diet}$ = -26.3‰ to -25.2‰) (Fig. 3). The mean $\delta^{18}O_{carb}$ values extend from -6.8‰ and -3.3‰. Horses and bovines overlap in their isotopic niche (Fig. 4), mainly due to the notably lower $\delta^{13}C_{carb}$ reported by bovines. The mean $\delta^{13}C_{carb}$ (-13‰) of the single red deer tooth is inside the variation range of bovines and horses but with a lower $\delta^{18}O_{carb}$ mean value (-6.8‰). Considering these isotopic compositions by levels, bovine mean $\delta^{13}C_{diet}$ values highly increase the variation range from Mousterian levels (20E and 21A) to Transitional Aurignacian levels (18C and 18B). In contrast, horses increase mean $\delta^{13}C_{diet}$ values (Fig. 5). Bovine mean $\delta^{18}O_{mw}$ values decrease from level 21A to level 18B, while horses from 18B have a large intra-level amplitude.

The mean $\delta^{18}O_{carb}$ values from horses have a more significant variation (range = 3.3‰) than bovines (range = 2.2‰). All individuals show flat $\delta^{13}C_{carb}$ intratooth profiles (<0.4‰), except for red deer (1‰) (Appendix C). Intratooth $\delta^{18}O_{carb}$ ranges of individuals are around 1-2‰ for horses and 1-3‰ for bovines. Some of the individuals analyzed do not show non-complete annual cycles. No precise $\delta^{18}O_{carb}$ sinusoidal profiles are detected in three teeth; the other six have particularly unclear profiles. After modelling, individual $\delta^{18}O_{carb}$ ranges oscillated between 2.7‰ and 7.4‰ (Appendix D). MATs oscillated between 4.6ºC and 12.6ºC (MATAs = -8.8ºC/-0.9ºC), with mean summer temperatures from around 20.5ºC and mean winter temperatures around -1.1ºC. MAPs extend between 376mm and 784mm (MAPAs = -656/-248mm) (Table 4). Non-important differences in rainfall estimations based on bovines and equids are noticed, probably because they feed on similar ecological resources. Diachronic trends are unclear along the sequence, but mean annual and winter temperatures from levels 18C and 18C seem slightly lower. MAPs estimations oscillated more in the upper levels.

505

506
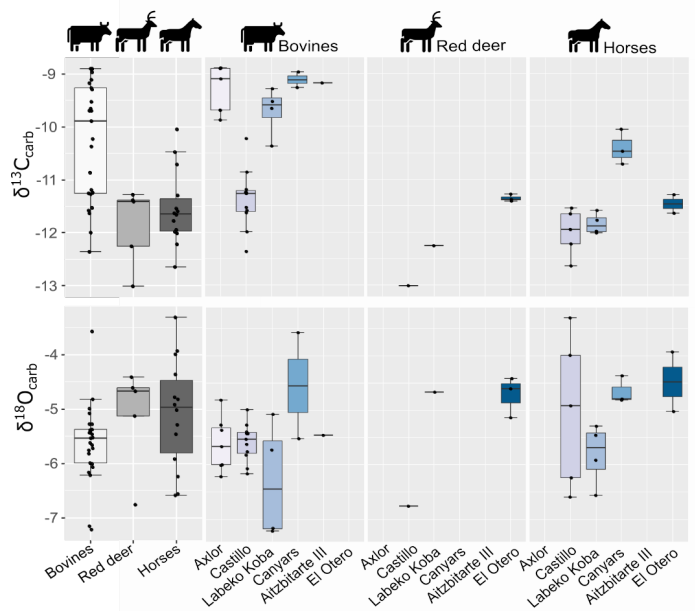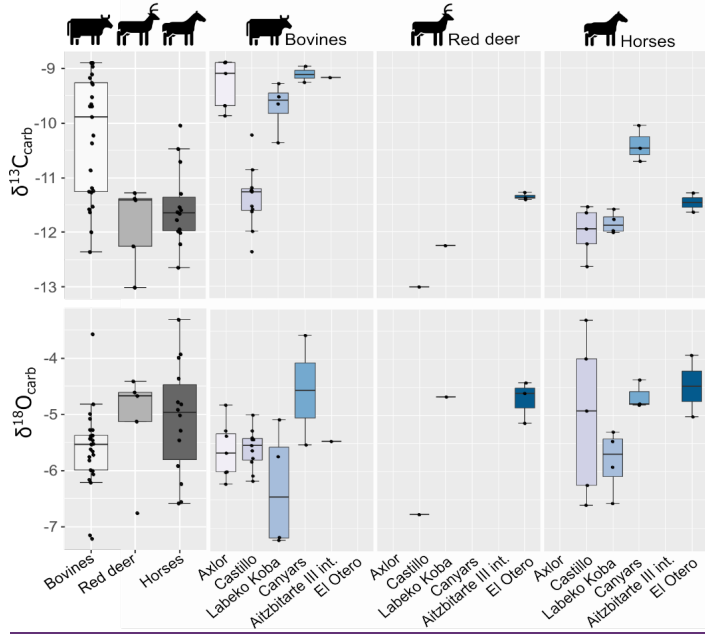
Figure 3. Distribution of mean carbon (δ¹³C$_{carb}$) and oxygen (δ¹⁸O$_{carb}$) isotopic values ~~from~~ of enamel carbonate ~~for~~ by species and archaeological site.

507
508
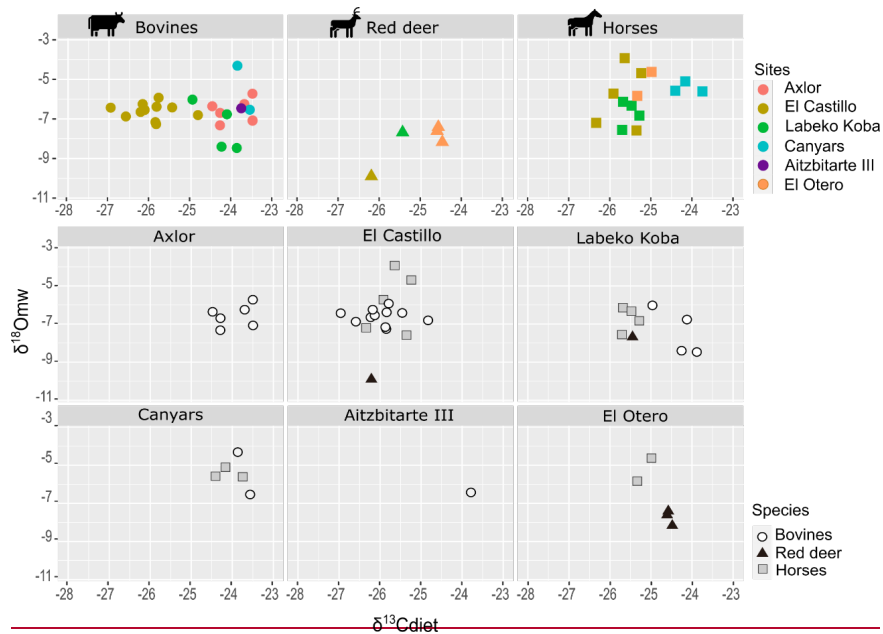
509
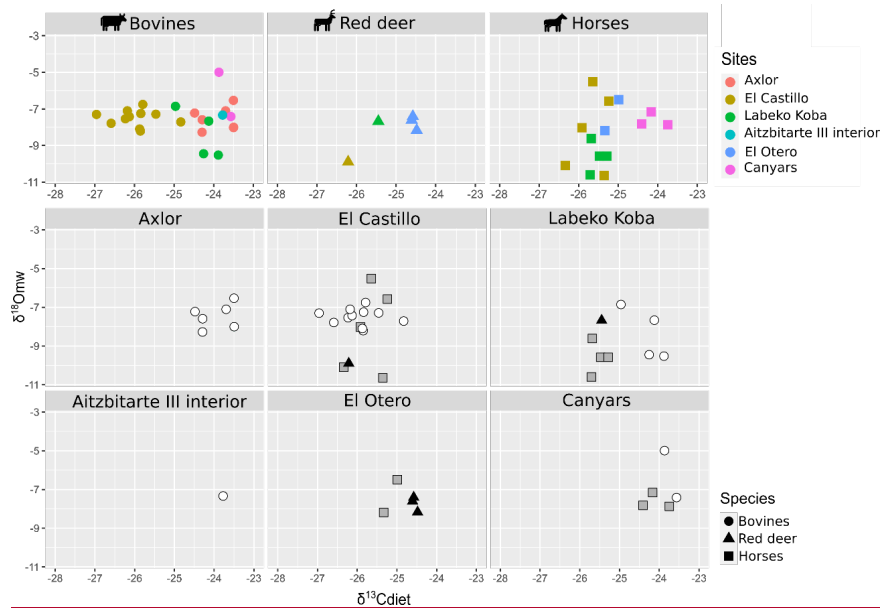
510

511 **Figure 4.** Biplot crossing δ13C from diet (δ13C$_{diet}$) and δ18O from meteoric waters (δ18O$_{mw}$) by species and archaeological sites.

512 **4.3 Labeko Koba (ca. 43.4-35.4 ka cal BP)**

513 This work includes ~~teeth of~~ bovines (n = 4), horses (n = 4), and red deer (n = 1) teeth from levels related to
514 Châtelperronian (IXb inf), ProtoAurignacian (VII), and Aurignacian (VI, V, and IV). Significant differentiation
515 in mean δ13C$_{carb}$ between bovines and horses is observed, with higher values between -9.3‰ and -10.4‰

in bovines ($\delta^{13}C_{diet}$ = -25 ~~23.8~~‰ to -23.8 ~~25~~‰) than equids, whose values extend from -12 ~~11.6~~‰ to -
~~12~~11.6‰ ($\delta^{13}C_{diet}$ = -25.8 ~~2~~‰ to -25.2 ~~8~~‰) (Fig. 3;). These horses' values are within the ranges observed
from this species in the region. Red deer have similar $\delta^{13}C_{carb}$ values to those of horses ($\delta^{13}C_{carb}$ = -12.3‰;
$\delta^{13}C_{diet}$ = -25.5‰). Mean $\delta^{18}O_{carb}$ values are similar between species from -7.2 ~~4.7~~‰ to -4.7 ~~7.2~~‰ ($\delta^{18}O_{mw}$ =
-8.5 ~~6.1~~‰ to -6.1 ~~8.5~~‰). However, bovines have a very high variation within mean $\delta^{18}O_{carb}$ values (2.1‰),
also reflected in the intratooth profiles. These $\delta^{18}O$ values are lower than in other Vasco-Cantabrian sites,
especially for two individuals in levels VII and V (Table 3). Differences in $\delta^{13}C_{diet}$ values between bovines
and horses result in isotopic niche differentiation between both species (Fig. 4). The red deer niche is placed
within the horses' niche. The evolution of ~~red~~ this ~~deer~~ niche over time cannot be evaluated by levels due to
the limited sample. Considering the isotopic compositions by levels (Fig. 5), both bovines and horses
experienced a slight increase in mean $\delta^{13}C_{diet}$ from levels IX_inf to IV ~~, that is~~, from Châtelperronian to
Aurignacian. Mean $\delta^{18}O_{mw}$ values of bovines decrease from VII to V, whereas ~~in the case of horses increase
from Xlinf to VI to then~~horses increase from Xlinf to VI to decrease from VI to IV.

Variability of $\delta^{13}C_{carb}$ values in intratooth profiles is slightly higher (0.1-0.7‰), especially in bovines (0.3-
0.9‰), with more oscillating profiles than generally flat profiles observed in horses and red deer (Appendix
C; D). Intratooth profiles ranges of $\delta^{18}O_{carb}$ are also larger within bovines (2-4‰) than in horses (1-2‰).
Inverse-modelled individual $\delta^{18}O_{carb}$ ranges oscillated between 5-8‰ and 2-4‰, respectively. Sinusoidal
curves are observed ~~both~~ in horses and bovines, but bovine profiles are noisier. The red deer has a ~~largn~~
extensive $\delta^{18}O_{carb}$ range (6.3‰) from summer peak to an incomplete winter thought. We detect an inverse
relation between $\delta^{13}C_{carb}$ and $\delta^{18}O_{carb}$ in some points of these individual profiles. MATs oscillated between
5.2 ~~7~~ºC and 11.4 ~~3.7~~ºC (MATAs = -5.6/+1.1ºC), with summer temperatures from 14.5 ~~3~~ºC to 27.3 ~~5~~ºC and
winter temperatures from 0 ~~1.9~~ºC to -4.9 ~~9.1~~ºC. MAPs extend between 248mm and 521mm, ~~which are
notable drier conditions~~notably drier than nowadays (MAPAs = -798/-525mm) (Table 4). Lower rainfall levels
and higher seasonal amplitudes are recorded along the sequence, especially in samples from the
ProtoAurignacian level VII. Relevant differences are noticed between MAPs estimated from bovines and
equids, the first providing more arid conditions.

4.4 Aitzbitarte III interior (ca. 30.8-26.9 ka cal BP)

A single bovine individual was analysed from Gravettian level V located in the inner part of the cave, ~~related
to Gravettian~~. It has a high mean $\delta^{13}C_{carb}$ (-9.2‰) considering the observed range in bovines from the Vasco-
Cantabrian region, whereas the $\delta^{18}O_{carb}$ mean value (-5.5‰) is inside the common $\delta^{18}O_{carb}$ variation
observed (Fig. 3). The mean $\delta^{13}C_{diet}$ value of -23.8‰ is comparable with Canyars and some individuals from
Axlor ~~,~~ but different from Labeko Koba and El Castillo individuals. The individual $\delta^{13}C_{carb}$ fluctuation is ~~small~~
slight (0.3‰) (Appendix C; D). These teeth show not quite sinusoidal profile shape in $\delta^{18}O_{carb}$, with an
intratooth range of around 2.2‰. Climatic information is extracted but may be considered cautiously due to
the profile shape and the limited sample size. From the inverse modelled mean $\delta^{18}O_{mw}$ value (-5.4‰), we
estimate a MAT of 13 ~~4.5~~ºC (MATA = -0.4 ~~+1.1~~ºC) with a summer temperature of 19.7 ~~5~~ºC and winter
temperature of -2.9 ~~4~~ºC. The MAP estimation reached 235mm (-1127mm to nowadays) (Table 4).

4.5 El Otero (ca. 19 ka cal BP)

Two equids and three cervids are included from level IV from El Otero, recently redate and chronologically
related to the Magdalenian ~~phase~~ (Marín-Arroyo et al., 2018). The mean $\delta^{13}C_{carb}$ values are close, between
-11.4 ~~3~~‰ and -11.3 ~~4~~‰ for red deer ($\delta^{13}C_{diet}$ = -24.4‰ and -24.6‰) and -11.6 ~~3~~‰ and -11.3 ~~6~~‰ for horse
($\delta^{13}C_{diet}$ = -25.3 ~~‰ and -~~25.3‰) (Fig. 3). These $\delta^{13}C$ values for both species are relatively high concerning
other studied samples, especially for cervids (around +1-2‰). Both species have higher $\delta^{18}O_{carb}$ values
concerning the common range of variation observed in the Vasco-Cantabria region, between -5 ~~3.9~~‰ and -
3.9 ~~5~~‰ for horses and between -5.1 ~~4.4~~‰ and -4.4 ~~5.1~~‰ for red deer. When values are transformed to $\delta^{13}C_{diet}$
and $\delta^{18}O_{mw}$, equids and cervids isotopic niches are separated (Fig. 4). All individuals show low- amplitude

562 δ¹³C_carb intratooth profiles (<0.3‰), but especially equids with an intratooth variation around 0.1‰ (Appendix

563 C; D). Equids and cervids show δ¹⁸O_carb sinusoidal profiles, with intratooth ranges between 1.4‰ and 2.4‰.

564 Climatic estimations are proposed only for equids, providing MATs estimations from ~~13.4~~8.8ºC to 12.~~6.7~~ºC

565 (MATAs = -4.9~~0.3ºC~~/-1~~+3~~ºC) and MAP between 400mm and 456mm (MAPAs = -755/-699mm) (Table 4). A

566 high-temperature seasonality can be seen, with summer temperatures between 19.~~7~~4ºC and 23.8~~2.5~~ºC and

567 winter temperatures from ~~0.7~~10.4ºC to -3.1~~7.2~~ºC.
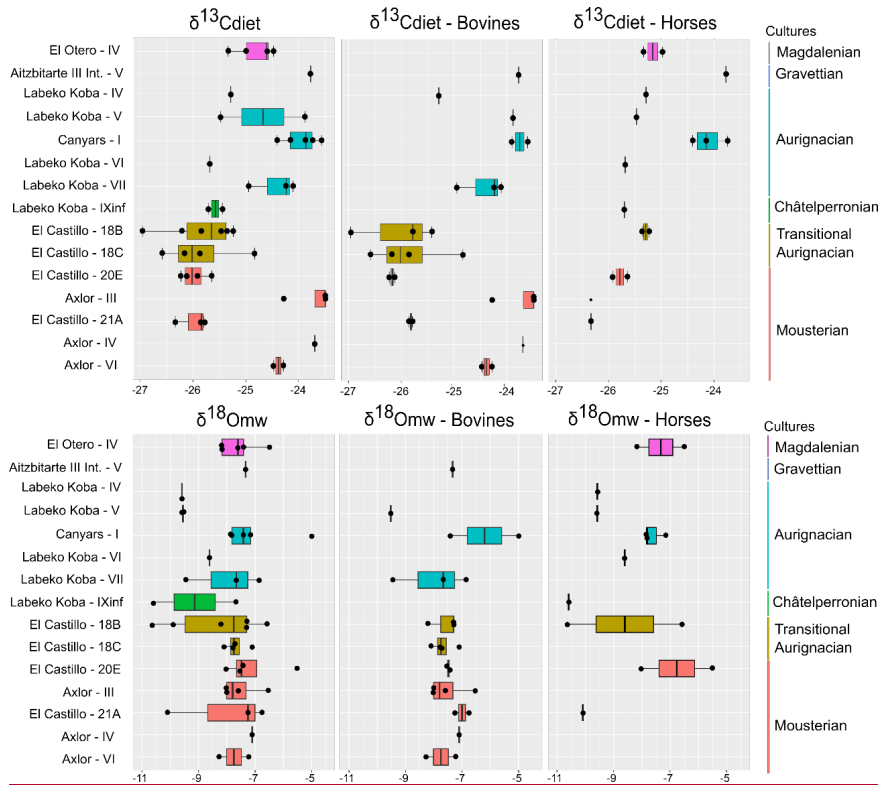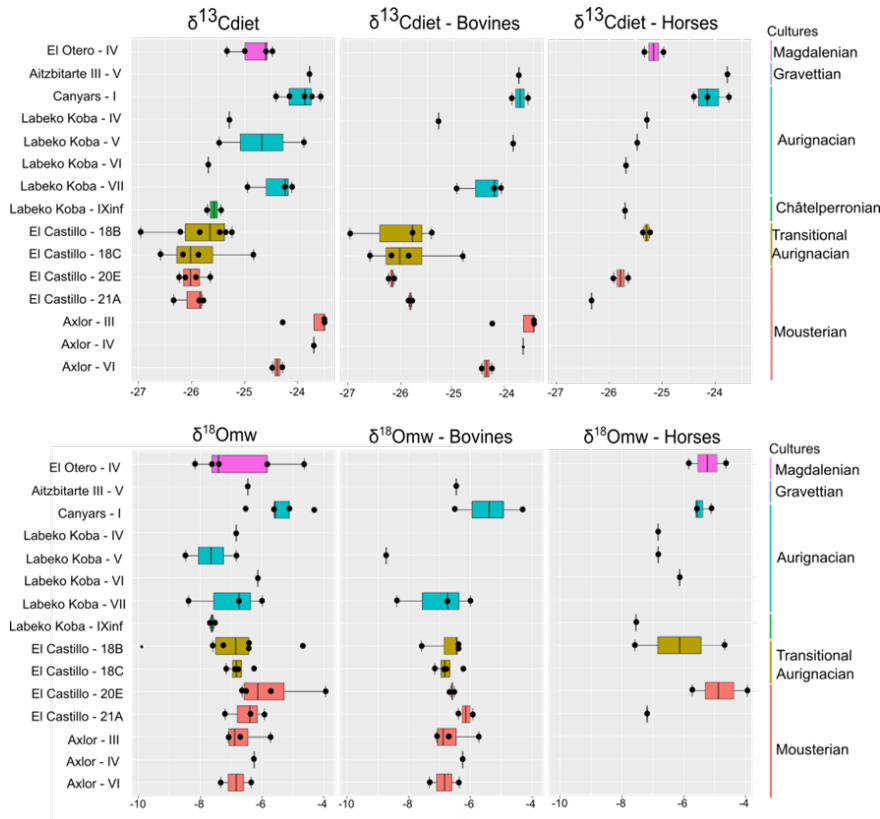
Figure 5. Evolution of δ13C in diet (δ13Cdiet) and δ18O in meteoric waters (δ18Omw) by archaeological levels in a diachronic order. From right to left: all species, including cervids, bovines and horses. Colours correspond to different chrono-cultures.

4.6 Canyars (ca. 40 ka cal BP)

From the archaeological ~~layer~~ level I at Canyars, corresponding to the Aurignacian, this work includes bovines (n = 2) and equids (n = 3) teeth. The mean δ13Ccarb values for bovines are between -9‰ to -9.3‰ (δ13Cdiet = -23.6‰ and -23.8‰), and for horses between -10‰ and -10.7‰ (δ13Cdiet = -23.7‰ and -24.4‰) (Fig.3). In this site, the δ13Ccarb values for horses are notably higher than ~~samples~~ in the Vasco-Cantabrian region (around +1-2‰) (Table 3). Both species have relatively high δ18Ocarb values, but they fall inside the range of variation observed in the Vasco-Cantabrian region, between ~~-5.5~~ -3.6‰ and ~~-5.5~~ -3.6‰ in bovines and between -4.~~84~~‰ and -4.~~48~~‰ in horses. ~~Different responses are seen in mean δ18O values between the two bovines, with one high mean value; ~~but~~but with close δ13C mean values.~~ Bovine and equid isotopic niches overlap (Fig. 4), but d~~i~~fferent responses are seen in mean δ18Omw values between the two bovines, with one high mean value but close δ13Cdiet mean values.

All individuals show flat δ13Ccarb intratooth profiles (<0.3‰ variation). Some individuals analysed do not show δ18Ocarb sinusoidal profiles, with intratooth profiles moderately flat and ranging from 1.1~~1~~‰ to 1.6~~6~~‰. We detect an inverse relation between δ13Ccarb and δ18Ocarb in some points of bovine individual isotopic profiles. MATs oscillated between ~~12.5~~9.8ºC and 1~~1~~4.~~9~~8ºC (MATAS = ~~-5.42~~-60.3ºC/-~~30.3~~2.6ºC), with summer temperatures from 1~~6.3~~5.2ºC to 2~~7.5~~.2ºC and winter temperatures from ~~7.3~~-0.5ºC to 1.~~8~~1.4ºC (Table 4).

588 MAPs extend between 211mm and 316mm (MAPAs = -431/-326mm). No substantial differences are noticed
589 in the estimations based on bovines and equids because mean δ¹³C diet values differed relatively little.

Site	Sample	Level	Species	MAT (ºC) Estimated	Relative	Summer (ºC) Estimated	Relative	Winter (ºC) Estimated	Relative	Seasonality (ºC)	MAP (mm) Estimated	Relative
Axlor	AXL59	III	*Bos/Bison* sp.	9.4	-2.8	17.6	-0.3	-3.9	-11.0	21.5	204	-843
	AXL60	III	*Bos/Bison* sp.	10.8	-1.4	22.7	4.7	4.8	-2.3	17.9	300	-747
	AXL65	III	*Bos/Bison* sp.	9.7	-2.5	22.7	4.8	-2.5	-9.6	25.2	204	-843
	AXL66	III	*Bos/Bison* sp.	12.6	0.4	22.8	4.8	-3.2	-10.3	26.0	204	-843
	AXL70	IV	*Bos/Bison* sp.	11.1	-1.1	21.9	3.9	-8.0	-15.1	29.9	227	-820
	AXL77	VI	*Bos/Bison* sp.	9.1	-3.1	20.4	2.5	-10.9	-17.9	31.3	300	-747
	AXL86	VI	*Bos/Bison* sp.	11.1	-1.1	25.9	8.0	3.1	-4.0	22.8	326	-721
El Castillo	CAS141	21A	*Bos/Bison* sp.	11.7	-1.7	24.2	5.6	-0.8	-9.9	25.1	546	-486
	CAS142	21A	*Bison priscus*	12.6	-0.9	19.6	1.0	3.1	-5.9	16.5	536	-496
	CAS143	21A	*Equus* sp.	5.7	-7.8	20.7	2.1	-5.6	-14.7	26.3	645	-387
	CAS60	20E	*Equus* sp.					1.6	-7.5		510	-522
	CAS61	20E	*Equus* sp.	9.7	-3.8	25.9	7.3	-4.1	-13.2	30.1	561	-471
	CAS139	20E	*Bos/Bison* sp.	11.2	-2.3	18.8	0.2	1.8	-7.3	17.0	622	-410
	CAS140	20E	*Bos/Bison* sp.	11.3	-2.1						602	-430
	CAS135	18C	*Bos/Bison* sp.			17.0	-1.6				551	-481
	CAS136	18C	*Bos/Bison* sp.	10.6	-2.9						699	-333
	CAS137	18C	*Bos/Bison* sp.					0.0	-9.1		376	-656
	CAS138	18C	*Bos/Bison* sp.	11.8	-1.7	18.3	-0.3	3.1	-6.0	15.3	612	-420
	CAS132	18B	*Bos/Bison* sp.	9.8	-3.6	26.3	7.6	-1.2	-10.3	27.5	548	-484
	CAS133	18B	*Bos/Bison* sp.					-0.1	-9.2		477	-555
	CAS134	18B	*Bos/Bison* sp.					0.8	-8.3		784	-248
	CAS58	18B	*Equus* sp.	4.6	-8.8	13.5	-5.1	-11.2	-20.3	24.7	460	-572
	CAS59	18B	*Equus* sp.	13.0	-0.5						440	-592
Labeko Koba	LAB38	IX inf	*Equus* sp.	5.2	-7.4	14.5	-4.1	-1.8	-9.1	16.2	521	-526
	LAB36	IV	*Equus* sp.	7.0	-5.6	16.3	-2.3	-2.4	-9.7	18.7	448	-599
	LAB42	V	*Equus* sp.	7.6	-5.0				-7.3		501	-546
	LAB69	V	*Bos primigenius*	6.3	-6.3	17.3	-1.2	-4.9	-12.2	22.2	248	-799
	LAB20	VI	*Equus* sp.	9.1	-3.5	15.7	-2.9	-0.9	-8.2	16.6	517	-530
	LAB53	VII	*Bos primigenius*	11.3	-1.3	27.3	8.7	-2.4	-9.7	29.7	278	-769
	LAB55	VII	*Bos primigenius*	11.4	-1.2	26.3	7.8	1.9	-5.4	24.4	397	-650
	LAB62	VII	*Bos/Bison* sp.	7.2	-5.4	20.6	2.1	-2.9	-10.2	23.5	295	-752
Canyars	CAN01	I	*Equus* sp.	9.8	-5.4	16.3	-5.9	1.7	-7.5	14.6	232	-410
	CAN02	I	*Equus ferus*	11.9	-3.3						284	-358
	CAN03	I	*Equus ferus*	10.4	-4.7	18.6	-3.6	-0.5	-9.7	19.1	316	-326
	CAN04	I	*Bos primigenius*	17.2	2.1	27.5	5.3				247	-395
	CAN05	I	*Bos primigenius*	11.3	-3.9	17.5	-4.7	1.8	-7.4	15.7	211	-431
Aitzbitarte III int	AITI10	V	*Bos/Bison* sp.	13.0	-0.4	19.7	0.7	-2.9	-11.4	22.6	235	-1127
Otero	OTE11	IV	*Equus* sp.	8.8	-4.9	19.7	0.9	-10.4	-19.8	30.1	456	-699
	OTE12	IV	*Equus* sp.	12.6	-1.0	23.8	5.0	-3.1	-12.5	26.8	400	-755

590

Site	Sample	Level	Species	MAT (°C)		Summer (°C)		Winter (°C)		MAP (mm)	
				Estimated	Relative	Estimated	Relative	Estimated	Relative	Estimated	Relative
Axlor	AXL59	III	*Bos/Bison* sp.	10.5	-1.7	15.4	-2.6	0.9	-6.2	204	-843
Axlor	AXL60	III	*Bos/Bison* sp.	12.0	-0.2	20.4	2.5	10.8	3.7	300	-747
Axlor	AXL65	III	*Bos/Bison* sp.	10.8	-1.4	20.5	2.5	2.5	-4.6	204	-843
Axlor	AXL66	III	*Bos/Bison* sp.	14.0	1.8	20.5	2.5	1.7	-5.4	204	-843
Axlor	AXL70	IV	*Bos/Bison* sp.	12.4	0.2	19.6	1.6	-3.8	-10.9	227	-820
Axlor	AXL77	VI	*Bos/Bison* sp.	10.1	-2.1	18.2	0.2	-7.0	-14.1	300	-747
Axlor	AXL86	VI	*Bos/Bison* sp.	12.3	0.2	23.7	5.7	8.9	1.8	326	-721
El Castillo	CAS141	21A	*Bos/Bison* sp.	13.1	-0.4	22.0	3.3	4.4	-4.7	546	-486
El Castillo	CAS142	21A	*Bison priscus*	14.0	0.5	17.3	-1.3	8.9	-0.2	536	-496
El Castillo	CAS143	21A	*Equus* sp.	10.8	-2.7	20.1	1.5	5.0	-4.1	645	-387
El Castillo	CAS60	20E	*Equus* sp.					11.3	2.3	510	-522
El Castillo	CAS61	20E	*Equus* sp.	14.2	0.7	24.2	5.6	6.3	-2.8	561	-471
El Castillo	CAS139	20E	*Bos/Bison* sp.	12.5	-1.0	16.5	-2.1	7.3	-1.8	622	-410
El Castillo	CAS140	20E	*Bos/Bison* sp.	12.6	-0.9					602	-430
El Castillo	CAS135	18C	*Bos/Bison* sp.			14.8	-3.8			551	-481
El Castillo	CAS136	18C	*Bos/Bison* sp.	11.8	-1.6					699	-333
El Castillo	CAS137	18C	*Bos/Bison* sp.					5.4	-3.7	376	-656
El Castillo	CAS138	18C	*Bos/Bison* sp.	13.1	-0.4	16.1	-2.5	8.8	-0.3	612	-420
El Castillo	CAS132	18B	*Bos/Bison* sp.	11.0	-2.5	24.0	5.4	4.0	-5.1	548	-484
El Castillo	CAS133	18B	*Bos/Bison* sp.					5.2	-3.9	477	-555
El Castillo	CAS134	18B	*Bos/Bison* sp.					6.2	-2.9	784	-248
El Castillo	CAS58	18B	*Equus* sp.	9.9	-3.6	14.5	-4.1	0.1	-9.0	460	-572
El Castillo	CAS59	18B	*Equus* sp.	17.0	3.6					440	-592
Labeko Koba	LAB38	IXinf	*Equus* sp.	10.3	-2.3	15.3	-3.3	8.4	1.1	521	-526
Labeko Koba	LAB36	IV	*Equus* sp.	11.9	-0.7	16.7	-1.9	7.8	0.5	448	-599
Labeko Koba	LAB42	V	*Equus* sp.	13.1	0.5					501	-546
Labeko Koba	LAB69	V	*Bos primigenius*	7.0	-5.6	15.1	-3.5	-0.2	-7.6	248	-799
Labeko Koba	LAB20	VI	*Equus* sp.	13.7	1.1	16.2	-2.3	9.1	1.8	517	-530
Labeko Koba	LAB53	VII	*Bos primigenius*	12.5	-0.1	25.0	6.4	2.6	-4.7	278	-769
Labeko Koba	LAB55	VII	*Bos primigenius*	12.7	0.1	24.0	5.4	7.5	0.2	397	-650
Labeko Koba	LAB62	VII	*Bos/Bison* sp.	8.1	-4.5	18.3	-0.2	2.1	-5.3	295	-752
Canyars	CAN01	I	*Equus* sp.	14.3	-0.9	16.7	-5.5	11.4	2.2	232	-410
Canyars	CAN02	I	*Equus ferus*							284	-358
Canyars	CAN03	I	*Equus ferus*	14.8	-0.3	18.5	-3.7	9.5	0.3	316	-326
Canyars	CAN04	I	*Bos primigenius*			25.2	3.0			247	-395
Canyars	CAN05	I	*Bos primigenius*	12.5	-2.6	15.2	-7.0	7.3	-1.8	211	-431
Aitzbitarte III	AITI10	V	*Bos/Bison* sp.	14.5	1.1	17.5	-1.5	2.1	-6.5	235	-1127
Otero	OTE11	IV	*Equus* sp.	13.4	-0.3	19.4	0.6	0.8	-8.6	456	-699
Otero	OTE12	IV	*Equus* sp.	16.7	3.0	22.5	3.7	7.2	-2.2	400	-755

Table 4. Summary of paleoclimatic estimations, based on $\delta^{18}O$ for temperatures (Mean Annual Temperatures, MAT; summer; winter) and in $\delta^{13}C$ for precipitation (Mean Annual Precipitations, MAP). ~~SOnly~~ teeth with validated seasonal curves are included in the ~~su~~mmer and winter temperature estimation~~s~~ were obtained from teeth with clear seasonal profiles after modelling, ~~teeth peaks and trough~~while MAT was averaged between summer and winter before mode~~lling profiles. For In~~ cases ~~some of profiles with an unclear seasonal shapes, MATs were~~ was deduced from the original average of all points of the teeth~~profiles with an unclear seasonal shape, MAT was deduced from the original average of all teeth points~~ without a seasonal profile (values marked in red~~italics~~). Mean ~~Details on teeth selection are presented in Appendix B.~~error associated to temperature estimations is 5.1±0.6 (see details in Appendix B). Seasonality is calculated as the temperature difference between summer and winter.

5. Discussion

5.1 Diet and ecological niches: carbon ratios

Carbon isotopic ratios are valuable indicators for discerning past animal diets ~~based on the ecosystems or parts of the ecosystem where the animals most frequently foraged. They are also~~, partially influenced by the physiology of the animal. Considering species trends in the studied sites, bovines have generally higher mean $\delta^{13}C_{carb}$ values (from -12.4‰ ~~-8.9‰~~ to ~~-12.4‰~~ -8.9‰) than horses (from -12.6‰ ~~-11.3‰~~ to -11.3‰ ~~-12.6‰~~), whereas the red deer fall within the horses'' range (from -13‰ ~~-11.3‰~~ to -11.3‰ ~~-13‰~~). ~~In Canyars,~~ ~~I~~In the Mediterranean site of Canyars~~area~~, bovines also show higher mean $\delta^{13}C_{carb}$ values (-9‰ to -9.3‰) compared to horses (-10.7‰ to -10.7‰). These differentiated isotopic ranges for equids and bovines can be potentially linked to feeding behaviour~~, but~~. Still, these species are expected to present different basal $\delta^{13}C_{carb}$ driven ~~not only by their feeding behavior but also by their~~by their feeding behaviour and distinct physiological characteristics~~considering their physiology and diet~~. Bovines, being ruminants, have been suggested in previous studies to exhibit higher $\delta^{13}C_{carb}$ values due to increased methane production (Cerling

and Harris, 1999; Tejada-Lara et al., 2018). Therefore, transforming $\delta^{13}C_{carb}$ to $\delta^{13}C_{diet}$ values using species-specific equations is crucial to mitigate the species-specific impact, particularly when comparing ruminants and non-ruminants. Bovines report $\delta^{13}C_{diet}$ values between -27.5‰ ~~-23.5‰~~ and -23.5‰ ~~-27.5‰~~ and horses between -26‰ ~~-25‰~~ and -26‰ ~~-25‰~~. These carbon compositions are typical of animals feeding on C3 plants (commonly accepted range between -34‰ and -23‰), as can be expected from high-latitude ecosystems during the Pleistocene (Cerling and Harris, 1999; Bocherens, 2003; Drucker, 2022).

Environmental factors such as light exposure, water stress, temperature fluctuations, salinity, and atmospheric CO_2 changes can influence variations in $\delta^{13}C$ values in a diet primarily based on C3 plants (Kohn, 2010; Bocherens, 2003). Typically, $\delta^{13}C_{diet}$ values below -27‰ ($\delta^{13}C_{carb}$ = -13‰) are associated with animals feeding on C3 vegetation found in closed forested environments, whereas $\delta^{13}C_{diet}$ values between -27‰ and -23‰ are linked to C3 open landscapes, which could include grasslands and steppe areas (Bocherens, 2003). The relatively high $\delta^{13}C_{diet}$ observed here points to animals predominantly feeding in open environments. The canopy effect, characterised by a depletion in ^{13}C isotopes due to dense tree cover, seems unlikely among the analysed samples since none of the individuals reported $\delta^{13}C_{diet}$ below the ~~common~~ standard cut-off of -27‰ (van der Merwe, 1991; Kohn, 2010; Drucker et al., 2008). Therefore, in general terms, open mosaic landscapes, ranging from light forests to meadows and grasslands, can be inferred for northwestern Iberia. Given the generally higher $\delta^{13}C_{diet}$ values reported by bovines, it is likely that they were foraging in more open environments than horses and can be considered predominantly grazers. Particularly, bovines from El Castillo exhibit distinct feeding behaviour compared to other Vasco-Cantabrian sites, as evidenced by their lower $\delta^{13}C_{diet}$ values, indicating a potential preference for browsing and feeding in closer environments, possibly in lightly forested areas. Both extinct aurochs (*Bos primigenius*) and steppe bison (*Bison priscus*) are usually classified as grass-dominant mix-feeders during the Pleistocene, although it should be noted that modern European bison (*Bison bonasus*) could include browsing in their diet (Rivals et al., 2022). For aurochs, a browse-dominated mixed feeding behaviour is also frequently described.

The $\delta^{13}C_{diet}$ range in equids also indicates feeding in open environments ~~as well~~, suggesting a general mixed-feeding pattern for the Vasco-Cantabrian region. However, individuals from the ~~the~~ northeastern ~~Mediterranean~~ Iberia ~~area~~ are likely grazing in more open environments, as evidenced by their notably higher $\delta^{13}C_{diet}$ values compared to the Vasco-Cantabrian region (+1-2‰). ~~It is important to evaluate if other factors are contributing to lower $\delta^{13}C_{diet}$ values in horses~~ Evaluating if other factors contribute to lower $\delta^{13}C_{diet}$ values in horses is critical. In the case of equid ~~samples~~ from the Vasco-Cantabrian region, it should be considered that they have been pretreated with a combination of NaClO and acetic acid, which could potentially affect the isotopic values. Samples after organic removal pretreatment can potentially show either higher or lower $\delta^{13}C$ values and higher $\delta^{18}O$ values based on previous experiments (Pellegrini and Snoeck, 2016; Snoeck and Pellegrini, 2015), with $\delta^{13}C$ values generally varying below 0.3‰. Based on the observation that horses in the Vasco-Cantabrian region present lower $\delta^{13}C_{carb}$ values compared to bovines but similar mean $\delta^{18}O_{carb}$ value ranges, the influence of the pre-treatment on our samples is deemed to be limited.

Furthermore, the high variability in $\delta^{18}O_{carb}$ values at El Castillo and Labeko Koba does not correlate with a significant variation in $\delta^{13}C_{carb}$ values. Based on dental wear and stable isotopes analysis, Middle and Late Pleistocene horses (*Equus ferus*) were primarily grazers, although some rare cases have been reported as mixed feeders or browsers, such as at Igue des Rameaux ~~amont or~~ and Schöningen (Kuitems et al., 2015; Rivals et al., 2009, 2015; Uzunidis, 2020). Horse populations from northern and eastern Europe were found to be browsers or mixed feeders, while those from the Mediterranean region tend to be grazers (Rivals et al., 2022).

658 Finally, the few cervids included in this study exhibit δ¹³C_diet values that frequently overlap with ~~those of~~
659 horses, indicating a mixed feeding behaviour that varies from more closed environments in El Castillo to
660 more open habitats in El Otero. During the Pleistocene, the red deer (*Cervus elaphus*) exhibit a flexible,
661 mixed-feeding ~~behavior~~behaviour, consuming leaves, shrubs, forbs, grass, and sedges, similar to their
662 present-day counterparts (Rivals et al., 2022; Merceron et al., 2021). Today, t~~T~~his species inhabits diverse
663 habitats ranging from steppes to closed temperate forests.

5.2 Seasonality, mobility and water acquisition: oxygen ratios and intratooth profiles

665 Average values of δ¹⁸O_carb in Vasco-Cantabrian individuals extend between -7.2‰ ~~-3.3‰~~ and -3.3‰ ~~-7.2‰~~
666 (Table 3). Even if no clear species patterns in δ¹⁸O_carb are observed, in general, bovines present slightly
667 lower δ¹⁸O_carb values from -7.2‰ ~~-4.8‰~~ to 4.8‰ ~~-7.2‰~~ than other species; horses have a ~~large~~ significant
668 variation from -6.6‰ ~~-3.3‰~~ to -3.3‰ ~~-6.6‰~~ and red deer from -6.8‰ to -4.4‰ ~~to -6.8‰~~. In Canyars, both
669 species have relatively high δ¹⁸O_carb values that fall inside the variation range observed in the Vasco-
670 Cantabrian region, between -5.5‰ and -3.6‰ ~~and -5.5‰~~ in bovines and between -4.8‰ -4.4‰ and -4.4‰ ~~-~~
671 ~~4.8‰~~ in horses. Each species show~~s~~ different δ¹⁸O_carb intratooth ranges, with bovines between 1‰ and 3‰,
672 ~~equids~~ horses mostly around 1.5%, and ~~cervids~~ red deer from 1‰ to 6‰ presenting the higher ranges~~, from~~
673 ~~1‰ to 6‰~~ (Table 3; Appendix C). After applying inverse modelling to correct the dampening effect (Passey
674 et al., 2005b)~~(Passey et al., 2005)~~, the majority of teeth increase the δ¹⁸O_carb intratooth range, between 3‰
675 and 8‰ for bovines and 2‰ and 7‰ for horses (Appendix D). Most bovines from Axlor and Labeko Koba
676 and ~~equids~~ horses from El Castillo and El Otero exhibit well-defined sinusoidal profiles in their δ¹⁸O_carb and
677 large intratooth individual ranges~~values~~, related to the predominant consumption of water sources that
678 reflect~~s~~ seasonal ~~indicating potential seasonal~~ fluctuations between ~~δ¹⁸O values of environmental~~ summer
679 and winter ~~meteoric waters.~~ A~~, a~~lthough not all samples consistently follow this pattern ~~consistently. c.~~
680 ~~Certain~~specific intratooth profiles, particularly those from bovines in El Castillo and Canyars, exhibit sharp
681 profiles with narrow ranges (<1.5‰). This phenomenon was previously reported in the region in preliminary
682 studies conducted at the sites of El Castillo (Jones et al., 2019) and in the Magdalenian levels of El Mirón
683 cave (Geiling, 2020).

684 Non-sinusoidal profiles observed in the data can be attributed to various factors, including ~~issues related to~~
685 ~~sample techniques and preservation~~sample techniques and preservation issues and the inherent variability
686 in the original isotopic signal. Factors related to sampling and methods can be connected to 1) the sampling
687 process (e.g. too deep or too distant sampling grooves); 2) the imprecision of the mass spectrometer
688 measurements; 3) uncontrolled effects of samples pretreatments; 4) diagenetic alterations affecting the
689 carbonate fraction. However, it must be noted that technical reasons, whether related to sampling or
690 pretreatment, do not appear to impact the obtained results significantly. First, this study reproduces the
691 same intratooth sampling methods that previously yielded reliable results in similar research (e.g., Pederzani
692 et al., 2023, 2021a). Second, non-significant alterations in intratooth profiles of pretreated horse samples
693 (El Castillo, Labeko Koba, Otero) are noticed in comparison to untreated bovid samples (Appendix C). Some
694 bovid samples ~~are equally showing these non-sinusoidal profiles~~show these non-sinusoidal profiles equally.
695 In sites where both species are analysed, no correlation is observed between δ¹⁸O_carb and δ¹³C_carb. In tooth
696 enamel, diagenetic alterations are generally less pronounced than in bone due to its ~~larger~~ higher mineral
697 content. However, carbonates within tooth enamel can be more susceptible to diagenesis and
698 recrystallisation compared to the phosphate fraction, which contains a ~~larger~~ more extensive reservoir of
699 oxygen and stronger oxygen bonds (Zazzo et al., 2004; Chenery et al., 2012; Bryant et al., 1996). The
700 carbonate content in our samples, ranging from 3.9% to 8.9%, is similar to the proportion found in modern
701 tooth enamel, suggesting no immediate indication of diagenetic alteration. Diagenesis can also be evaluated
702 by comparing the isotopic values of the carbonate and phosphate fractions in a sample, as there is a
703 predictable difference between them. However, phosphate fraction measurements were still unavailable in

704 our study, except ~~in~~at ~~the site of~~ Axlor (Pederzani et al., 2023) ~~–~~where good preservation was attested.
705 Additionally, in the case of diagenetic alteration, we would expect specimens from the same archaeological
706 levels to be affected similarly, which is not the case.

707 Based on these arguments, it is suggested that the non-sinusoidal $\delta^{18}O_{carb}$ signal observed in some
708 individuals may not be attributed to poor preservation; instead, it ~~is~~ likely ~~attributed to the preservation~~
709 ~~of~~reflects the original isotopic signature from water input, which appears to be non-seasonal. Several factors
710 can explain why some teeth do not reflect a ~~clea~~n evident seasonal fluctuation, which could be related to
711 animals' mobility ~~or,~~ the isotopic composition of the water sources, and seasonal buffering within those water
712 sources (Pederzani and Britton, 2019). The main factors considered in our study are 1) the high mobility of
713 the animals analysed among ecosystems with different isotopic baselines due to large migrations; 2) the
714 inland-coastal or short altitudinal movements through the region, which lead to the acquisition of water from
715 sources with different isotopic signal; and 3) the acquisition of water from sources with no clear seasonal
716 signal, such as large bodies of water, rivers, groundwaters, or meltwaters. Furthermore, variability between
717 species and within the same species, even within populations living in the same habitat, is also possible.
718 This can be attributed to multiple factors, from minor differences in foraging and drinking ~~behavior~~behaviour
719 to slight metabolic and physiological variations, including body size, metabolic rate, breathing rate, moisture
720 content of food, and f~~a~~eces, among others (Kohn, 1996; Magozzi et al., 2019; Hoppe et al., 2004).

721 Analyses of nitrogen and sulphur stable isotopes on ungulate bone collagen from Axlor, El Castillo and
722 Labeko Koba (Jones et al., 2019, 2018; Pederzani et al., 2023) have already revealed large variation ranges
723 linked to the existence of several microenvironments just in a few kilometres within the Vasco-Cantabria
724 region. Long migrations and long hunting distances cannot solely explain these ~~diversified~~ diverse values,
725 because of the range of species involved and their likely small-scale movements. In our study, the minimal
726 $\delta^{13}C_{carb}$ intratooth variation within individuals (<1‰) indicates limited seasonal changes in their feeding
727 ~~behavior~~behaviour that influenced the carbon isotopic composition (Appendix C). Therefore, considering the
728 diverse topography of the Vasco-Cantabrian, characterized by steep ~~diverse orography with perpendicular~~
729 valleys ~~that~~ connecting the Cantabrian Cordillera with the Atlantic Ocean through rivers over short distances
730 (30-50 km), the availability in the past of a wide range of water sources in small areas seems highly likely.
731 Certain drinking ~~behavior~~behaviours can influence $\delta^{18}O$, as animals may acquire water from various
732 sources, with small streams better reflecting seasonal isotopic oscillations than large lakes or evaporating
733 ponds (see synthesis in Pederzani and Britton, 2019). Systematic consumption of highly buffered water
734 sources can significantly attenuate the final recorded signal. Furthermore, rivers in the region frequently
735 contain meltwater from snow during the winter-spring months, and water springs ~~are also common~~.

736

737 **5.3 Regional trends and ecological niches**

738 This study provides valuable insights despite the limited sample size at each archaeological level. It
739 establishes a baseline of isotopic values for northern Iberia, allowing for the evaluation of regional trends.
740 In the northwest, in the Vasco-Cantabrian region, the $\delta^{13}C_{carb}$ values obtained oscillated between -13‰ -
741 8.9‰ ~~and -13‰~~ -8.9‰ and between -7.2‰ -3.3‰ ~~and -3.3‰~~-7.2‰ in the case of $\delta^{18}O_{carb}$ values. These
742 values are within the range expected, considering previous regional studies in ungulates (Lécuyer et al.,
743 2021; Pederzani et al., 2023; Jones et al., 2019; Carvalho et al., 2022). Although oxygen variability trends
744 are less precise, the main factor distinguishing the observed changes over time is the variation of carbon
745 isotopic composition among species and regions. The combination of mean $\delta^{13}C_{diet}$ and $\delta^{18}O_{mw}$ values (Fig.
746 4; 5) accentuates disparities in ecological niche overlap between horses and bovines, whereas cervids and
747 horses frequently exhibit shared ecological niches. The dissimilarities between bovines and horses could

be attributed to shifts in feeding ~~behavior~~behaviour, which may be accompanied by ecological and environmental changes, either independently or in parallel.

~~Upon evaluating the entire dataset by sites~~Comparing the entire dataset and across all sites, the consistently lower $\delta^{13}C_{diet}$ values in horses compared to bovids throughout time suggest both animals inhabited open landscapes, with bovines exhibiting a grazer preference while horses show a mix-feeding diet. Only in the Middle-to-Upper Paleolithic transition 18B and 18C levels of El Castillo, an exception is observed with lower $\delta^{13}C_{diet}$ values in bovines, linked to a higher browser input due to a higher habitat in closer environments, such as open forests, similar to those inhabited by the horses. This generates a niche overlapping between horses and bovines, most likely reflecting stable conditions that could support both species in similar ecosystems. Contrarily, in the Châtelperronian and early Aurignacian levels from Labeko Koba, a clear differentiation between horses and bovines is observed, mainly in $\delta^{13}C_{diet}$ values, highlighting the occupation of different ~~landscapes~~parts of the landscape by both species. This ~~niche fractionation~~spatially-driven niche separation between species could result from resource competition derived from an unstable climatic period, where species needed to specialise to adapt to the changing conditions. Notable changes are also observed in the $\delta^{18}O_{carb}$ values from Labeko Koba compared to the older El Castillo and Axlor sites, with bovines exhibiting a higher fluctuation range and the lowest values in the region. These trends are consistent with values observed on bone collagen from previous studies in the ~~studied~~se sites. During the Middle-to-Upper Paleolithic transition in the region, by comparing horses and red deer, a decrease in mean $\delta^{13}C$ (from -21~~0~~‰ to -20~~4~~‰) and $\delta^{15}N$ values (from 2.5~~6~~‰ to 6~~2.5~~‰) in bone collagen was observed in contrast to stable red deer mean $\delta^{13}C$ (Fernández-García et al., 2023; Jones et al., 2018, 2019). This decrease was ~~already~~previously interpreted as niche fractionation, derived from an opening landscape, that drove equids into low-quality pastures compared to cervids. Pollen evidence in the region suggests a prevalence of steppe vegetation and low tree cover for the Châtelperronian and Aurignacian (Iriarte-Chiapusso, 2000).

In the same period, Canyars in the northeastern ~~at the Mediterranean site~~area of ~~Canyars,~~ higher mean $\delta^{13}C_{diet}$ are observed in both species (between -23.6‰ and -24.4‰), indicating a preference for more open landscapes by bovines and equids. The indication of open areas could be linked to the arid climatic conditions associated with the Heinrich Event 4, which coincides with the formation of the ~~archaeological~~ studied level ~~at Canyars~~. This predominance of open areas coincides with the presence of typical steppe herbivore species, such as *Equus hydruntinus* and *Coelodonta antiquitatis*, the microfauna and pollen taxa, and the data offered by the use-wear analysis on ungulate remains identified at the site (Daura et al., 2013; López-García et al., 2022; Rivals et al., 2017).

Aridity is a plausible explanation for the higher niche partitioning observed in Labeko Koba and the higher $\delta^{13}C_{diet}$ values found in Canyars for both species ~~in~~during the Aurignacian ~~levels~~. The $\delta^{13}C_{diet}$ results of bovines from Aitzbitarte III interior during the Gravettian are consistent with the trend observed in Labeko Koba, ~~and~~where previous studies have already suggested this time to be notably arid and cold (Arrizabalaga et al., 2010). Finally, in the Magdalenian level of El Otero, higher $\delta^{13}C_{diet}$ values resemble those observed in Canyars. However, this time, carbon values are related to niche partitioning between horses and red deer. In contrast, higher $\delta^{18}O_{mw}$ values might indicate warmer conditions but are still associated with open landscapes in the Vasco-Cantabrian area.

5.4 Late Pleistocene climatic evolution in Northern Iberia

Carbon and oxygen isotopes were used to estimate quantitative parameters related to past temperatures and precipitation. In the case of oxygen isotopic compositions, an evaluation of environmental water composition can be addressed before approaching temperature estimations. When transformed to $\delta^{18}O_{mw}$ using species-adapted correlations and correcting bias in sea water $\delta^{18}O_{mw}$, the summer $\delta^{18}O_{mw}$ values obtained from the modelled teeth range from -8~~4.9~~-1‰ to -~~12.2~~4.9‰, while the winter values range from -

793 $17.0.16$ 4.2‰ to -$8.94.2$ 10.6‰. These values ~~agree~~ can be tentatively compared with the current trends
794 observed in δ^{18}O$_{mw}$ range ~~of values~~ recorded by the IAEA station (IAEA/ WMO, 2022) in Santander (from -
795 3.5‰ in summer to -6.6‰ in winter) and in Barcelona (from -2.2‰ in summer to -6.3‰ in winter) and the
796 OIPC (Bowen, 2022) estimations for studied locations (from -1‰ to -9‰) (Appendix B). As observed in the
797 present, Canyars exhibit ~~higher~~ mean annual δ^{18}O$_{mw}$ values ~~of~~ around -$8.25.5$‰, which ~~are close~~ is lower ~~to~~
798 than the current δ^{18}O$_{mw}$ estimated for this location (-5.4‰) but higher than Labeko Koba mean annual δ^{18}O$_{mw}$
799 (-9.5‰). This raises the question of whether ~~suggests that~~ the baseline δ^{18}O$_{mw}$ differences between
800 Canyars and the other sites can be ~~primarily~~ attributed to ~~the~~ Mediterranean influence rather than the
801 Atlantic, assuming equivalent air circulation patterns and moisture sources ~~in the past as~~ experienced in the
802 past as in the present ~~-~~ (Moreno et al., 2021; Araguas-Araguas and Diaz Teijeiro, 2005; García-Alix et al.,
803 2021)~~and considering IAEA stations~~.

804 ~~Considering this work's climatic reconstruction,~~As indicated by the climate reconstructed here, temperatures
805 ~~are~~ were ~~generally~~ colder ~~and precipitation levels were~~are ~~notably lower in the Late Pleistocene period in~~
806 ~~this region than~~, and precipitation levels were notably lower in the Late Pleistocene period in this region than
807 they are nowadays (Table 4; Appendix B). From 80,~~000~~ to 57 46 ka,~~000 cal~~ BP, in the Mousterian levels of
808 ~~the~~ Axlor ~~site~~, temperatures ~~we~~are ~~generally~~ sligthly colder than today, ~~but there is no clear trend observed~~
809 ~~throughout the sequence,~~ but ~~with~~ older levels ~~showing~~ showed higher differences between summer and
810 winter temperatures. Rainfall estimations ~~in these levels~~ exhibit an unusual arid pattern, possibly affected
811 by bovines ~~mainly~~ predominantly feeding in open areas at that time. ~~Indeed, even if the species' impact has~~
812 ~~been corrected through δ^{13}C$_{diet}$ estimation (Tejada-Lara et al., 2018), t~~This aligns ~~study observed that~~ with
813 the impact ~~the influence~~ of basal feeding ~~behavior~~behaviour on rainfall estimations, as previously advised
814 by Lécuyer et al. (2021) ~~should be considered~~. In this case, it is not possible to isolate the effect of diet from
815 environmental interference, but previous studies have highlighted stable climatic conditions ~~for~~at the site
816 (Pederzani et al., 2023). Climatic reconstruction, relying on a compilation of lake sediments from northern
817 Iberia (Moreno et al., 2012) suggests that from late MIS4 to 60 ka cal BP, cold but relatively humid conditions
818 predominated, with drier conditions emerging later. Additionally, stalagmites from the Ejulve cave in the
819 Iberian range indicate a dry climate until 65.5 ka BP, preceding HE6, followed by more humid conditions
820 afterwards (Pérez-Mejías et al., 2019).

821

822 During the late Middle ~~to Upper~~ Paleolithic ~~transition~~ and early Aurignacian occupations, the observed~~a~~ shift
823 in the niche configuration of species ~~is observed,~~ suggests potential ~~indicating~~ climatic perturbations. There
824 is a decreasing trend in temperatures from the Transitional Aurignacian levels in El Castillo (18C and 18B;
825 ca. 47 ka,~~000~~ cal BP) to the Châtelperronian (Xinf; 42.1 ka,~~100~~ cal BP) and Early Aurignacian (VII-V; from
826 41,~~136~~.1 to 37.88,~~570~~ ka cal BP) levels in Labeko Koba. Lower mean annual and winter temperatures are
827 particularly notable at~~in~~ El Castillo and ~~, while~~ Labeko Koba. Labeko Koba levels exhibit~~s~~ high seasonal
828 amplitude, especially ~~in~~ at level VII. Additionally, there is a slight decrease in rainfall and increased
829 fluctuations from the Transitional Aurignacian levels from~~in~~ El Castillo (18B-18C) to the Aurignacian levels
830 in Labeko Koba (VII-V). Previous studies in the northern Iberian region underlined an environmental and
831 ecological shift after GS13/HE5, from 48,~~000~~ to 44 ka,~~000~~ cal BP, based on a progressive trend to colder
832 temperatures, aridity increase, and open environmental conditions, matching with the late Neanderthal
833 occupations, followed by a population hiatus before the arrival of Anatomically Modern Humans (Vidal-
834 Cordasco et al., 2022; Fernández-García et al., 2023). This episode coincides with the ~~region's maximum~~
835 ~~extension of the glaciers~~maximum extent of glaciers in this region, as recorded in Lake Enol and Vega
836 Comeya and ~~the~~an ~~associated a~~ significant decrease in plant biomass and herbivore abundance around
837 44 to 38 ka BP (Jiménez-Sánchez et al., 2013; Ruiz-Fernández et al., 2022; Ballesteros et al., 2020; Vidal-
838 Cordasco et al 2022). Moreover, previous isotopic analyses in the region pointed to some ecological

839 alterations considering perturbations observed in the δ¹³C and δ¹⁵N of bone collagen (Jones et al., 2019,

840 2018). This tendency of increased aridity aligns with observations made in regional lake sediments from

841 northern Iberia between 60 and 23.5 ka cal BP, marked by abrupt climate changes associated with HE

842 (Moreno et al., 2012). Supporting this, the marine core MD04-2845 in the northern margin of Iberia reveals

843 a decline in the Atlantic forest and an expansion of steppe and cold grasses from 47 to 40 ka BP (Fourcade

844 et al., 2022).

845 When comparing the environmental reconstruction of the Aurignacian period ~~in~~ between the Vasco-

846 Cantabrian ~~region~~ (levels V-IV from Labeko Koba) and the ~~Mediterranean~~ northeastern region (Layer I from

847 Canyars), which are synchronous to HE4 (39~~,000~~ ka BP), thi~~s~~e study reveals notably lower rainfall levels for

848 the ~~northeastern site~~latter~~Mediterranean~~. This is~~,~~ ~~consistent with implied by~~due to the feeding

849 ~~behavior~~behaviour ~~described for~~ observed in animals ~~mainly feeding,~~ mainly in open areas. ~~But~~However,

850 t~~T~~hese drier conditions ~~align~~align with the ~~unique~~ specific climatic ~~expectations~~ conditions expected for this

851 period and support previous findings ~~suggesting~~revealing aridity and the predominance of open landscapes

852 (Rivals et al., 2017; Daura et al., 2013). The temperature data indicates that, at Canyars, colder conditions

853 were experienced, ~~colder conditions,~~ especially during the winter season, compared to the present.

854 However, in comparison to Labeko Koba, Canyars experienced warmer conditions. As explained earlier, the

855 Mediterranean basin had consistently higher temperatures, even during colder periods. ~~In line with this,~~

856 ~~previous studies conducted at the site have also highlighted the~~This is consistent with the persistence of

857 Mediterranean open forests in the surroundings, as indicated by other studies (Rivals et al., 2017; López-

858 García et al., 2013). Continuous natural records are lacking in the northeastern Iberian margin. However,

859 the inland stalagmite record from Ejulve Cave (Pérez-Mejías et al., 2019) and the sedimentary lacustrine

860 sequence of Cañizar de Villarquemado (González-Sampériz et al., 2020) have identified the most arid

861 intervals during HE5 and HE4. These periods were characterized by steppe vegetation expansions, followed

862 by deciduous woodland expansion. To the south, the Padul sequence agrees with cold and dry conditions

863 alternating with forest recovery (Camuera et al., 2019), as documented in the Alborean Sea (Martrat et al.,

864 2004).

865 Finally, the sites Aitzbitarte III interior (26.7~~,692~~ ka cal BP) and El Otero (19.~~303~~ ka cal BP) provided

866 valuable climatic insights into the Vasco-Cantabrian region during the Upper Paleolithic, specifically during

867 the Gravettian and Magdalenian ~~periods~~, respectively. Considering previous research in the region, the

868 climatic trend reported for the Aurignacian, characterised by colder and more arid conditions, was expected

869 to continue or even intensify during the Gravettian ~~period~~ (Fernández-García et al., 2023; Garcia-

870 Ibaibarriaga et al., 2019b; Lécuyer et al., 2021). Both sites ~~exhibit~~ indicate lower precipitation ~~levels~~

871 ~~compared to the present~~than ~~presently found in these area, indicating significant aridity, supported by~~

872 ~~the~~with ungulates ~~animals predominantly feeding in open landscapes predominantly~~today in this area,

873 indicating significant aridity, with ungulates feeding predominantly in open landscapes. ~~Finally,~~However,

874 E~~E~~l Otero's higher mean annual temperatures ~~recorded in the Magdalenian horses respect to other sites~~

875 within the Vasco-Cantabrian, are consistent with a climatic amelioration following the Last Glacial Maximum

876 (Jones et al., 2021). MIS 2 is marked by the most extreme glacial conditions, as indicated by NGRIP and

877 marine cores in Iberian margins (Sánchez Goñi et al., 2002; Martrat et al., 2004). However, other regional

878 proxies, such as lake sediment and the stalagmite sequence in Pindal Cave (Moreno et al., 2010), suggest

879 a complex and highly variable climate during MIS 2. These proxies identify the coldest and most arid period

880 within MIS 2 as the interval from 18 to 14 ka cal BP, rather than the global Last Glacial Maximum (23 to 19

881 ka cal BP).

882 **5. Conclusions**

883 This study provides a ~~comprehensive~~ detailed analysis of the temporal evolution of the environment and

884 climatic conditions in northern Iberia, spanning from the ~~late~~ Middle Paleolithic to the late Upper Paleolithic,

this is from the GS21 to the GS2, ranging from ca. 80 ka BP~~,000~~ to 1~~9~~75 ka cal~~,000 cal~~ BP. In the Vasco-Cantabrian region, the results reveal a heterogeneous open mosaic landscape ~~characterised by an open mosaic~~, ranging from light forest to meadows and grasslands. This landscape reconstruction is primarily ~~influenced~~ inferred by the feeding locations of the studied animals and, consequently, related to the ecosystems where hominins captured them. Despite shifts in niche configuration observed between equids and bovines, both species typically foragi~~e~~ng in open areas, with bovines showing a higher preference for grazing. Only in El Castillo, during the late Mousterian and the Transitional Aurignacian levels, bovines show unusually low $\delta^{13}C_{diet}$ related to higher browsing and overlapping with horse isotopic niche. This might indicate a slightly closed mosaic landscape that could sustain both species. In contrast, only horses from Canyars exhibit a preference for grazing ~~behavior~~behaviour.

Stable climatic conditions are described for Mousterian in Axlor and El Castillo levels from 80,~~000~~ to 50,~~000~~ ka cal BP. However, some elements indicate ~~some~~ environmental perturbations initiated during the Transitional Aurignacian levels ~~from~~of El Castillo, around 4~~8~~6-43 ka ~~,000~~ BP and after HE5/GS13. After GS12 (44.~~2~~00-43.~~3~~ ka~~00~~ BP), horses and bovines are potentially occupying different ecological niches during the Châtelperronian and early Aurignacian levels ~~from~~ of Labeko Koba, pointing to a species' environmental specialisation, which can be a consequence of competition for food resources during an unstable ecological period. The climatic estimations indicate a temperature shift during this period, with a slight decrease in temperatures and evidence of fluctuations in rainfall ~~from the Transitional Aurignacian levels of El Castillo to the early Aurignacian levels of Labeko Koba~~. Previous environmental studies on the region have underlined ecological stress and ~~aridity increase~~increasing aridity from around 42.5~~8~~~~,000~~ ka cal BP, ~~which could sustain this biological impoverishment~~which may relate to a ~~wi~~broader ecosystem decline. When comparing the environmental conditions during the Aurignacian period in the ~~Mediterranean~~northeast (Canyars) and the ~~Vasco-Cantabrian region~~northwest (Labeko Koba), the ~~Mediterranean are~~first~~a~~ had higher baseline temperatures but also experienced higher aridity. Animals continued to feed on open landscapes during the Gravettian and Magdalenian levels in the Vasco-Cantabrian region, represented by Aitzbitarte III interior and El Otero ~~sites~~. However, there is evidence of a temperature recovery after the LGM at the El Otero ~~site~~.

~~For the first time, a regional approach is obtained by measuring δ13C and δ18O in enamel carbonates from ungulates teeth for the late Middle and Upper Paleolithic in northern Iberia. Stable isotope composition of oxygen and carbon from ungulate teeth has provided valuable insights into the diet and foraging areas of bovines, equids, and cervids. These results,~~The results presented here, derived from ~~this~~the first extensive sampling in the Vasco-Cantabrian, establish the basis of future stable isotopic studies on ~~teeth~~ faunal tooth enamel in ~~this region~~Iberia~~, which were slightly explored in the region~~. Despite the uncertainties inherent in this work, ~~derived from using the carbonate enamel fraction for paleoclimatic estimations,~~ both $\delta^{18}O$ and $\delta^{13}C$ contributed to the regional climatic characterisation, including the estimation of temperatures and precipitations, as well as the seasonality range between summer and winter. The potential influence of pretreatment effects and uncontrolled diagenetic alterations on the enamel carbonate fraction has been assessed. However, ~~further investigation~~complementary diagenetic~~al~~ test, using new techniques like $\delta^{18}O_{phos}$ ~~phosphate analysis~~ and FTIR analyses are ~~needed~~advised ~~in further works in the region,~~ to gain more insights into sample preservation. Ongoing sulphur, hydrogen and strontium studies will provide additional information on the ~~animal~~ mobility patterns of animals ~~that were~~ hunted by Late Pleistocene ~~consumed for~~hominins and, therefore, will help better understand~~us better understand~~ the ~~landscape exploitation~~ecological and environmental context ~~of~~occupied by ~~the~~ ~~through this transition between late~~ Neanderthal and ~~early~~ modern human~~s groups~~~~habitations in this region~~ and their landscape use in this particular region. Finally, a ~~A~~ more comprehensive characterisation of the baseline oxygen values ~~in the region~~would also enhance the environmental interpretation of the existing data.

Appendices

Appendices A, C and D are presented after bibliography. Raw data is ~~found~~ presented in Appendix B. ~~All~~ available at https://github.com/ERC-Subsilience/Ungulate_enamel-carbonate

Code availability

R code used to perform plots, error calculations, and models in this manuscript can be accessed at GitHub (https://github.com/ERC-Subsilience/Ungulate_enamel-carbonate).

Data availability

The available datasets used for this article are provided in the supplementary materials (Appendix A-D).

Author contribution

A.B.M.-A. got the funding and designed the research. A.B.M.-A and M.F.-G. get the permissions for sampling in the regional museums. M.F.-G., K.B, and S.P. defined the analysis strategy. M.F.-G. analysed the data and wrote the manuscript with critical inputs from A.B.M.-A., K.B, and S.P. J.M.G., L.A., M.F.-G., and A.C. M.F.-G., L.A., J.M.G., and A.C. achieved the teeth sampling and lab sample preparation. J.D. and M.S. are responsible for the excavations in Canyars and contribute to the discussion. All the authors revised and commented on the manuscript.

Competing interests

The contact author has declared that none of the authors has any competing interests.

Acknowledgements

We acknowledge the Museo de Arqueología y Prehistoria de Cantabria (MUPAC), the Consejería de Educación, Cultura y Deporte del Gobierno de Cantabria, the Museo de Arqueología de Bizkaia (Arkeologi Museoa) and the Centro de Colecciones Patrimoniales de la Diputación Foral de Gipuzkoa (Gordailua) -— Provincial Government of Guipuzkoa"s Heritage Collection Centre for the access to the archaeological collections. We do appreciate the work achieved by H. Reade during the initial sampling, pretreatment and analyses of samples undertaken at the University of Cantabria and Cambridge. We want to thank the two anonymous referees for their valuable comments, which significantly improved the quality of the paper.

Financial support

Funding for Vasco-Cantabria research was obtained from the Spanish Ministry of Science and Innovation (PID2021-125818NB-I00, HAR2017-84997-P and HAR2012-33956) and the European Research Council under the European Union"s Horizon 2020 Research and Innovation Programme (grant agreement number 818299; SUBSILIENCE project). Research for Canyars was funded by the Spanish Ministry of Science and Innovation (PID2020-113960GB-100), Departament de Cultura de la Generalitat de Catalunya (CLT/2022/ARQ001SOLC/128) and AGAUR (SGR2021-00337). M.F.-G. is supported by the APOSTD postdoctoral fellowship (CIAPOS/2022/081/AEI/10.13039/501100011033), funded by the Generalitat Valenciana and the European Social Fund. S.P. was supported by a German Academy of Sciences Leopoldina postdoctoral fellowship (LPDS 2021-13) during this project. M.S. benefited from financial support from a Ramon y Cajal postdoctoral grant (RYC2021-032999-I) funded by the Spanish Ministry of Science and Innovation and the European Union-NextGenerationEU.

References

Allué, E., Martínez-Moreno, J., Roy, M., Benito-Calvo, A., and Mora, R.: Montane pine forests in NE Iberia during MIS 3 and MIS 2. A study based on new anthracological evidence from Cova Gran (Santa Linya, Iberian Pre-Pyrenees), Review of

Palaeobotany and Palynology, 258, 62–72, https://doi.org/10.1016/j.revpalbo.2018.06.012, 2018.

Álvarez-Lao, D. J., Rivals, F., Sánchez-Hernández, C., Blasco, R., and Rosell, J.: Ungulates from Teixoneres Cave (Moià, Barcelona, Spain): Presence of cold-adapted elements in NE Iberia during the MIS 3, Palaeogeography, Palaeoclimatology, Palaeoecology, 466, 287–302, https://doi.org/10.1016/j.palaeo.2016.11.040, 2017.

Ambrose, S. H. and Norr, L.: Experimental Evidence for the Relationship of the Carbon Isotope Ratios of Whole Diet and Dietary Protein to Those of Bone Collagen and Carbonate, in: Prehistoric Human Bone, Springer Berlin Heidelberg, Berlin, Heidelberg, 1–37, https://doi.org/10.1007/978-3-662-02894-0_1, 1993.

Araguas-Araguas, L. J. and Diaz Teijeiro, M. F.: Isotope composition of precipitation and water vapour in the Iberian Peninsula. First results of the Spanish Network of Isotopes in Precipitation, in: Isotopic Composition of Precipitation in the Mediterranean Basin in Relation to Air Circulation Patterns and Climate. IAEA-TECDOC-1453, Vienna, 173–190, 2005.

Balasse, M., Ambrose, S. H., Smith, A. B., and Price, T. D.: The Seasonal Mobility Model for Prehistoric Herders in the South-western Cape of South Africa Assessed by Isotopic Analysis of Sheep Tooth Enamel, Journal of Archaeological Science, 29, 917–932, https://doi.org/10.1006/jasc.2001.0787, 2002.

Ballesteros, D., Álvarez-Vena, A., Monod-Del Dago, M., Rodríguez-Rodríguez, L., Sanjurjo-Sánchez, J., Álvarez-Lao, D., Pérez-Mejías, C., Valenzuela, P., DeFelipe, I., Laplana, C., Cheng, H., and Jiménez-Sánchez, M.: Paleoenvironmental evolution of Picos de Europa (Spain) during marine isotopic stages 5c to 3 combining glacial reconstruction, cave sedimentology and paleontological findings, Quaternary Science Reviews, 248, 106581, https://doi.org/10.1016/j.quascirev.2020.106581, 2020.

Bendrey, R., Vella, D., Zazzo, A., Balasse, M., and Lepetz, S.: Exponentially decreasing tooth growth rate in horse teeth: implications for isotopic analyses, Archaeometry, 57, 1104–1124, https://doi.org/10.1111/arcm.12151, 2015.

Blumenthal, S. A., Cerling, T. E., Chritz, K. L., Bromage, T. G., Kozdon, R., and Valley, J. W.: Stable isotope time-series in mammalian teeth: In situ $\delta^{18}O$ from the innermost enamel layer, Geochimica et Cosmochimica Acta, 124, 223–236, https://doi.org/10.1016/j.gca.2013.09.032, 2014.

Blumenthal, S. A., Cerling, T. E., Smiley, T. M., Badgley, C. E., and Plummer, T. W.: Isotopic records of climate seasonality in equid teeth, Geochimica et Cosmochimica Acta, 260, 329–348, https://doi.org/10.1016/j.gca.2019.06.037, 2019.

Bocherens, H.: Isotopic biogeochemistry and the paleoecology of the mammoth steppe fauna, Deinsea, 91, 57–76, 2003.

Brand, W. A., Coplen, T. B., Vogl, J., Rosner, M., and Prohaska, T.: Assessment of international reference materials for isotope-ratio analysis (IUPAC Technical Report), Pure and Applied Chemistry, 86, 425–467, https://doi.org/10.1515/pac-2013-1023, 2014.

Britton, K., Pederzani, S., Kindler, L., Roebroeks, W., Gaudzinski-Windheuser, S., Richards, M. P., and Tütken, T.: Oxygen isotope analysis of Equus teeth evidences early Eemian and early Weichselian palaeotemperatures at the Middle Palaeolithic site of Neumark-Nord 2, Saxony-Anhalt, Germany, Quaternary Science Reviews, 226, 106029, https://doi.org/10.1016/j.quascirev.2019.106029, 2019.

Bryant, J. D., Luz, B., and Froelich, P. N.: Oxygen isotopic composition of fossil horse tooth phosphate as a record of continental paleoclimate, Palaeogeography, Palaeoclimatology, Palaeoecology, 107, 303–316, https://doi.org/10.1016/0031-0182(94)90102-3, 1994.

Bryant, J. D., Koch, P. L., Froelich, P. N., Showers, W. J., and Genna, B. J.: Oxygen isotope partitioning between phosphate and carbonate in mammalian apatite, Geochimica et Cosmochimica Acta, 60, 5145–5148, https://doi.org/10.1016/S0016-7037(96)00308-0, 1996.

Camuera, J., Jiménez-Moreno, G., Ramos-Román, M. J., García-Alix, A., Toney, J. L., Anderson, R. S., Jiménez-Espejo, F., Bright, J., Webster, C., Yanes, Y., and Carrión, J. S.: Vegetation and climate changes during the last two glacial-interglacial cycles in the western Mediterranean: A new long pollen record from Padul (southern Iberian Peninsula), Quaternary Science Reviews, 205, 86–105, https://doi.org/10.1016/j.quascirev.2018.12.013, 2019.

Carvalho, M., Jones, E. L., Ellis, M. G., Cascalheira, J., Bicho, N., Meiggs, D., Benedetti, M., Friedl, L., and Haws, J.: Neanderthal palaeoecology in the late Middle Palaeolithic of western Iberia: a stable isotope analysis of ungulate teeth from Lapa do Picareiro (Portugal), Journal of Quaternary Science, 37, 300–319, https://doi.org/10.1002/jqs.3363, 2022.

Cascalheira, J., Alcaraz-Castaño, M., Alcolea-González, J., de Andrés-Herrero, M., Arrizabalaga, A., Aura Tortosa, J. E., Garcia-Ibaibarriaga, N., and Iriarte-Chiapusso, M.-J.: Paleoenvironments and human adaptations during the Last Glacial Maximum in the Iberian Peninsula: A review, Quaternary International, 581–582, 28–51, https://doi.org/10.1016/j.quaint.2020.08.005, 2021.

Cerling, T. E. and Harris, J. M.: Carbon isotope fractionation between diet and bioapatite in ungulate mammals and implications for ecological and paleoecological studies, Oecologia, 120, 347–363, https://doi.org/10.1007/s004420050868, 1999.

Chappell, J. and Shackleton, N. J.: Oxygen isotopes and sea level, Nature, 324, 137–140, https://doi.org/10.1038/324137a0, 1986.

Chesson, L. A., Beasley, M. M., Bartelink, E. J., Jans, M. M. E., and Berg, G. E.: Using bone bioapatite yield for quality control in stable isotope analysis applications, Journal of Archaeological Science: Reports, 35, 102749, https://doi.org/10.1016/j.jasrep.2020.102749, 2021.

Chillón, B. S., Alberdi, M. T., Leone, G., Bonadonna, F. P., Stenni, B., and Longinelli, A.: Oxygen isotopic composition of fossil equid tooth and bone phosphate: an archive of difficult interpretation, Palaeogeography, Palaeoclimatology, Palaeoecology, 107, 317–328, https://doi.org/10.1016/0031-0182(94)90103-1, 1994.

Coplen, T. B.: Guidelines and recommended terms for expression of stable-isotope-ratio and gas-ratio measurement results, Rapid Communications in Mass Spectrometry, 25, 2538–2560, https://doi.org/10.1002/rcm.5129, 2011.

Coplen, T. B., Kendall, C., and Hopple, J.: Comparison of stable isotope reference samples, Nature, 302, 236–238, https://doi.org/10.1038/302236a0, 1983.

D'Angela, D. and Longinelli, A.: Oxygen isotopes in living mammal's bone phosphate: Further results, Chemical Geology, 86, 75–82, 1990.

D'Errico, F. and Sánchez Goñi, M. F.: Neandertal extinction and the millennial scale climatic variability of OIS 3, Quaternary Science Reviews, 22, 769–788, https://doi.org/10.1016/S0277-3791(03)00009-X, 2003.

1038 Dansgaard, W.: Stable isotopes in precipitation, Tellus, XVI, 436–468, 1964.
1039 Daura, J., Sanz, M., García, N., Allué, E., Vaquero, M., Fierro, E., Carrión, J. S., López-García, J. M., Blain, H. a., Sánchez-Marco,
1040   a., Valls, C., Albert, R. M., Fornós, J. J., Julià, R., Fullola, J. M., and Zilhão, J.: Terrasses de la Riera dels Canyars (Gavà,
1041   Barcelona): The landscape of Heinrich Stadial 4 north of the " Ebro frontier" and implications for modern human dispersal
1042   into Iberia, Quaternary Science Reviews, 60, 26–48, https://doi.org/10.1016/j.quascirev.2012.10.042, 2013.
1043 Delgado Huertas, A., Iacumin, P., Stenni, B., Sánchez Chillón, B., and Longinelli, A.: Oxygen isotope variations of phosphate in
1044   mammalian bone and tooth enamel, Geochimica et Cosmochimica Acta, 59, 4299–4305, https://doi.org/10.1016/0016-
1045   7037(95)00286-9, 1995.
1046 Drucker, D. G.: The Isotopic Ecology of the Mammoth Steppe, Annual Review of Earth and Planetary Sciences, 50, 395–418,
1047   https://doi.org/10.1146/annurev-earth-100821-081832, 2022.
1048 Drucker, D. G., Bridault, A., Hobson, K. A., Szuma, E., and Bocherens, H.: Can carbon-13 in large herbivores reflect the canopy
1049   effect in temperate and boreal ecosystems? Evidence from modern and ancient ungulates, Palaeogeography,
1050   Palaeoclimatology, Palaeoecology, 266, 69–82, https://doi.org/10.1016/j.palaeo.2008.03.020, 2008.
1051 Eggleston, S., Schmitt, J., Bereiter, B., Schneider, R., and Fischer, H.: Evolution of the stable carbon isotope composition of
1052   atmospheric CO2 over the last glacial cycle, Paleoceanography and Paleoclimatology, 31, 434–452,
1053   https://doi.org/10.1002/2015PA002874, 2016.
1054 Fagoaga, A.: Aproximacion34iomineraliz paleoclimática y paisajística durante el MIS3 a partir del estudio de los micromamíferos
1055   del yacimiento de El Salt (Alcoi, Alicante)., Universidad de Burgos, 34 pp., 2014.
1056 Fernández-García, M., Royer, A., López-García, J. M., Bennàsar, M., Goedert, J., Fourel, F., Julien, M.-A., Bañuls-Cardona, S.,
1057   Rodríguez-Hidalgo, A., Vallverdú, J., and Lécuyer, C.: Unravelling the oxygen isotope signal (δ18O) of rodent teeth from
1058   northeastern Iberia, and implications for past climate reconstructions, Quaternary Science Reviews, 218, 107–121,
1059   https://doi.org/10.1016/j.quascirev.2019.04.035, 2019.
1060 Fernández-García, M., López-García, J. M., Royer, A., Lécuyer, C., Allué, E., Burjachs, F., Chacón, M. G., Saladié, P., Vallverdú,
1061   J., and Carbonell, E.: Combined palaeoecological methods using small-mammal assemblages to decipher environmental
1062   context of a long-term Neanderthal settlement in northeastern Iberia, Quaternary Science Reviews, 228, 106072,
1063   https://doi.org/10.1016/j.quascirev.2019.106072, 2020.
1064 Fernández-García, M., Vidal-Cordasco, M., Jones, J. R., and Marín-Arroyo, A. B.: Reassessing palaeoenvironmental conditions
1065   during the Middle to Upper Palaeolithic transition in the Cantabrian region (Southwestern Europe), Quaternary Science
1066   Reviews, 301, 107928, https://doi.org/10.1016/j.quascirev.2022.107928, 2023.
1067 Fick, S. E. and Hijmans, R. J.: WorldClim 2: new 1-km spatial resolution climate surfaces for global land areas, International Journal
1068   of Climatology, 37, 4302–4315, https://doi.org/10.1002/joc.5086, 2017.
1069 Finlayson, C. and Carrión, J. S.: Rapid ecological turnover and its impact on Neanderthal and other human populations, Trends in
1070   Ecology and Evolution, 22, 213–222, https://doi.org/10.1016/j.tree.2007.02.001, 2007.
1071 Fourcade, T., Sánchez Goñi, M. F., Lahaye, C., Rossignol, L., and Philippe, A.: Environmental changes in SW France during the
1072   Middle to Upper Paleolithic transition from the pollen analysis of an eastern North Atlantic deep-sea core, Quaternary
1073   Research, 1–18, https://doi.org/10.1017/qua.2022.21, 2022.
1074 France, C. A. M., Sugiyama, N., and Aguayo, E.: Establishing a preservation index for bone, dentin, and enamel bioapatite mineral
1075   using ATR-FTIR, Journal of Archaeological Science: Reports, 33, 102551, https://doi.org/10.1016/j.jasrep.2020.102551,
1076   2020.
1077 García-Alix, A., Camuera, J., Ramos-Román, M. J., Toney, J. L., Sachse, D., Schefuß, E., Jiménez-Moreno, G., Jiménez-Espejo,
1078   F. J., López-Avilés, A., Anderson, R. S., and Yanes, Y.: Paleohydrological dynamics in the Western Mediterranean during
1079   the last glacial cycle, Global and Planetary Change, 202, 103527, https://doi.org/10.1016/j.gloplacha.2021.103527, 2021.
1080 Garcia-Ibaibarriaga, N., Suárez-Bilbao, A., Iriarte-Chiapusso, M. J., Arrizabalaga, A., and Murelaga, X.: Palaeoenvironmental
1081   dynamics in the Cantabrian Region during Greenland stadial 2 approached through pollen and micromammal records:
1082   State of the art, Quaternary International, 506, 14–24, https://doi.org/10.1016/j.quaint.2018.12.004, 2019a.
1083 Garcia-Ibaibarriaga, N., Suárez-Bilbao, A., Iriarte-Chiapusso, M. J., Arrizabalaga, A., and Murelaga, X.: Palaeoenvironmental
1084   dynamics in the Cantabrian Region during Greenland stadial 2 approached through pollen and micromammal records:
1085   State of the art, Quaternary International, 506, 14–24, https://doi.org/10.1016/j.quaint.2018.12.004, 2019b.
1086 Geiling, J. M.: Human Ecodynamics in the Late Upper Pleistocene of Northern Spain: An Archeozoological Study of Ungulate
1087   Remains from the Lower Magdalenian and other Periods in El Mirón Cave (Cantabria), Universidad de Cantabria, 734
1088   pp., 2020.
1089 González-Sampériz, P., Gil-Romera, G., García-Prieto, E., Aranbarri, J., Moreno, A., Morellón, M., Sevilla-Callejo, M., Leunda, M.,
1090   Santos, L., Franco-Múgica, F., Andrade, A., Carrión, J. S., and Valero-Garcés, B. L.: Strong continentality and effective
1091   moisture drove unforeseen vegetation dynamics since the last interglacial at inland Mediterranean areas: The
1092   Villarquemado sequence in NE Iberia, Quaternary Science Reviews, 242,
1093   https://doi.org/10.1016/j.quascirev.2020.106425, 2020.
1094 Hoppe, K. A.: Correlation between the oxygen isotope ratio of North American bison teeth and local waters: Implication for
1095   paleoclimatic reconstructions, Earth and Planetary Science Letters, 244, 408–417,
1096   https://doi.org/10.1016/j.epsl.2006.01.062, 2006.
1097 Hoppe, K. A., Stover, S. M., Pascoe, J. R., and Amundson, R.: Tooth enamel biomineralization in extant horses: implications for
1098   isotopic microsampling, Palaeogeography, Palaeoclimatology, Palaeoecology, 206, 355–365,
1099   https://doi.org/10.1016/j.palaeo.2004.01.012, 2004.
1100 Iacumin, P., Bocherens, H., Mariotti, A., and Longinelli, A.: Oxygen isotope analyses of co-existing carbonate and phosphate in
1101   biogenic apatite: a way to monitor diagenetic alteration of bone phosphate?, Earth and Planetary Science Letters, 142,
1102   1–6, https://doi.org/10.1016/0012-821X(96)00093-3, 1996.
1103 Iriarte-Chiapusso, M. J.: El entorno vegetal del yacimiento paleolítico de Labeko Koba (Arrasate, País Vasco): análisis polínico.,
1104   Labeko Koba (País Vasco). Hienas y humanos en los albores del Paleolítico superior., Munibe, 89–106, 2000.

Jiménez-Sánchez, M., Rodríguez-Rodríguez, L., García-Ruiz, J. M., Domínguez-Cuesta, M. J., Farias, P., Valero-Garcés, B., Moreno, A., Rico, M., and Valcárcel, M.: A review of glacial geomorphology and chronology in northern Spain: Timing and regional variability during the last glacial cycle, Geomorphology, 196, 50–64, https://doi.org/10.1016/j.geomorph.2012.06.009, 2013.

Jones, J. R., Richards, M. P., Straus, L. G., Reade, H., Altuna, J., Mariezkurrena, K., and Marín-Arroyo, A. B.: Changing environments during the Middle-Upper Palaeolithic transition in the eastern Cantabrian Region (Spain): direct evidence from stable isotope studies on ungulate bones, Scientific Reports, 8, 14842, https://doi.org/10.1038/s41598-018-32493-0, 2018.

Jones, J. R., Richards, M. P., Reade, H., Bernaldo de Quirós, F., and Marín-Arroyo, A. B.: Multi-Isotope investigations of ungulate bones and teeth from El Castillo and Covalejos caves (Cantabria, Spain): Implications for paleoenvironment reconstructions across the Middle-Upper Palaeolithic transition, Journal of Archaeological Science: Reports, 23, 1029–1042, https://doi.org/10.1016/j.jasrep.2018.04.014, 2019.

Jones, J. R., Marín-Arroyo, A. B., Corchón Rodríguez, M. S., and Richards, M. P.: After the Last Glacial Maximum in the refugium of northern Iberia: Environmental shifts, demographic pressure and changing economic strategies at Las Caldas Cave (Asturias, Spain), Quaternary Science Reviews, 262, 106931, https://doi.org/10.1016/j.quascirev.2021.106931, 2021.

Klein, K., Weniger, G.-C., Ludwig, P., Stepanek, C., Zhang, X., Wegener, C., and Shao, Y.: Assessing climatic impact on transition from Neanderthal to anatomically modern human population on Iberian Peninsula: a macroscopic perspective, Science Bulletin, 68, 1176–1186, https://doi.org/10.1016/j.scib.2023.04.025, 2023.

Kohn, M. J.: Predicting animal δ18O: Accounting for diet and physiological adaptation, Geochimica et Cosmochimica Acta, 60, 4811–4829, https://doi.org/10.1016/S0016-7037(96)00240-2, 1996.

Kohn, M. J.: Comment: Tooth Enamel Mineralization in Ungulates: Implications for Recovering a Primary Isotopic Time-Series, by B. H. Passey and T. E. Cerling (2002), Geochimica et Cosmochimica Acta, 68, 403–405, https://doi.org/10.1016/S0016-7037(03)00443-5, 2004.

Kohn, M. J.: Carbon isotope compositions of terrestrial C3 plants as indicators of (paleo)ecology and (paleo)climate, Proceedings of the National Academy of Sciences, 107, 19691–19695, https://doi.org/10.1073/pnas.1004933107, 2010.

Lécuyer, C., Hillaire-Marcel, C., Burke, A., Julien, M.-A., and Hélie, J.-F.: Temperature and precipitation regime in LGM human refugia of southwestern Europe inferred from δ13C and δ18O of large mammal remains, Quaternary Science Reviews, 255, 106796, https://doi.org/10.1016/j.quascirev.2021.106796, 2021.

Leuenberger, M., Siegenthaler, U., and Langway, C.: Carbon isotope composition of atmospheric CO2 during the last ice age from an Antarctic ice core, Nature, 357, 488–490, https://doi.org/10.1038/357488a0, 1992.

López-García, J. M., Blain, H.-A., Bennàsar, M., Sanz, M., and Daura, J.: Heinrich event 4 characterized by terrestrial proxies in southwestern Europe, Climate of the Past, 9, 1053–1064, https://doi.org/10.5194/cp-9-1053-2013, 2013.

López-García, J. M., Blain, H.-A., Bennàsar, M., and Fernández-García, M.: Environmental and climatic context of Neanderthal occupation in southwestern Europe during MIS3 inferred from the small-vertebrate assemblages, Quaternary International, 326–327, 319–328, https://doi.org/10.1016/j.quaint.2013.09.010, 2014.

López-García, J. M., Blain, H. A., Fagoaga, A., Bandera, C. S., Sanz, M., and Daura, J.: Environment and climate during the Neanderthal-AMH presence in the Garraf Massif mountain range (northeastern Iberia) from the late Middle Pleistocene to Late Pleistocene inferred from small-vertebrate assemblages, Quaternary Science Reviews, 288, https://doi.org/10.1016/j.quascirev.2022.107595, 2022.

Luz, B., Kolodny, Y., and Horowitz, M.: Fractionation of oxygen isotopes between mammalian, Geochimica et Cosmochimica Acta, 48, 1689–1693, 1984.

Magozzi, S., Vander Zanden, H. B., Wunder, M. B., and Bowen, G. J.: Mechanistic model predicts tissue–environment relationships and trophic shifts in animal hydrogen and oxygen isotope ratios, Oecologia, 191, 777–789, https://doi.org/10.1007/s00442-019-04532-8, 2019.

Marín-Arroyo, A. B. and Sanz-Royo, A.: What Neanderthals and AMH ate: reassessment of the subsistence across the Middle–Upper Palaeolithic transition in the Vasco-Cantabrian region of SW Europe, Journal of Quaternary Science, 37, 320–334, https://doi.org/10.1002/jqs.3291, 2022.

Martrat, B., Grimalt, J. O., Lopez-Martinez, C., Cacho, I., Sierro, F. J., Flores, J. A., Zahn, R., Canals, M., Curtis, J. H., and Hodell, D. A.: Abrupt Temperature Changes in the Western Mediterranean over the Past 250,000 Years, Science, 306, 1762–1765, https://doi.org/10.1126/science.1101706, 2004.

Merceron, G., Berlioz, E., Vonhof, H., Green, D., Garel, M., and Tütken, T.: Tooth tales told by dental diet proxies: An alpine community of sympatric ruminants as a model to decipher the ecology of fossil fauna, Palaeogeography, Palaeoclimatology, Palaeoecology, 562, 110077, https://doi.org/10.1016/j.palaeo.2020.110077, 2021.

Van der Merwe, N. J.: Light Stable Isotopes and the Reconstruction of Prehistoric Diets, Proceedings of the British Academy, 77, 247–264, 1991.

Moreno, A., Stoll, H., Jiménez-Sánchez, M., Cacho, I., Valero-Garcés, B., Ito, E., and Edwards, R. L.: A speleothem record of glacial (25–11.6 kyr BP) rapid climatic changes from northern Iberian Peninsula, Global and Planetary Change, 71, 218–231, https://doi.org/10.1016/j.gloplacha.2009.10.002, 2010.

Moreno, A., González-Sampériz, P., Morellón, M., Valero-Garcés, B. L., and Fletcher, W. J.: Northern Iberian abrupt climate change dynamics during the last glacial cycle: A view from lacustrine sediments, Quaternary Science Reviews, 36, 139–153, https://doi.org/10.1016/j.quascirev.2010.06.031, 2012.

Moreno, A., Iglesias, M., Azorin-Molina, C., Pérez-Mejías, C., Bartolomé, M., Sancho, C., Stoll, H., Cacho, I., Frigola, J., Osácar, C., Muñoz, A., Delgado-Huertas, A., Bladé, I., and Vimeux, F.: Measurement report: Spatial variability of northern Iberian rainfall stable isotope values – investigating atmospheric controls on daily and monthly timescales, Atmospheric Chemistry and Physics, 21, 10159–10177, https://doi.org/10.5194/acp-21-10159-2021, 2021.

Naughton, F., Sánchez-Goñi, M. F., Desprat, S., Turon, J.-L., and Duprat, J.: Present-day and past (last 25 000 years) marine pollen signal off western Iberia, Marine micropaleontology, 62, 91–114, https://doi.org/10.1016/j.marmicro.2006.07.006, 2007.

1172 North Greenland Ice Core Project members: High-resolution record of Northern Hemisphere climate extending into the last
1173   interglacial period, Nature, 431, 147–151, https://doi.org/10.1038/nature02805, 2004.
1174 Ochando, J., Amorós, G., Carrión, J. S., Fernández, S., Munuera, M., Camuera, J., Jiménez-Moreno, G., González-Sampériz, P.,
1175   Burjachs, F., Marín-Arroyo, A. B., Roksandic, M., and Finlayson, C.: Iberian Neanderthals in forests and savannahs,
1176   Journal of Quaternary Science, 1–28, https://doi.org/10.1002/jqs.3339, 2021.
1177 Passey, B. H. and Cerling, T. E.: Tooth enamel mineralization in ungulates: implications for recovering a primary isotopic time-
1178   series, Geochimica et Cosmochimica Acta, 66, 3225–3234, https://doi.org/10.1016/S0016-7037(02)00933-X, 2002.
1179 Passey, B. H., Robinson, T. F., Ayliffe, L. K., Cerling, T. E., Sponheimer, M., Dearing, M. D., Roeder, B. L., and Ehleringer, J. R.:
1180   Carbon isotope fractionation between diet, breath CO_2, and bioapatite in different mammals, Journal of Archaeological
1181   Science, 32, 1459–1470, https://doi.org/10.1016/j.jas.2005.03.015, 2005a.
1182 Passey, B. H., Cerling, T. E., Schuster, G. T., Robinson, T. F., Roeder, B. L., and Krueger, S. K.: Inverse methods for estimating
1183   primary input signals from time-averaged isotope profiles, Geochimica et Cosmochimica Acta, 69, 4101–4116,
1184   https://doi.org/10.1016/j.gca.2004.12.002, 2005b.
1185 Pederzani, S. and Britton, K.: Oxygen isotopes in bioarchaeology: Principles and applications, challenges and opportunities, Earth-
1186   Science Reviews, 188, 77–107, https://doi.org/10.1016/j.earscirev.2018.11.005, 2019.
1187 Pederzani, S., Aldeias, V., Dibble, H. L., Goldberg, P., Hublin, J. J., Madelaine, S., McPherron, S. P., Sandgathe, D., Steele, T. E.,
1188   Turq, A., and Britton, K.: Reconstructing Late Pleistocene paleoclimate at the scale of human ~~behavior~~behaviour: an
1189   example from the Neandertal occupation of La Ferrassie (France), Scientific Reports, 11, 1–10,
1190   https://doi.org/10.1038/s41598-020-80777-1, 2021a.
1191 Pederzani, S., Britton, K., Aldeias, V., Bourgon, N., Fewlass, H., Lauer, T., McPherron, S. P., Rezek, Z., Sirakov, N., Smith, G. M.,
1192   Spasov, R., Tran, N. H., Tsanova, T., and Hublin, J. J.: Subarctic climate for the earliest Homo sapiens in Europe, Science
1193   Advances, 7, 1–11, https://doi.org/10.1126/sciadv.abi4642, 2021b.
1194 Pederzani, S., Britton, K., Jones, J. R., Agudo Pérez, L., Geiling, J. M., and Marín-Arroyo, A. B.: Late Pleistocene Neanderthal
1195   exploitation of stable and mosaic ecosystems in northern Iberia shown by multi-isotope evidence, Quaternary Research,
1196   1–25, https://doi.org/10.1017/qua.2023.32, 2023.
1197 Pellegrini, M. and Snoeck, C.: Comparing bioapatite carbonate pre-treatments for isotopic measurements: Part 2 — Impact on
1198   carbon and oxygen isotope compositions, Chemical Geology, 420, 88–96,
1199   https://doi.org/10.1016/j.chemgeo.2015.10.038, 2016.
1200 Pellegrini, M., Lee-Thorp, J. A., and Donahue, R. E.: Exploring the variation of the $\delta^{18}O_p$ and $\delta^{18}O_c$ relationship in enamel
1201   increments, Palaeogeography, Palaeoclimatology, Palaeoecology, 310, 71–83,
1202   https://doi.org/10.1016/j.palaeo.2011.02.023, 2011.
1203 Pérez-Mejías, C., Moreno, A., Sancho, C., Martín-García, R., Spötl, C., Cacho, I., Cheng, H., and Edwards, R. L.: Orbital-to-
1204   millennial scale climate variability during Marine Isotope Stages 5 to 3 in northeast Iberia, Quaternary Science Reviews,
1205   224, https://doi.org/10.1016/j.quascirev.2019.105946, 2019.
1206 Posth, C., Yu, H., Ghalichi, A., Rougier, H., Crevecoeur, I., Huang, Y., Ringbauer, H., Rohrlach, A. B., Nägele, K., Villalba-Mouco,
1207   V., Radzeviciute, R., Ferraz, T., Stoessel, A., Tukhbatova, R., Drucker, D. G., Lari, M., Modi, A., Vai, S., Saupe, T.,
1208   Scheib, C. L., Catalano, G., Pagani, L., Talamo, S., Fewlass, H., Klaric, L., Morala, A., Rué, M., Madelaine, S., Crépin,
1209   L., Caverne, J.-B., Bocaege, E., Ricci, S., Boschin, F., Bayle, P., Maureille, B., Le Brun-Ricalens, F., Bordes, J.-G., Oxilia,
1210   G., Bortolini, E., Bignon-Lau, O., Debout, G., Orliac, M., Zazzo, A., Sparacello, V., Starnini, E., Sineo, L., van der Plicht,
1211   J., Pecqueur, L., Merceron, G., Garcia, G., Leuvrey, J.-M., Garcia, C. B., Gómez-Olivencia, A., Połtowicz-Bobak, M.,
1212   Bobak, D., Le Luyer, M., Storm, P., Hoffmann, C., Kabaciński, J., Filimonova, T., Shnaider, S., Berezina, N., González-
1213   Rabanal, B., González Morales, M. R., Marín-Arroyo, A. B., López, B., Alonso-Llamazares, C., Ronchitelli, A., Polet, C.,
1214   Jadin, I., Cauwe, N., Soler, J., Coromina, N., Rufí, I., Cottiaux, R., Clark, G., Straus, L. G., Julien, M.-A., Renhart, S.,
1215   Talaa, D., Benazzi, S., Romandini, M., Amkreutz, L., Bocherens, H., Wißing, C., Villotte, S., de Pablo, J. F.-L., Gómez-
1216   Puche, M., Esquembre-Bebia, M. A., Bodu, P., Smits, L., Souffi, B., Jankauskas, R., Kozakaitė, J., Cupillard, C., Benthien,
1217   H., Wehrberger, K., Schmitz, R. W., Feine, S. C., et al.: Palaeogenomics of Upper Palaeolithic to Neolithic European
1218   hunter-gatherers, Nature, 615, 117–126, https://doi.org/10.1038/s41586-023-05726-0, 2023.
1219 Pryor, A. J. E., Stevens, R. E., Connell, T. C. O., and Lister, J. R.: Quantification and propagation of errors when converting
1220   vertebrate biomineral oxygen isotope data to temperature for palaeoclimate reconstruction, Palaeogeography,
1221   Palaeoclimatology, Palaeoecology, 412, 99–107, https://doi.org/10.1016/j.palaeo.2014.07.003, 2014.
1222 Ramsey, C. B.: Bayesian Analysis of Radiocarbon Dates, Radiocarbon, 51, 337–360, https://doi.org/10.1017/S0033822200033865,
1223   2009.
1224 Rasmussen, S. O., Bigler, M., Blockley, S. P., Blunier, T., Buchardt, S. L., Clausen, H. B., Cvijanovic, I., Dahl-Jensen, D., Johnsen,
1225   S. J., Fischer, H., Gkinis, V., Guillevic, M., Hoek, W. Z., Lowe, J. J., Pedro, J. B., Popp, T., Seierstad, I. K., Steffensen,
1226   J. P., Svensson, A. M., Vallelonga, P., Vinther, B. M., Walker, M. J. C., Wheatley, J. J., and Winstrup, M.: A stratigraphic
1227   framework for abrupt climatic changes during the Last Glacial period based on three synchronized Greenland ice-core
1228   records: Refining and extending the INTIMATE event stratigraphy, Quaternary Science Reviews, 106, 14–28,
1229   https://doi.org/10.1016/j.quascirev.2014.09.007, 2014.
1230 Reimer, P. J., Austin, W. E. N., Bard, E., Bayliss, A., Blackwell, P. G., Bronk Ramsey, C., Butzin, M., Cheng, H., Edwards, R. L.,
1231   Friedrich, M., Grootes, P. M., Guilderson, T. P., Hajdas, I., Heaton, T. J., Hogg, A. G., Hughen, K. A., Kromer, B., Manning,
1232   S. W., Muscheler, R., Palmer, J. G., Pearson, C., van der Plicht, J., Reimer, R. W., Richards, D. A., Scott, E. M., Southon,
1233   J. R., Turney, C. S. M., Wacker, L., Adolphi, F., Büntgen, U., Capano, M., Fahrni, S. M., Fogtmann-Schulz, A., Friedrich,
1234   R., Köhler, P., Kudsk, S., Miyake, F., Olsen, J., Reinig, F., Sakamoto, M., Sookdeo, A., and Talamo, S.: The IntCal20
1235   Northern Hemisphere Radiocarbon Age Calibration Curve (0–55 cal kBP), Radiocarbon, 62, 725–757,
1236   https://doi.org/10.1017/RDC.2020.41, 2020.
1237 Rey, K., Amiot, R., Lécuyer, C., Koufos, G. D., Martineau, F., Fourel, F., Kostopoulos, D. S., and Merceron, G.: Late Miocene climatic
1238   and environmental variations in northern Greece inferred from stable isotope compositions ($\delta^{18}O$, $\delta^{13}C$) of equid teeth

apatite, Palaeogeography, Palaeoclimatology, Palaeoecology, 388, 48–57, https://doi.org/10.1016/j.palaeo.2013.07.021, 2013.

Rivals, F., Uzunidis, A., Sanz, M., and Daura, J.: Faunal dietary response to the Heinrich Event 4 in southwestern Europe, Palaeogeography, Palaeoclimatology, Palaeoecology, 473, 123–130, https://doi.org/10.1016/j.palaeo.2017.02.033, 2017.

Rivals, F., Bocherens, H., Camarós, E., and Rosell, J.: Diet and ecological interactions in the Middle and Late Pleistocene, in: Updating Neanderthals. Understanding Behavioural Complexity in the Late Middle Palaeolithic, 39–54, 2022.

Roucoux, K. H., Shackleton, N. J., Abreu, L. De, Schönfeld, J., and Tzedakis, P. C.: Combined marine proxy and pollen analyses reveal rapid Iberian vegetation response to North Atlantic millennial-scale climate oscillations, Quaternary Research, 56, 128–132, https://doi.org/10.1006/qres.2001.2218, 2001.

Rozanski, K., Araguás-Araguás, L., and Gonfiantini, R.: Relation Between Long-Term Trends of Oxygen-18 Isotope Composition of Precipitation and Climate, Science, 258, 981–985, 1992.

Rufí, I., Solés, A., Soler, J., and Soler, N.: A mammoth (Mammuthus primigenius Blumenbach 1799, Proboscidea) calf tooth from the Mousterian of Arbreda Cave (Serinyà, NE Iberian Peninsula), Estudios Geológicos, 74, e079, https://doi.org/10.3989/egeol.43130.478, 2018.

Ruiz-Fernández, J., García-Hernández, C., and Gallinar Cañedo, D.: The glaciers of the Picos de Europa, in: Iberia, Land of Glaciers, Elsevier, 237–263, https://doi.org/10.1016/B978-0-12-821941-6.00012-8, 2022.

Sánchez-Goñi, M. F., Eynaud, F., Turon, J.-L., and Shackleton, N. J.: High resolution palynological record off the Iberian margin: direct land-sea correlation for the Last Interglacial complex, Earth and Planetary Science Letters, 171, 123–137, 1999.

Sánchez-Goñi, M. F., Landais, A., Cacho, I., Duprat, J., and Rossignol, L.: Contrasting intrainterstadial climatic evolution between high and middle North Atlantic latitudes: A close-up of Greenland Interstadials 8 and 12, Geochemistry, Geophysics, Geosystems, 10, 1–16, https://doi.org/10.1029/2008GC002369, 2009.

Sánchez Goñi, M., Cacho, I., Turon, J., Guiot, J., Sierro, F., Peypouquet, J., Grimalt, J., and Shackleton, N.: Synchroneity between marine and terrestrial responses to millennial scale climatic variability during the last glacial period in the Mediterranean region, Climate Dynamics, 19, 95–105, https://doi.org/10.1007/s00382-001-0212-x, 2002.

Sánchez Goñi, M. F.: Regional impacts of climate change and its relevance to human evolution, Evolutionary Human Sciences, 2, e55, https://doi.org/10.1017/ehs.2020.56, 2020.

Schmitt, J., Schneider, R., Elsig, J., Leuenberger, D., Lourantou, A., Chappellaz, J., Köhler, P., Joos, F., Stocker, T. F., Leuenberger, M., and Fischer, H.: Carbon Isotope Constraints on the Deglacial CO 2 Rise from Ice Cores, Science, 336, 711–714, https://doi.org/10.1126/science.1217161, 2012.

Schrag, D. P., Adkins, J. F., Mcintyre, K., Alexander, J. L., Hodell, A., Charles, C. D., and Mcmanus, J. F.: The oxygen isotopic composition of seawater during the Last Glacial Maximum, Quaternary Science Reviews, 21, 331–342, 2002.

Sepulchre, P., Ramstein, G., Kageyama, M., Vanhaeren, M., Krinner, G., Sánchez-Goñi, M. F., and d'Errico, F.: H4 abrupt event and late Neanderthal presence in Iberia, Earth and Planetary Science Letters, 258, 283–292, https://doi.org/10.1016/j.epsl.2007.03.041, 2007.

Shackleton, N. J.: Oxygen isotopes, ice volume and sea level, Quaternary Science Reviews, 6, 183–190, https://doi.org/10.1016/0277-3791(87)90003-5, 1987.

Skrzypek, G., Wiśniewski, A., and Grierson, P. F.: How cold was it for Neanderthals moving to Central Europe during warm phases of the last glaciation?, Quaternary Science Reviews, 30, 481–487, https://doi.org/10.1016/j.quascirev.2010.12.018, 2011.

Skrzypek, G., Sadler, R., and Wi, A.: Reassessment of recommendations for processing mammal phosphate δ18O data for paleotemperature reconstruction, Palaeogeography, Palaeoclimatology, Palaeoecology, 446, 162–167, https://doi.org/10.1016/j.palaeo.2016.01.032, 2016.

Snoeck, C. and Pellegrini, M.: Comparing bioapatite carbonate pre-treatments for isotopic measurements: Part 1—Impact on structure and chemical composition, Chemical Geology, 417, 394–403, https://doi.org/10.1016/j.chemgeo.2015.10.004, 2015.

Staubwasser, M., Drăgusin, V., Onac, B. P., Assonov, S., Ersek, V., Hoffmann, D. L., and Veres, D.: Impact of climate change on the transition of Neanderthals to modern humans in Europe, Proceedings of the National Academy of Sciences, 115, 9116–9121, https://doi.org/10.1073/pnas.1808647115, 2018.

Tejada-Lara, J. V., MacFadden, B. J., Bermudez, L., Rojas, G., Salas-Gismondi, R., and Flynn, J. J.: Body mass predicts isotope enrichment in herbivorous mammals, Proceedings of the Royal Society B: Biological Sciences, 285, 20181020, https://doi.org/10.1098/rspb.2018.1020, 2018.

Timmermann, A.: Quantifying the potential causes of Neanderthal extinction: Abrupt climate change versus competition and interbreeding, Quaternary Science Reviews, 238, 106331, https://doi.org/10.1016/j.quascirev.2020.106331, 2020.

Trayler, R. B. and Kohn, M. J.: Tooth enamel maturation reequilibrates oxygen isotope compositions and supports simple sampling methods, Geochimica et Cosmochimica Acta, 198, 32–47, https://doi.org/10.1016/j.gca.2016.10.023, 2017.

Tütken, T., Furrer, H., and Vennemann, T. W.: Stable isotope compositions of mammoth teeth from Niederweningen, Switzerland: Implications for the Late Pleistocene climate, environment, and diet, Quaternary International, 164–165, 139–150, https://doi.org/10.1016/j.quaint.2006.09.004, 2007.

Vidal-Cordasco, M., Ocio, D., Hickler, T., and Marín-Arroyo, A. B.: Ecosystem productivity affected the spatiotemporal disappearance of Neanderthals in Iberia, Nature Ecology & Evolution, 6, 1644–1657, https://doi.org/10.1038/s41559-022-01861-5, 2022.

Vidal-Cordasco, Terlaro, G., M., Ocio, D., T., Marín-Arroyo, A.B., 2023. Neanderthal coexistence with Homo sapiens in Europe was affected by herbivore carrying capacity. Science Advances 9 (38), https://www.science.org/doi/10.1126/sciadv.adi4099

Zazzo, A., Bendrey, R., Vella, D., Moloney, A. P., Monahan, F. J., and Schmidt, O.: A refined sampling strategy for intra-tooth stable isotope analysis of mammalian enamel, Geochimica et Cosmochimica Acta, 84, 1–13, https://doi.org/10.1016/j.gca.2012.01.012, 2012.

Allué, E., Martínez-Moreno, J., Roy, M., Benito-Calvo, A., and Mora, R.: Montane pine forests in NE Iberia during MIS 3 and MIS 2. A study based on new anthracological evidence from Cova Gran (Santa Linya, Iberian Pre-Pyrenees), Rev. Palaeobot. Palynol., 258, 62–72, https://doi.org/10.1016/j.revpalbo.2018.06.012, 2018.

Álvarez-Lao, D. J., Rivals, F., Sánchez-Hernández, C., Blasco, R., and Rosell, J.: Ungulates from Teixoneres Cave (Moià, Barcelona, Spain): Presence of cold-adapted elements in NE Iberia during the MIS 3, Palaeogeogr. Palaeoclimatol. Palaeoecol., 466, 287–302, https://doi.org/10.1016/j.palaeo.2016.11.040, 2017.

Balasse, M., Ambrose, S. H., Smith, A. B., and Price, T. D.: The Seasonal Mobility Model for Prehistoric Herders in the South-western Cape of South Africa Assessed by Isotopic Analysis of Sheep Tooth Enamel, J. Archaeol. Sci., 29, 917–932, https://doi.org/10.1006/jasc.2001.0787, 2002.

Bendrey, R., Vella, D., Zazzo, A., Balasse, M., and Lepetz, S.: Exponentially decreasing tooth growth rate in horse teeth: implications for isotopic analyses, Archaeometry, 57, 1104–1124, https://doi.org/10.1111/arcm.12151, 2015.

Blumenthal, S. A., Cerling, T. E., Chritz, K. L., Bromage, T. G., Kozdon, R., and Valley, J. W.: Stable isotope time-series in mammalian teeth: In situ δ18O from the innermost enamel layer, Geochim. Cosmochim. Acta, 124, 223–236, https://doi.org/10.1016/j.gca.2013.09.032, 2014.

Blumenthal, S. A., Cerling, T. E., Smiley, T. M., Badgley, C. E., and Plummer, T. W.: Isotopic records of climate seasonality in equid teeth, Geochim. Cosmochim. Acta, 260, 329–348, https://doi.org/10.1016/j.gca.2019.06.037, 2019.

Bocherens, H.: Isotopic biogeochemistry and the paleoecology of the mammoth steppe fauna, Deinsea, 91, 57–76, 2003.

Brand, W. A., Coplen, T. B., Vogl, J., Rosner, M., and Prohaska, T.: Assessment of international reference materials for isotope-ratio analysis (IUPAC Technical Report), Pure Appl. Chem., 86, 425–467, https://doi.org/10.1515/pac-2013-1023, 2014.

Britton, K., Pederzani, S., Kindler, L., Roebroeks, W., Gaudzinski-Windheuser, S., Richards, M. P., and Tütken, T.: Oxygen isotope analysis of Equus teeth evidences early Eemian and early Weichselian palaeotemperatures at the Middle Palaeolithic site of Neumark-Nord 2, Saxony-Anhalt, Germany, Quat. Sci. Rev., 226, 106029, https://doi.org/10.1016/j.quascirev.2019.106029, 2019.

Bryant, J. D., Luz, B., and Froelich, P. N.: Oxygen isotopic composition of fossil horse tooth phosphate as a record of continental paleoclimate, Palaeogeogr. Palaeoclimatol. Palaeoecol., 107, 303–316, https://doi.org/10.1016/0031-0182(94)90102-3, 1994.

Bryant, J. D., Koch, P. L., Froelich, P. N., Showers, W. J., and Genna, B. J.: Oxygen isotope partitioning between phosphate and carbonate in mammalian apatite, Geochim. Cosmochim. Acta, 60, 5145–5148, https://doi.org/10.1016/S0016-7037(96)00308-0, 1996.

Carvalho, M., Jones, E. L., Ellis, M. G., Cascalheira, J., Bicho, N., Meiggs, D., Benedetti, M., Friedl, L., and Haws, J.: Neanderthal palaeoecology in the late Middle Palaeolithic of western Iberia: a stable isotope analysis of ungulate teeth from Lapa do Picareiro (Portugal), J. Quat. Sci., 37, 300–319, https://doi.org/10.1002/jqs.3363, 2022.

Cascalheira, J., Alcaraz-Castaño, M., Alcolea-González, J., de Andrés-Herrero, M., Arrizabalaga, A., Aura Tortosa, J. E., Garcia-Ibaibarriaga, N., and Iriarte-Chiapusso, M. J.: Paleoenvironments and human adaptations during the Last Glacial Maximum in the Iberian Peninsula: A review, Quat. Int., 581–582, 28–51, https://doi.org/10.1016/j.quaint.2020.08.005, 2021.

Cerling, T. E. and Harris, J. M.: Carbon isotope fractionation between diet and bioapatite in ungulate mammals and implications for ecological and paleoecological studies, Oecologia, 120, 347–363, https://doi.org/10.1007/s004420050868, 1999.

Chillón, B. S., Alberdi, M. T., Leone, G., Bonadonna, F. P., Stenni, B., and Longinelli, A.: Oxygen isotopic composition of fossil equid tooth and bone phosphate: an archive of difficult interpretation, Palaeogeogr. Palaeoclimatol. Palaeoecol., 107, 317–328, https://doi.org/10.1016/0031-0182(94)90103-1, 1994.

Coplen, T. B.: Guidelines and recommended terms for expression of stable-isotope-ratio and gas-ratio measurement results, Rapid Commun. Mass Spectrom., 25, 2538–2560, https://doi.org/10.1002/rcm.5129, 2011.

Coplen, T. B., Kendall, C., and Hopple, J.: Comparison of stable isotope reference samples, Nature, 302, 236–238, https://doi.org/10.1038/302236a0, 1983.

D''Angela, D. and Longinelli, A.: Oxygen isotopes in living mammal''s bone phosphate: Further results, Chem. Geol., 86, 75–82, 1990.

Dansgaard, W.: Stable isotopes in precipitation, Tellus, XVI, 436–468, 1964.

Daura, J., Sanz, M., García, N., Allué, E., Vaquero, M., Fierro, E., Carrión, J. S., López-García, J. M., Blain, H. a., Sánchez-Marco, a., Valls, C., Albert, R. M., Fornós, J. J., Julià, R., Fullola, J. M., and Zilhão, J.: Terrasses de la Riera dels Canyars (Gavà, Barcelona): The landscape of Heinrich Stadial 4 north of the ""Ebro frontier"" and implications for modern human dispersal into Iberia, Quat. Sci. Rev., 60, 26–48, https://doi.org/10.1016/j.quascirev.2012.10.042, 2013.

Delgado Huertas, A., Iacumin, P., Stenni, B., Sánchez Chillón, B., and Longinelli, A.: Oxygen isotope variations of phosphate in mammalian bone and tooth enamel, Geochim. Cosmochim. Acta, 59, 4299–4305, https://doi.org/10.1016/0016-7037(95)00286-9, 1995.

Drucker, D. G.: The Isotopic Ecology of the Mammoth Steppe, Annu. Rev. Earth Planet. Sci., 50, 395–418, https://doi.org/10.1146/annurev-earth-100821-081832, 2022.

Drucker, D. G., Bridault, A., Hobson, K. A., Szuma, E., and Bocherens, H.: Can carbon-13 in large herbivores reflect the canopy effect in temperate and boreal ecosystems? Evidence from modern and ancient ungulates, Palaeogeogr. Palaeoclimatol. Palaeoecol., 266, 69–82, https://doi.org/10.1016/j.palaeo.2008.03.020, 2008.

Fagoaga, A.: Aproximacion paleoclimática y paisajística durante el MIS3 a partir del estudio38iomin de los micromamíferos del yacimiento de El Salt (Alcoi, Alicante)., Universidad de Burgos, 34 pp., 2014.

Fernández-García, M., Royer, A., López-García, J. M., Bennàsar, M., Goedert, J., Fourel, F., Julien, M.-A., Bañuls-Cardona, S., Rodríguez-Hidalgo, A., Vallverdú, J., and Lécuyer, C.: Unravelling the oxygen isotope signal (δ18O) of rodent teeth from northeastern Iberia, and implications for past climate reconstructions, Quat. Sci. Rev., 218, 107–121, https://doi.org/10.1016/j.quascirev.2019.04.035, 2019.

Fernández-García, M., López-García, J. M., Royer, A., Lécuyer, C., Allué, E., Burjachs, F., Chacón, M. G., Saladié, P., Vallverdú,

1373   J., and Carbonell, E.: Combined palaeoecological methods using small-mammal assemblages to decipher environmental
1374   context of a long-term Neanderthal settlement in northeastern Iberia, Quat. Sci. Rev., 228, 106072,
1375   https://doi.org/10.1016/j.quascirev.2019.106072, 2020.
1376 Fernández-García, M., Vidal-Cordasco, M., Jones, J. R., and Marín-Arroyo, A. B.: Reassessing palaeoenvironmental conditions
1377   during the Middle to Upper Palaeolithic transition in the Cantabrian region (Southwestern Europe), Quat. Sci. Rev., 301,
1378   107928, https://doi.org/10.1016/j.quascirev.2022.107928, 2023.
1379 Fick, S. E. and Hijmans, R. J.: WorldClim 2: new 1-km spatial resolution climate surfaces for global land areas, Int. J. Climatol., 37,
1380   4302–4315, https://doi.org/10.1002/joc.5086, 2017.
1381 Garcia-Ibaibarriaga, N., Suárez-Bilbao, A., Iriarte-Chiapusso, M. J., Arrizabalaga, A., and Murelaga, X.: Palaeoenvironmental
1382   dynamics in the Cantabrian Region during Greenland stadial 2 approached through pollen and micromammal records:
1383   State of the art, Quat. Int., 506, 14–24, https://doi.org/10.1016/j.quaint.2018.12.004, 2019a.
1384 Garcia-Ibaibarriaga, N., Suárez-Bilbao, A., Iriarte-Chiapusso, M. J., Arrizabalaga, A., and Murelaga, X.: Palaeoenvironmental
1385   dynamics in the Cantabrian Region during Greenland stadial 2 approached through pollen and micromammal records:
1386   State of the art, Quat. Int., 506, 14–24, https://doi.org/10.1016/j.quaint.2018.12.004, 2019b.
1387 Geiling, J. M.: Human Ecodynamics in the Late Upper Pleistocene of Northern Spain: An Archeozoological Study of Ungulate
1388   Remains from the Lower Magdalenian and other Periods in El Mirón Cave (Cantabria), Universidad de Cantabria, 734
1389   pp., 2020.
1390 Hoppe, K. A.: Correlation between the oxygen isotope ratio of North American bison teeth and local waters: Implication for
1391   paleoclimatic reconstructions, Earth Planet. Sci. Lett., 244, 408–417, https://doi.org/10.1016/j.epsl.2006.01.062, 2006.
1392 Hoppe, K. A., Stover, S. M., Pascoe, J. R., and Amundson, R.: Tooth enamel biomineralisation39iomineralization in extant horses:
1393   implications for isotopic microsampling, Palaeogeogr. Palaeoclimatol. Palaeoecol., 206, 355–365,
1394   https://doi.org/10.1016/j.palaeo.2004.01.012, 2004.
1395 Iacumin, P., Bocherens, H., Mariotti, A., and Longinelli, A.: Oxygen isotope analyses of co-existing carbonate and phosphate in
1396   biogenic apatite: a way to monitor diagenetic alteration of bone phosphate?, Earth Planet. Sci. Lett., 142, 1–6,
1397   https://doi.org/10.1016/0012-821X(96)00093-3, 1996.
1398 Iriarte-Chiapusso, M. J.: El entorno vegetal del yacimiento paleolítico de Labeko Koba (Arrasate, País Vasco): análisis polínico.,
1399   Labeko Koba (País Vasco). Hienas y humanos en los albores del Paleolítico Super., Munibe, 89–106, 2000.
1400 Jiménez-Sánchez, M., Rodríguez-Rodríguez, L., García-Ruiz, J. M., Domínguez-Cuesta, M. J., Farias, P., Valero-Garcés, B.,
1401   Moreno, A., Rico, M., and Valcárcel, M.: A review of glacial geomorphology and chronology in northern Spain: Timing
1402   and regional variability during the last glacial cycle, Geomorphology, 196, 50–64,
1403   https://doi.org/10.1016/j.geomorph.2012.06.009, 2013.
1404 Jones, J. R., Richards, M. P., Straus, L. G., Reade, H., Altuna, J., Mariezkurrena, K., and Marín-Arroyo, A. B.: Changing
1405   environments during the Middle-Upper Palaeolithic transition in the eastern Cantabrian Region (Spain): direct evidence
1406   from stable isotope studies on ungulate bones, Sci. Rep., 8, 14842, https://doi.org/10.1038/s41598-018-32493-0, 2018.
1407 Jones, J. R., Richards, M. P., Reade, H., Bernaldo de Quirós, F., and Marín-Arroyo, A. B.: Multi-Isotope investigations of ungulate
1408   bones and teeth from El Castillo and Covalejos caves (Cantabria, Spain): Implications for paleoenvironment
1409   reconstructions across the Middle-Upper Palaeolithic transition, J. Archaeol. Sci. Reports, 23, 1029–1042,
1410   https://doi.org/10.1016/j.jasrep.2018.04.014, 2019.
1411 Jones, J. R., Marín-Arroyo, A. B., Corchón Rodríguez, M. S., and Richards, M. P.: After the Last Glacial Maximum in the refugium
1412   of northern Iberia: Environmental shifts, demographic pressure and changing economic strategies at Las Caldas Cave
1413   (Asturias, Spain), Quat. Sci. Rev., 262, 106931, https://doi.org/10.1016/j.quascirev.2021.106931, 2021.
1414 Kohn, M. J.: Comment: Tooth Enamel Mineralization in Ungulates: Implications for Recovering a Primary Isotopic Time-Series, by
1415   B. H. Passey and T. E. Cerling (2002), Geochim. Cosmochim. Acta, 68, 403–405, https://doi.org/10.1016/S0016-
1416   7037(03)00443-5, 2004.
1417 Kohn, M. J.: Carbon isotope compositions of terrestrial C3 plants as indicators of (paleo)ecology and (paleo)climate, Proc. Natl.
1418   Acad. Sci., 107, 19691–19695, https://doi.org/10.1073/pnas.1004933107, 2010.
1419 Lécuyer, C., Hillaire-Marcel, C., Burke, A., Julien, M.-A., and Hélie, J.-F.: Temperature and precipitation regime in LGM human
1420   refugia of southwestern Europe inferred from δ13C and δ18O of large mammal remains, Quat. Sci. Rev., 255, 106796,
1421   https://doi.org/10.1016/j.quascirev.2021.106796, 2021.
1422 Leuenberger, M., Siegenthaler, U., and Langway, C.: Carbon isotope composition of atmospheric CO2 during the last ice age from
1423   an Antarctic ice core, Nature, 357, 488–490, https://doi.org/10.1038/357488a0, 1992.
1424 López-García, J. M., Blain, H.-A., Bennàsar, M., Sanz, M., and Daura, J.: Heinrich event 4 characterised by terrestrial proxies in
1425   southwestern Europe, Clim. Past, 9, 1053–1064, https://doi.org/10.5194/cp-9-1053-2013, 2013.
1426 López-García, J. M., Blain, H.-A., Bennàsar, M., and Fernández-García, M.: Environmental and climatic context of Neanderthal
1427   occupation in southwestern Europe during MIS3 inferred from the small-vertebrate assemblages, Quat. Int., 326–327,
1428   319–328, https://doi.org/10.1016/j.quaint.2013.09.010, 2014.
1429 López-García, J. M., Blain, H. A., Fagoaga, A., Bandera, C. S., Sanz, M., and Daura, J.: Environment and climate during the
1430   Neanderthal-AMH presence in the Garraf Massif mountain range (northeastern Iberia) from the late Middle Pleistocene
1431   to Late Pleistocene inferred from small-vertebrate assemblages, Quat. Sci. Rev., 288,
1432   https://doi.org/10.1016/j.quascirev.2022.107595, 2022.
1433 Marín-Arroyo, A. B. and Sanz-Royo, A.: What Neanderthals and AMH ate: reassessment of the subsistence across the Middle-
1434   Upper Palaeolithic transition in the Vasco-Cantabrian region of SW Europe, J. Quat. Sci., 37, 320–334,
1435   https://doi.org/10.1002/jqs.3291, 2022.
1436 Merceron, G., Berlioz, E., Vonhof, H., Green, D., Garel, M., and Tütken, T.: Tooth tales told by dental diet proxies: An alpine
1437   community of sympatric ruminants as a model to decipher the ecology of fossil fauna, Palaeogeogr. Palaeoclimatol.
1438   Palaeoecol., 562, 110077, https://doi.org/10.1016/j.palaeo.2020.110077, 2021.
1439 van der Merwe, N. J.: Light Stable Isotopes and the Reconstruction of Prehistoric Diets, Proc. Br. Acad., 77, 247–264, 1991.

North Greenland Ice Core Project members: High-resolution record of Northern Hemisphere climate extending into the last interglacial period, Nature, 431, 147–151, https://doi.org/10.1038/nature02805, 2004.

Ochando, J., Amorós, G., Carrión, J. S., Fernández, S., Munuera, M., Camuera, J., Jiménez-Moreno, G., González-Sampériz, P., Burjachs, F., Marín-Arroyo, A. B., Roksandic, M., and Finlayson, C.: Iberian Neanderthals in forests and savannahs, J. Quat. Sci., 1–28, https://doi.org/10.1002/jqs.3339, 2021.

Passey, B. H. and Cerling, T. E.: Tooth enamel mineralisation in ungulates: implications for recovering a primary isotopic time-series, Geochim. Cosmochim. Acta, 66, 3225–3234, https://doi.org/10.1016/S0016-7037(02)00933-X, 2002.

Passey, B. H., Robinson, T. F., Ayliffe, L. K., Cerling, T. E., Sponheimer, M., Dearing, M. D., Roeder, B. L., and Ehleringer, J. R.: Carbon isotope fractionation between diet, breath CO2, and bioapatite in different mammals, J. Archaeol. Sci., 32, 1459–1470, https://doi.org/10.1016/j.jas.2005.03.015, 2005.

Pederzani, S. and Britton, K.: Oxygen isotopes in bioarchaeology: Principles and applications, challenges and opportunities, Earth-Science Rev., 188, 77–107, https://doi.org/10.1016/j.earscirev.2018.11.005, 2019.

Pederzani, S., Aldeias, V., Dibble, H. L., Goldberg, P., Hublin, J. J., Madelaine, S., McPherron, S. P., Sandgathe, D., Steele, T. E., Turq, A., and Britton, K.: Reconstructing Late Pleistocene paleoclimate at the scale of human behavior: an example from the Neandertal occupation of La Ferrassie (France), Sci. Rep., 11, 1–10, https://doi.org/10.1038/s41598-020-80777-1, 2021a.

Pederzani, S., Britton, K., Aldeias, V., Bourgon, N., Fewlass, H., Lauer, T., McPherron, S. P., Rezek, Z., Sirakov, N., Smith, G. M., Spasov, R., Tran, N. H., Tsanova, T., and Hublin, J. J.: Subarctic climate for the earliest Homo sapiens in Europe, Sci. Adv., 7, 1–11, https://doi.org/10.1126/sciadv.abi4642, 2021b.

Pederzani, S., Britton, K., Jones, J. R., Agudo Pérez, L., Geiling, J. M., and Marín-Arroyo, A. B.: Late Pleistocene Neanderthal exploitation of stable and mosaic ecosystems in northern Iberia shown by multi-isotope evidence, Quat. Res., 1–25, https://doi.org/10.1017/qua.2023.32, 2023.

Pellegrini, M. and Snoeck, C.: Comparing bioapatite carbonate pre-treatments for isotopic measurements: Part 2 — Impact on carbon and oxygen isotope compositions, Chem. Geol., 420, 88–96, https://doi.org/10.1016/j.chemgeo.2015.10.038, 2016.

Pellegrini, M., Lee-Thorp, J. A., and Donahue, R. E.: Exploring the variation of the δ18Op and δ18Oc relationship in enamel increments, Palaeogeogr. Palaeoclimatol. Palaeoecol., 310, 71–83, https://doi.org/10.1016/j.palaeo.2011.02.023, 2011.

Posth, C., Yu, H., Ghalichi, A., Rougier, H., Crevecoeur, I., Huang, Y., Ringbauer, H., Rohrlach, A. B., Nägele, K., Villalba-Mouco, V., Radzeviciute, R., Ferraz, T., Stoessel, A., Tukhbatova, R., Drucker, D. G., Lari, M., Modi, A., Vai, S., Saupe, T., Scheib, C. L., Catalano, G., Pagani, L., Talamo, S., Fewlass, H., Klaric, L., Morala, A., Rué, M., Madelaine, S., Crépin, L., Caverne, J. B., Bocaege, E., Ricci, S., Boschin, F., Bayle, P., Maureille, B., Le Brun-Ricalens, F., Bordes, J. G., Oxilia, G., Bortolini, E., Bignon-Lau, O., Debout, G., Orliac, M., Zazzo, A., Sparacello, V., Starnini, E., Sineo, L., van der Plicht, J., Pecqueur, L., Merceron, G., Garcia, G., Leuvrey, J. M., Garcia, C. B., Gómez-Olivencia, A., Połtowicz-Bobak, M., Bobak, D., Le Luyer, M., Storm, P., Hoffmann, C., Kabaciński, J., Filimonova, T., Shnaider, S., Berezina, N., González-Rabanal, B., González Morales, M. R., Marín-Arroyo, A. B., López, B., Alonso-Llamazares, C., Ronchitelli, A., Polet, C., Jadin, I., Cauwe, N., Soler, J., Coromina, N., Rufí, I., Cottiaux, R., Clark, G., Straus, L. G., Julien, M.-A., Renhart, S., Talaa, D., Benazzi, S., Romandini, M., Amkreutz, L., Bocherens, H., Wißing, C., Villotte, S., de Pablo, J. F.-L., Gómez-Puche, M., Esquembre-Bebia, M. A., Bodu, P., Smits, L., Souffi, B., Jankauskas, R., Kozakaitė, J., Cupillard, C., Benthien, H., Wehrberger, K., Schmitz, R. W., Feine, S. C., et al.: Palaeogenomics of Upper Palaeolithic to Neolithic European hunter-gatherers, Nature, 615, 117–126, https://doi.org/10.1038/s41586-023-05726-0, 2023.

Pryor, A. J. E., Stevens, R. E., Connell, T. C. O., and Lister, J. R.: Quantification and propagation of errors when converting vertebrate biomineral oxygen isotope data to temperature for palaeoclimate reconstruction, Palaeogeogr. Palaeoclimatol. Palaeoecol., 412, 99–107, https://doi.org/10.1016/j.palaeo.2014.07.003, 2014.

Rasmussen, S. O., Bigler, M., Blockley, S. P., Blunier, T., Buchardt, S. L., Clausen, H. B., Cvijanovic, I., Dahl-Jensen, D., Johnsen, S. J., Fischer, H., Gkinis, V., Guillevic, M., Hoek, W. Z., Lowe, J. J., Pedro, J. B., Popp, T., Seierstad, I. K., Steffensen, J. P., Svensson, A. M., Vallelonga, P., Vinther, B. M., Walker, M. J. C., Wheatley, J. J., and Winstrup, M.: A stratigraphic framework for abrupt climatic changes during the Last Glacial period based on three synchronised Greenland ice-core records: Refining and extending the INTIMATE event stratigraphy, Quat. Sci. Rev., 106, 14–28, https://doi.org/10.1016/j.quascirev.2014.09.007, 2014.

Rey, K., Amiot, R., Lécuyer, C., Koufos, G. D., Martineau, F., Fourel, F., Kostopoulos, D. S., and Merceron, G.: Late Miocene climatic and environmental variations in northern Greece inferred from stable isotope compositions (δ18O, δ13C) of equid teeth apatite, Palaeogeogr. Palaeoclimatol. Palaeoecol., 388, 48–57, https://doi.org/10.1016/j.palaeo.2013.07.021, 2013.

Rivals, F., Uzunidis, A., Sanz, M., and Daura, J.: Faunal dietary response to the Heinrich Event 4 in southwestern Europe, Palaeogeogr. Palaeoclimatol. Palaeoecol., 473, 123–130, https://doi.org/10.1016/j.palaeo.2017.02.033, 2017.

Rivals, F., Bocherens, H., Camarós, E., and Rosell, J.: Diet and ecological interactions in the Middle and Late Pleistocene, in: Updating Neanderthals. Understanding Behavioural Complexity in the Late Middle Palaeolithic, 39–54, 2022.

Rozanski, K., Araguás-Araguás, L., and Gonfiantini, R.: Relation Between Long-Term Trends of Oxygen-18 Isotope Composition of Precipitation and Climate, Science (80-.), 258, 981–985, 1992.

Rufí, I., Solés, A., Soler, J., and Soler, N.: Un diente de cría de mamut (Mammuthus primigenius Blumenbach 1799, Proboscidea) procedente del Musteriense de la Cueva de la Arbreda (Serinyà, NE de la Península Ibérica), Estud. Geológicos, 74, e079, https://doi.org/10.3989/egeol.43130.478, 2018.

Ruiz-Fernández, J., García-Hernández, C., and Gallinar Cañedo, D.: The glaciers of the Picos de Europa, in: Iberia, Land of Glaciers, Elsevier, 237–263, https://doi.org/10.1016/B978-0-12-821941-6.00012-8, 2022.

Schmitt, J., Schneider, R., Elsig, J., Leuenberger, D., Lourantou, A., Chappellaz, J., Köhler, P., Joos, F., Stocker, T. F., Leuenberger, M., and Fischer, H.: Carbon Isotope Constraints on the Deglacial CO2 Rise from Ice Cores, Science (80-.), 336, 711–714, https://doi.org/10.1126/science.1217161, 2012.

Skrzypek, G., Sadler, R., and Wi, A.: Reassessment of recommendations for processing mammal phosphate δ18O data for

paleotemperature reconstruction, Palaeogeogr. Palaeoclimatol. Palaeoecol., 446, 162–167, https://doi.org/10.1016/j.palaeo.2016.01.032, 2016.

Snoeck, C. and Pellegrini, M.: Comparing bioapatite carbonate pre-treatments for isotopic measurements: Part 1—Impact on structure and chemical composition, Chem. Geol., 417, 394–403, https://doi.org/10.1016/j.chemgeo.2015.10.004, 2015.

Tejada-Lara, J. V., MacFadden, B. J., Bermudez, L., Rojas, G., Salas-Gismondi, R., and Flynn, J. J.: Body mass predicts isotope enrichment in herbivorous mammals, Proc. R. Soc. B Biol. Sci., 285, 20181020, https://doi.org/10.1098/rspb.2018.1020, 2018.

Trayler, R. B. and Kohn, M. J.: Tooth enamel maturation reequilibrates oxygen isotope compositions and supports simple sampling methods, Geochim. Cosmochim. Acta, 198, 32–47, https://doi.org/10.1016/j.gca.2016.10.023, 2017.

Vidal-Cordasco, M., Ocio, D., Hickler, T., and Marín-Arroyo, A. B.: Ecosystem productivity affected the spatiotemporal disappearance of Neanderthals in Iberia, Nat. Ecol. Evol., 6, 1644–1657, https://doi.org/10.1038/s41559-022-01861-5, 2022.

Zazzo, A., Bendrey, R., Vella, D., Moloney, A. P., Monahan, F. J., and Schmidt, O.: A refined sampling strategy for intra-tooth stable isotope analysis of mammalian enamel, Geochim. Cosmochim. Acta, 84, 1–13, https://doi.org/10.1016/j.gca.2012.01.012, 2012.

Appendix A. Sites description Formatted: English (United States)

A1. Vasco-Cantabrian sites

Axlor (Dima, Vizcaya, País Vasco)

Axlor is a rock-shelter located in Dima (43.2706; -1.8905), with a continuous Middle Paleolithic sequence from the MIS5 to the MIS3 (DeMuro et al., 2023; Pederzani et al., 2023; Marín-Arroyo et al., 2018). It is placed on the southwestern slope of the Dima valleyValley, with an elevation of approximately 320 m above sea level (a.s.l.), at 33 km straight from the present-day coastline, next to one of the lowest mountain passes linking the Cantabrian basins and the Alavese Plateau. The site was discovered in 1932 and initial excavations were performed by Barandiarán (1967-1974). J. M. Barandiarán undertook the excavations between 1967 and 1974, identifying eight Mousterian levels (I-VIII) (Barandiarán, 1980).

From 2000 to 2008, new excavations by González-Urquijo, Ibáñez-Estévez and Rios-Garaizar were achieved and, since 2019, these are ongoing by González-Urquijo and Lazuén. Due to the lack of chronology during Barandiarán excavations, among other aspects, work was focused on obtaining a detailed stratigraphy on the new excavation areas to correlate it with Barandiarán's levels (González-Urquijo & Ibáñez-Estévez, 2021; González Urquijo et al., 2005). The new stratigraphic sequence is roughly equivalent to the previous one,. but with additional levels, not previously identified or excavated by Barandiarán. Some of these levels were deposited before Level VIII (Gómez-Olivencia et al., 2018; 2020). The Middle Paleolithic sequence extends from layers VIII to III (or from N to B-C). Levallois production is predominant in the lower levels (VI to VIII), while Quina Mousterian technocomplex does in the upper ones (from III to V) (Rios-Garaizar, 2012, 2017). New Recent chronological data by radiocarbon (Pederzani et al., 2023; Marín-Arroyo et al., 2018) and OSL (Demuro et al., 2023) methods confirm that a sequence Axlor levels VI, VIII, and VIII probably accumulated during MIS5d–a (109–82 ka), while levels D to B probably were formed during the period encompassing the start of MIS 4 (71–57 ka) through to the beginning or middle of MIS 3 (57–29 ka) (Demuro et al., 2023) and upper Level III to 46,200 ±3,000 BP, which calibrates between 45,510 350 cal BP and the end ofbeyond the calibration curve at > 55,000 cal BP (see Pederzani et al., 2023: Fig. 1)..

The archaeozoological study indicates an anthropic origin of the faunal assemblage with scarce carnivore activity documented (Altuna, 1989; Castaños, 2005; Gómez-Olivencia et al., 2018). In lower layers, the most abundant taxa are *Cervus elaphus* (VIII) and *Capra pyrenaica* (VII), while in upper layers III-V, *Cervus elaphus* is substituted by *Bos primigenious/Bison priscus* and *Equus sp*. The material included in this work comes from the faunal collection of the Barandiarán excavation currently curated at the Bizkaia Museum of Archaeology (Bilbao), where teeth were sampled, and the stable isotope analyses on enamel phosphate were included in Pederzani et al. (2023).

El Castillo (Puente Viesgo, Cantabria)

El Castillo is cave is located in Puente Viesgo (43.2924; -3.9656), with an elevation of approximately 195m a.s.l., at 17 km straight from the present-day coastline. The cave belongs to the karstic system that was formed in the Monte Castillo, which dominates the Pas valleyValley. The site was discovered in 1903 by H. Alcalde del Río. H. Obermaier carried out the first excavation seasons between 1910 and 1914, when many of the archaeological remains were recovered, mainly from the hall of the cavecave hall. These interventions were done under the supervision of the "Institut de Paléontologie Humaine" (IPH) and of Prince Albert I of Monaco. From 1980 to 2011, V. Cabrera and F. Bernaldo de Quirós underwent new excavations focusing on the cave entrance, on the Middle to Upper Paleolithic transitional levels, mainly 16, 18 and 20 (Cabrera-Valdes, 1984). The site has yielded an important stratigraphic sequence, composed by 26 sedimentological

units (1-26) related to different anthropic occupational units, often separated by archaeologically sterile units: Eneolithic (2), Azilian (4), Magdalenian (6 and 8), Solutrean (10), Aurignacian (12, 14, 16 and 18), Mousterian (20, 21 and 22) and Acheulean (24) (Cabrera-Valdés, 1984).

Unit 21 is mostly sterile (Cabrera Valdés, 1984; Martín-Perea et al., 2023), and ~~it was dated by ESR~~ESR dated it, yielding a mean date of 69,000 ± 9,200 years BP (Rink et al., 1997). However, Martín-Perea et al. (2023) suggested some dating uncertainty ~~arising~~ from ~~the interpretation of~~interpreting the initial stratigraphic nomenclature. They suggest that the ESR dates provided for level 21 by Rink et al. (1997) were erroneously attributed to this unit and it might correspond to 20E, indicating that below that subunit, the chronology is older than 70,000 years BP (Martín-Perea et al., 2023). The Mousterian Unit 20 cave is divided into several subunits (Martín-Perea et al., 2023). In Unit 20, a cave roof collapse took place, transforming the cave system into an open rock shelter. This unit contains abundant archaeological and paleontological remains. Lithic industry ~~consistent~~ consists ~~in~~of sidescrapers, denticulates, notches and cleavers, the majority on quartzite and presents both unifacial, bifacial discoid debitage and Levallois debitage. Unit 20E was attributed to Quina Mousterian by Sánchez-Fernández and Bernaldo De Quiros (2009) and contains a Neanderthal tooth ~~remain~~ (Garralda, 2005). Considering the geochronological uncertainties for dates on 20E related ~~with~~ to Rink et al. (1997), we have decided to ~~solely r~~rely sol~~ely~~ on E~~R~~SR date of 47,000 ± 9400 BP provided by Liberda et al. (2010) for this level. Unit 20C presents clear evidence of the Mousterian lithic industry and radiocarbon dates of 48,700±3,400 uncal BP (OxA-22204) and 49,400±3,700 uncal BP (OxA-22205) (Wood et al., 2018) and mean ESR date of 42,700 ±9900 BP (Liberda et al., 2010). Level 19 is archaeologically sterile and separates Unit 20 from Unit 18 (Wood et al., 2018).

Unit 18 is divided into ~~three parts:~~ 18A (archaeologically sterile), 18B, and 18C. Levels 18B and 18C were classified as Transitional Aurignacian, representing a gradual transformation from the Mousterian to the Aurignacian, which is unique to El Castillo cave (Cabrera et al., 2001; Maíllo and Bernaldo de Quirós, 2010; Wood et al., 2018). The ~~dates and the cultural attribution of these levels~~se levels" dates and cultural attribution have been the subject of much debate (e.g. Zilhao and D'Errico, 2003; Wood et al., 2018). According to Wood et al. (2018), the last dates of these levels range between 42,000±1,500 uncal BP (OxA-22203) and 46,000±2,400 uncal BP (OxA-21973), which is much earlier than the start of the Aurignacian period in the Cantabrian region (Marín-Arroyo et al., 2018; Vidal-Cordasco et al., ~~2023~~2022). The lithic assemblage of Unit 18 appears to be dominated by Discoid/Levallois technology (Bernaldo de Quirós and Maíllo-Fernández, 2009) but with a high percentage of "~~"~~Upper Paleolithic~~"~~" pieces. Additionally, punctual bone industry~~, as well as pieces with incisions and engravings,~~ and pieces with incisions and engravings were discovered in Unit 18 (Cabrera-Valdés et al., 2001). Three deciduous tooth crowns attributed to Neanderthals were found in Unit 18B (Garralda et al., 2022). Above, Unit 17 is sterile but contains scarce lithic and faunal materials, while Level 16 was attributed to the Proto-Aurignacian, with dates of 38,600±1,000 uncal BP (OxA-22200) (Wood et al., 2018).

According to Luret et al. (2020), there was a shift in hunting practices between the Late Mousterian (unit 20) and the Transitional Aurignacian (unit 18). During the Late Mousterian, hunting strategies were less specialized, and the species hunted included red deer, horses, and bovines. However, in Unit 18, a specialization in red deer hunting is observed. However, the explanation of this shift has been proposed as a response to a cultural choice or induced by climatic changes. However, recent taphonomic studies by Sanz-Royo et al. (2023) on the old collections of Aurignacian Delta level reveal a more significant role of carnivores than shown by Luret et al. (2020). The material included in this work comes from the faunal collection recovered during the Cabrera-Valdés and Bernaldo de Quirós excavations curated at Museo de Prehistoria y Arqueología de Cantabria (MUPAC, Santander).

Labeko Koba (Arrastre, Guipúzcoa, País Vasco)

Labeko Koba is a cave located in the Kurtzetxiki Hill (43.0619; -2.4833), at 246 m a.s.l. and 29 km straight from the present-day Atlantic coast. In 1987 and 1988, due to the construction of the Arrasate ring road, the site was discoverethe site was discovered due to the construction of the Arrasate ring road, and a savage excavation was carried out (Arrizabalaga, 2000a). Unfortunately, the site was destroyed after that. The stratigraphic sequence identified nine different levels. The lower Level IX was attributed to the Châtelperronian, based on the presence of three Châtelperron points. Although there is a lack of human remains in few Cantabrian Châtelperronian sites, recent research has suggested that this techno-complex was produced by Neanderthals (Maroto et al., 2012; Rios-Garaizar et al., 2022). Level VII marks the beginning of the Aurignacian sequence, likely Proto-Aurignacian, with a lithic assemblage dominated by Dufour bladelets (Arrizabalaga, 2000a). Levels VI, V, and IV contain lithic assemblages that suggested an Early Aurignacian attribution (Arrizabalaga, 2000b; Arrizabalaga et al., 2009). This site is significant because it is one of the few sites with Châtelperronian assemblages and with both Proto-Aurignacian and Early Aurignacian separated (Arrizabalaga et al., 2009).

Initial radiocarbon dates were inconsistent with the stratigraphy of the site and much more recent than expected for the Early Upper Paleolithic (Arrizabalaga, 2000a). This incoherence was determined to be affected by taphonomic alterations (Wood et al., 2014). Later radiocarbon dates undertaken with an ultrafiltrarte pre-treatment provided a new regional framework for the regional Early Upper Paleolithic (Wood et al., 2014). The Châtelperronian layer IX inf is dated to 38,100±900 uncal BP (OxA-22562) and 37,400±800 uncal BP (OxA-22560). The Proto-Aurignacian levels cover a period from 36,850±800 uncal BP (OxA-21766) to 35,250±650 uncal BP (OxA-21793). The three Early Aurignacian levels are dated to 35,100±600 uncal BP (OxA-21778) for level VI, ~ 34,000 uncal BP (OxA-21767 and OxA-21779) for level V, and ~ 33,000 BP (OxA-21768 and OxA-21780) for level IV (Arrizabalaga et al., 2009).

Taphonomic studies indicate an alternation in the use of the cave between carnivores and humans, the latter ones during short occupation periods (Villaluenda et al., 2012; Ríos-Garaizar et al., 2012; Arrizabalaga et al., 2010). Labeko Koba is considered to have functioned as a natural trap where carnivores, mainly hyenas, accessed to animal carcasses. At least in the base of Labeko Koba IX, carnivore activity was higher, and they would have consumed the same prey as humans (Villaluenga et al., 2012). The presence of humans is linked to strategic use as a campsite associated with a small assemblage of lithic artifacts. The most consumed species by Châtelperronian groups were red deer, followed by the consumption of large bovids, equids, and woolly rhinoceros. During the Aurignacian period, there was some stability in human occupations, although they still alternated with carnivore occupations (Arrizabalaga et al., 2010). Cold-adapted fauna such as reindeer and woolly rhinoceros were identified in association with the Châtelperronian. Reindeer were still present during the Aurignacian levels, as well as the woolly mammoth and arctic foxand the woolly mammoth and arctic fox were still present during the Aurignacian levels. The original sampling of the studied teeth studied by this work was performed in the San Sebastian Heritage Collection headquarters, where the Guipuzcoa archaeological materials were deposited at that time.

Aitzbitarte III interior (Renteriia, Guipúzcoa, País Vasco)

Aitzbitarte III is an archaeological site located within a the Landarbaso karstic system comprising of nine caves in Renteria (43.270; -1.8905). The cave is situated 220 m.a.s.l. and is 10 km away from the present-day coastline. Initial archaeological interventions were carried out at the end of the 19th century by P.M. de Soraluce (Altuna, 2011). Recent excavations were initially conducted in the deep zone inside the cave between 1986 and 1993, where the studied tooth was recovered, and later focused on the cave entrance between 1994 and 2002, by J. Altuna, K. Mariezkurrena, and J. Ríos-Garaizar (Altuna et al., 2011; 2017).

While the cave's entrance area contains a sequence comprising possible Mousterian and ~~,~~ Evolved Aurignacian~~,~~ and Gravettian ~~layers~~ levels (Altuna et al., 2011; 2013), the stratigraphy in the inner cave presents ~~8~~ eight levels: level VIII (some tools with Mousterian features), VII (sterile), VIb, VIa and V (Middle Gravettian technocomplex with abundance of Noailles burins), IV-II (disturbed archaeological levels) and I (surface) (Altuna et al., 2017). Levels V have dates of 24,910 uncal BP (I-15208) and 23,230 uncal BP (Ua-2243); whereas level VI extends from 23,830 ± 345 uncal BP (Ua-2628) and 25,380± 430 uncal BP (Ua-2244) (Altuna, 1992; Altuna et al., 2017), with a possible outlier dated at 21,130 uncal BP (Ua-1917).

The Gravettian occupation in the inner part of the cave was ~~originally~~ initially thought to be more recent than the one~~s~~ in the cave entrance. However, it was not ~~difficult~~ easy to correlate the two excavation areas due to different sedimentation rates. The ~~rich~~ abundant human occupations took place during a singular cold phase in the Middle Gravettian with a specialized paleoeconomy focused on the hunting of *Bos primigenius* and *Bison priscus* (85% in level VI and 68% in level V), which is unusual in the Cantabrian region mostly focused on red deer and ibex. Other ungulates present are *Cervus elaphus* and *Rupicapra rupicapra*, and to a lesser extent *Capra pyrenaica, Capreolus capreolus, Rangifer tarandus*, and *Equus ferus* (Altuna et al., 2017; Altuna & Mariezkurrena, 2020). There is a scarce representation of carnivores. The tooth studied was sampled at the Gordailua Center for Heritage Collections of the Provincial Council of Gipuzkoa.

El Otero (Secadura, Voto, Cantabria)

El Otero cave is located in Secadura (Voto) (43.3565; -3.5360), at 129 m.s.a.l and 12 km ~~straight~~ from the present-day coastline~~. N,~~ near the Matienzo valley in a coastal plain environment covered by meadows and gentle hills. The discovery was made in 1908 by Lorenzo Sierra. The site was excavated in 1963 by J. Gonzalez Echegaray and M.A. García Guinea, in two different sectors (Sala I and Sala II) with an equivalent stratigraphic sequence (González Echegaray, 1966). ~~A total of n~~Nine levels were identified in Sala I, from level IX to level I. Levels IX and VIII were ~~originally~~ initially related to the "Aurignacian-Mousterian, based on lithics assemblages with a combination of both technocomplex features. The overlying levels VI-IV were separated by a speleothem crust (level VII) and were initially related to Aurignacian, due to the presence of end-scrappers, bone points, blades, or burins on truncation (Freeman, 1964; Rios-Garaizar, 2013). Also, perforated deer, ibex, and fox teeth were found in levels V and IV. This site lacked chronological dating methods, until a selection of material from levels VI, V and IV revealed a difference in chrono-cultural attribution (Marín-Arroyo et al., 2018). Radiocarbon results yielded younger dates for such a cultural attribution and show~~ed~~ significant stratigraphic inconsistency. Level VI gave a result of 12,415±55 (OxA-32585), two dates in Level V are 12,340±55 (OxA-32509) and 10,585±50 (OxA-32510), and a date in Level IV is 15,990±80 (OxA-32508). All these results fall into the range of the Late Upper Paleolithic (Magdalenian-Azilian initially identified in levels III-I), eliminating attribution of these levels to the Aurignacian~~,~~ despite the presence of apparently characteristic artefacts. Further assessments of archaeological materials will be needed.

Red deer dominate the assemblage, except for level IV where horses are more abundant. Wild boar, roe deer, and ibex are also present, but large bovids are relatively rare (González Echegaray, 1966). Level IV is the richest and most anthropogenic level, with evidence of butchering in red deer (captured in winter and early summer) and chamois (in autumn). The formation of this level involved humans and carnivores, and although certain data may suggest an anthropogenic predominance, the limited sample analyzed taphonomically and the pre-selection of preserved pieces do not allow for a definitive conclusion (Yravedra & Gómez-Castanedo, 2010). The material included in this work is curated at the Museo de Prehistoria y Arqueología de Cantabria (MUPAC, Santander).

A2. Mediterranean sites

Terrasses de la Riera dels Canyars (Gavà, Barcelona, Cataluña)

Terrasses de la Riera dels Canyars (henceforth, Canyars) is an open-air site located near Gavà (Barcelona) (41.2961;1.9797), at 28 m.s.a.l and 3 km straight from the present-day coastline. The site lies on a fluvial terrace at the confluence of Riera dels Canyars, a torrential stream between Garraf Massif, Llobregat delta and Riera de Can Llong (Daura et al., 2013). Archaeo-paleontological remains were discovered during quarries activities in 2005 and was complete excavated on 2007 by the *Grup de Recerca del Quaternari* (Daura and Sanz, 2006; Daura et al., 2013). This intervention determined nine lithological units. The paleontological and archaeological remains come exclusively from one unit, the middle luthitic unit (MLU), and specifically from layer I. The MLU is composed of coarse sandy clays and gravels, filling a paleochannel network named lower detrital unit (LDU) (Daura et al., 2013). Five radiocarbon dates were obtained on charcoals from layer I, which yield statistically consistent ages from 33,800 ±350 uncal BP to 34,900 ±340 uncal BP, which results in mean age of 39,600 cal BP (from 37,405 to 40,916 cal BP) (Daura et al., 2013).

The layer I of the site has yielded a rich faunal assemblage, consisting of over 5,000 remains. Among the herbivores, the most common species found are *Equus ferus*, *Bos primigenius*, *Equus hydruntinus*, and *Cervus elaphus* (Daura et al., 2013; Sanz-Royo et al., 2020). *Capra* sp. and *Sus scrofa are* also present, although in lower frequencies. The carnivores found at the site are also noteworthy, with *Crocuta crocuta* and *Lynx pardinus* being the most frequent. Presence of cold-adapted fauna associated to stepped environments is recorded, such as cf. *Mammuthus* sp., *Coelodonta antiquitatis*, and *Equus hydruntinus*. Small mammal analysis, pollen, and use-wear analysis have provided further evidence that a steppe-dominated landscape surrounded the Canyars site, supporting a correlation with the Heinrich Event 4, in coherence with the chronology obtained for the layer (López-García et al. 2013; 2023; Rivals et al., 2017). However, the presence of woodland is also attested by forest taxa within charcoal and pollen assemblages (Daura et al., 2013).

Taphonomic study is ongoing. But several evidences point that hyenas have played an important role in the accumulation of the faunal assemblage (Daura et al., 2013; Jimenez et al. 2019). However, sporadic human presence is documented by few human modifications found in faunal remains (cutmarks and fire alterations). Although the paucity of the lithic assemblage in the site, it shows a clear attribution to Upper Palaeolithic technocomplex, most likely the Early Aurignacian (Daura et al., 2013). Recently, it was documented a perforated bone fragment, which has been identified as a perforated board for leather production (Doyon et al., 2023). All teeth included in this work were sampled in *Laboratori de la Guixera* (Ajuntament de Casteldefels) where the material is stored.

References Appendix A

Altuna, J., Mariezkurrena, K., de la Peña, P., Rios-Garaizar, J. 2011. Ocupaciones Humanas En La Cueva de Aitzbitarte III (Renteria, País Vasco) Sector Entrada: 33.000-18.000 BP. Servicio Central de Publicaciones del Gobierno Vasco; EKOB: 11–21.

Altuna, J., Mariezkurrena, K., de la Peña, P., Rios-Garaizar, J. 2013. Los niveles gravetienses de la cueva de Aitzbitarte III (Gipuzkoa). Industrias y faunas asociadas, in: de las Heras, C., Lasheras, J.A., Arrizabalaga, Á., de la Rasilla, M. editors. Pensando El Gravetiense: Nuevos Datos Para La Región Cantábrica En Su Contexto Peninsular Y Pirenaico. Monografías Del Museo Nacional Y Centro de Investigación de Altamira, 23. Madrid: Ministerio de Educación, Cultura; pp. 184–204.

Altuna, J. & Mariezkurrena, K. 2020. Estrategias de caza en el Paleolítico superior de la Región Cantábrica. El caso de Aitzbitarte II (zona profunda de la cueva). Sagvntvm-Extra 21, Homenaje al Profesor Manuel Pérez Ripoll: 219-225.

Altuna, J., Mariezkurrena, K., Ríos Garaizar, J., & San Emeterio Gómez, A. 2017. Ocupaciones Humanas en Aitzbitarte III (País Vasco) 26.000 - 13.000 BP (zona profunda de la cueva). Servicio Central de Publicaciones del Gobierno Vasco. EKOB; 8: 348pp.

Arrizabalaga, A., 2000a. El yacimiento arqueológico de Labeko Koba (Arrasate, País Vasco). Entorno. Crónica de las investigaciones. Estratigrafía y estructuras. Cronología absoluta. In: Arrizabalaga, A., Altuna, J. (Eds.), Labeko Koba

1750   (País Vasco). Hienas y Humanos en los Albores del Paleolítico Superior, Munibe (Antropologia-Arkeologia) 52. Sociedad
1751   de Ciencias Aranzadi, San Sebastián-Donostia, pp. 15-72.
1752 Arrizabalaga, A., 2000b. Los tecnocomplejos líticos del yacimiento arqueológico de Labeko Koba (Arrasate, País Vasco). In:
1753   Arrizabalaga, A., Altuna, J. (Eds.), Labeko Koba (País Vasco). Hienas y Humanos en los Albores del Paleolítico Superior,
1754   Munibe (Antropologia-Arkeologia) 52. Sociedad de Ciencias Aranzadi, San Sebastián-Donostia, pp. 193-343.
1755 Arrizabalaga, A., Iriarte, E., Ríos-Garaizar, J., 2009. The Early Aurignacian in the Basque Country. Quaternary International, 207:
1756   25–36.
1757 Arrizabalaga, A., Iriarte, M.J. & Villaluenga, A. 2010. Labeko Koba y Lezetxiki (País Vasco). Dos yacimientos, una problemática
1758   común. Zona Arqueológica, 13: 322-334.
1759 Barandiarán JM. 1980. Excavaciones en Axlor. 1967- 1974. En: Barandiarán, J. M.: Obras Completas. Tomo XVII; pp. 127-384.
1760 Bernaldo de Quirós, F., Maíllo-Fernández, J.-M. 2009. Middle to Upper Palaeolithic at Cantabrian Spain. In: Camps M, Chauhan
1761   PR (eds) A sourcebook of Palaeolithic transitions: methods, theories and interpretations. Springer, New York, pp. 341–
1762   359.
1763 Cabrera-Valdes, V. 1984. El Yacimiento de la cueva de «El Castillo» (Puente Viesgo, Santander). Bibliotheca Praehistorica Hispana
1764   22, C.S.I.C., 485 p.
1765 Cabrera-Valdes, V., Maillo-Fernandez, J.M., Lloret, M., Bernaldo De Quiros, F. 2001. La transition vers le Paléolithique supérieur
1766   dans la grotte du Castillo (Cantabrie, Espagne) la couche 18. L'Anthropologie 105, pp. 505–532.
1767 Daura, J., Sanz, M. (2006). Informe de la troballa del jaciment arqueològic "Terrasses dels Canyars" (Castelldefels-Gavà).
1768   Notificació de la descoberta i propostes d'actuació. Grup de Recerca del Quaternari, SERP, UB. Servei d'Arqueologia i
1769   Paleontologia, Departament de Cultura i Mitjans de Comunicació, Generalitat de Catalunya. Unpublished Archaeological
1770   Report.
1771 Daura, J., Sanz, M., García, N., Allué, E., Vaquero, M., Fierro, E., Carrión, J. S., López-García, J. M., Blain, H. A., Sánchez-Marco,
1772   A., Valls, C., Albert, R. M., Fornós, J. J., Julià, R., Fullola, J. M., Zilhão, J. 2013. Terrasses de la Riera dels Canyars
1773   (Gavà, Barcelona): The landscape of Heinrich stadial 4 north of the "Ebro frontier" and implications for modern human
1774   dispersal into Iberia. Quaternary Science Reviews, 60, 26–48.
1775 Demuro, M., Arnold, L., González-Urquijo, J., Lazuen, T., Frochoso, M. 2023. Chronological constraint of Neanderthal cultural and
1776   environmental changes in southwestern Europe: MIS 5–MIS 3 dating of the Axlor site (Biscay, Spain). Journal of
1777   Quaternary Research
1778 Doyon, L., Faure, T., Sanz, M., Daura, J., Cassard, L., D'Errico, F., 2023. A 39,600-year-old leather punch board from Canyars,
1779   Gavà, Spain. Scientific Advances, 9. https://doi.org/10.1126/sciadv.adg0834
1780 Freeman, L.G. 1964. Mousterian Developments in Cantabrian Spain. Ph.D. thesis. Dept. of Anthropology, University of Chicago,
1781   Chicago.
1782 Garralda, M.D. 2005. Los Neandertales en la Península Ibérica:The Neandertals from the Iberian Peninsula. Munibe (Antropologia-
1783   Arkeologia) 57, Homenaje a Jesús Altuna. pp. 289–314.
1784 Garralda, M.D., Madrigal, T., Zapata, J., & Rosell, J. 2022. Neanderthal deciduous tooth crowns from the Early Upper Paleolithic at
1785   El Castillo Cave (Cantabria, Spain). Archaeological and Anthropological Sciences.
1786 Gómez-Olivencia, A., Arceredillo, D., Álvarez-Lao, D.J., Garate, D., San Pedro, Z., Castaños, P., Rios-Garaizar, J., 2014. New
1787   evidence for the presence of reindeer (Rangifer tarandus) on the Iberian Peninsula in the Pleistocene: an
1788   archaeopalaeontological and chronological reassessment. Boreas 43, 286–308.
1789 Gómez-Olivencia, A., Sala, N., Núñez-Lahuerta, C., Sanchis, A., Arlegi, M., Rios-Garaizar, J., 2018. First data of Neandertal bird
1790   and carnivore exploitation in the Cantabrian Region (Axlor; Barandiaran excavations; Dima, Biscay, Northern Iberian
1791   Peninsula). Scienti. Rep. 8, 10551.
1792 González Echegaray, J.G. 1966. Cueva del Otero. Excavaciones Arqueológicas en España, 53. Madrid: Ministerio de Educación
1793   Nacional Dirección General de Bellas Artes Servicio Nacional de Excavaciones.
1794 González-Urquijo, J.E., Ibáñez-Estévez, J.J. 2001. Abrigo de Axlor (Dima). Arkeoikuska: Investigación arqueológica 2001; 2002:
1795   90–93.
1796 González Urquijo, J.E., Ibáñez Estévez, J.J., Rios-Garaizar, J., Bourguignon, L., Castaños Ugarte, P., Tarriño Vinagre, A. 2005.
1797   Excavaciones recientes en Axlor. Movilidad y planificación de actividades en grupos de neandertales. In: Montes Barquín
1798   R, Lasheras Corruchaga JA, editors. Actas de La Reunión Científica: Neandertales Cantábricos. Estado de La Cuestión.
1799   Monografías Del Museo Nacional Y Centro de Investigación de Altamira No 20. Madrid: Ministerio de Cultura; 2005. pp.
1800   527–539.
1801 Jimenez, I. J., Sanz, M., Daura, J., Gaspar, I. D., García, N. 2019. Ontogenetic dental patterns in Pleistocene hyenas (Crocuta
1802   crocuta Erxleben, 1777) and their palaeobiological implications. International Journal of Osteoarchaeology, 29, 808–821.
1803 Liberda, J.J., Thompson, J.W., Rink, W.J., Bernaldo de Quirós, F., Jayaraman, R., Selvaretinam, K., Chancellor-Maddison, K.,
1804   Volterra, V., 2010. ESR dating of tooth enamel in Mousterian layer 20, El Castillo, Spain. Geoarchaeology n/a-n/a.
1805 López-García, J.M., Blain, H.A., Fagoaga, A., Bandera, C.S., Sanz, M., Daura, J., 2022. Environment and climate during the
1806   Neanderthal-AMH presence in the Garraf Massif mountain range (northeastern Iberia) from the late Middle Pleistocene
1807   to Late Pleistocene inferred from small-vertebrate assemblages. Quaternary Science Reviews, 288.
1808 López-García, J. M., Blain, H.-A., Bennàsar, M., Sanz, M., Daura, J. 2013. Heinrich event 4 characterized by terrestrial proxies in
1809   southwestern Europe. Climate of the Past, 9: 1053–1064.

Luret, M., Blasco, R., Arsuaga, J.L., Baquedano, E., Pérez-González, A., Sala, N., & Aranburu, A. 2020. A multi-proxy approach to the chronology of the earliest Aurignacian at the El Castillo Cave (Spain). Journal of Archaeological Science: Reports, 33: 102339.

Maroto, J., Vaquero, M., Arrizabalaga, Á., Baena, J., Baquedano, E., Jordá, J., Julià, R., Montes, R., Van Der Plicht, J., Rasines, P., Wood, R., 2012. Current issues in late Middle Palaeolithic chronology: New assessments from Northern Iberia. Quaternary International, 247: 15–25.

Marín-Arroyo, A.B., Rios-Garaizar, J., Straus, L.G., Jones, J.R., de la Rasilla, M., González Morales, M.R., Richards, M., Altuna, J., Mariezkurrena, K., Ocio, D., 2018. Chronological reassessment of the Middle to Upper Paleolithic transition and Early Upper Paleolithic cultures in Cantabrian Spain. PLoS One 13: 1–20.

Martín-Perea, D.M., Maíllo-Fernández, J., Marín, J., Arroyo, X., Asiaín, R., 2023. A step back to move forward: a geological re-evaluation of the El Castillo Cave Middle Palaeolithic lithostratigraphic units (Cantabria, northern Iberia). Journal of Quaternary Science, 38: 221–234.

Pederzani, S., Britton, K., Jones, J.R., Agudo Pérez, L., Geiling, J.M., Marín-Arroyo, A.B., 2023. Late Pleistocene Neanderthal exploitation of stable and mosaic ecosystems in northern Iberia shown by multi-isotope evidence. Quaternary Research: 1–25.

Rink, W.J., Schwarcz, H.P., Lee, H.K., Cabrera Valdés, V., Bernaldo de Quirós, F., Hoyos, M. 1997. ESR dating of Mousterian levels at El Castillo Cave, Cantabria, Spain. Journal of Archaeological Science, 24 (7): 593-600.

Rios-Garaizar J. 2012. Industria lítica y sociedad en la Transición del Paleolítico Medio al Superior en torno al Golfo de Bizkaia. Santander: PUbliCan - Ediciones de la Universidad de Cantabria.

Rios-Garaizar, J. 2017. A new chronological and technological synthesis for Late Middle Paleolithic of the Eastern Cantabrian Region. Quaternary International, 433: 50-63.

Rios-Garaizar, J., Arrizabalaga, A. & Villaluenga, A. 2012. Haltes de chasse du Châtelperronien de la Péninsule Ibérique: Labeko Koba et Ekain (Pays Basque Péninsulaire). L'Anthropologie, 116: 532–549.

Rios-Garaizar, J., de la Peña, P., Maillo-Fernández, J.M. 2013. El final del Auriñaciense y el comienzo del Gravetiense en la región cantábrica: una visión tecno-tipológica. In: de las Heras C., Lasheras J.A., Arrizabalaga Á., de la Rasilla M. (Eds.), Pensando El Gravetiense: Nuevos Datos Para La Región Cantábrica En Su Contexto Peninsular Y Pirenaico. Monografías Del Museo Nacional Y Centro de Investigación de Altamira, 23. Madrid: Ministerio de Educación, Cultura; pp. 369–382.

Rios-Garaizar, J., Iriarte, E., Arnold, L.J., Sánchez-Romero, L., Marín-Arroyo, A.B., San Emeterio, A., Gómez-Olivencia, A., Pérez-Garrido, C., Demuro, M., Campaña, I., Bourguignon, L., Benito-Calvo, A., Iriarte, M.J., Aranburu, A., Arranz-Otaegi, A., Garate, D., Silva-Gago, M., Lahaye, C., Ortega, I. 2022. The intrusive nature of the Châtelperronian in the Iberian Peninsula. PLoS One 17, e0265219.

Rivals, F., Uzunidis, A., Sanz, M., Daura, J., 2017. Faunal dietary response to the Heinrich Event 4 in southwestern Europe. Palaeogeogr. Palaeoclimatol. Palaeoecol. 473, 123–130.

Sanz-Royo, A., Sanz, M., Daura, J. (2020). Upper Pleistocene equids from Terrasses de la Riera dels Canyars (NE Iberian Peninsula): The presence of Equus ferus and Equus hydruntinus based on dental criteria and their implications for palaeontological identification and palaeoenvironmental reconstruction. Quaternary International, 566–567, 78–90.

Sanz-Royo, A., Terlato, G., Marín-Arroyo, A.B., 2024. Taphonomic data from the transitional Aurignacian of El Castillo cave (Spain) reveals the role of carnivores at the Aurignacian Delta level. Quaternary Science Advances, 13: 100147. https://doi.org/10.1016/j.qsa.2023.100147

Vidal-Cordasco, M., Ocio, D., Hickler, T., Marín-Arroyo, A.B., 2022. Ecosystem productivity affected the spatiotemporal disappearance of Neanderthals in Iberia. Nat. Ecol. Evol. 6, 1644–1657.

Villaluenga, A., Arrizabalaga, A. & Rios-Garaizar, J. 2012. Multidisciplinary approach to two Châtelperronian series: lower IX layer of Labeko Koba and X Level of Ekain (Basque country, Spain). Journal of Taphonomy, 10: 525–548.

Wood, R.E., Arrizabalaga, A., Camps, M., Fallon, S., Iriarte-Chiapusso, M.J., Jones, R., Maroto, J., De la Rasilla, M., Santamaría, D., Soler, J., Soler, N., Villaluenga, A., Higham, T.F.G. 2014. The chronology of the earliest Upper Palaeolithic in northern Iberia: New insights from L'Arbreda, Labeko Koba and La Viña. Journl of Human Evolution, 69: 91–109. https://doi.org/10.1016/j.jhevol.2013.12.017

Wood, R., Bernaldo de Quirós, F., Maíllo-Fernández, J.M., Tejero, J.M., Neira, A., Higham, T. 2018. El Castillo (Cantabria, northern Iberia) and the Transitional Aurignacian: Using radiocarbon dating to assess site taphonomy. Quaternary International, 474: 56–70.

Yravedra, J., & Gómez-Castanedo, A. 2010. Estudio zooarqueológico y tafonómico del yacimiento del Otero (Secadura, Voto, Cantabria). Espacio, Tiempo y Forma. Serie I, Nueva época. Prehistoria y Arqueología, 3: 21-38

Zilhao, J., DEerrico, F. 2003 The chronology of the Aurignacian and Transitional technocomplexes. Where do we stand? In Zilhão, J. et d'Errico, F. eds., The chronology of the Aurignacian and of the transitional technocomplexes Dating, stratigraphies, cultural implications Proceedings of Symposium 6.1 of the XIVth Congress of the UISPP, pp. 313–349.

 Appendix C. Intratooth curve plots

1868 Original curves derived from enamel intratooth sampling on enamel carbonate. Provided by sites. In blue,
1869 oxygen stable isotope composition (δ¹⁸O), and, in brown, carbon stable isotope composition (δ¹³C). In the
1870 x-axis, the distance from Enamel Rooth Junction (ERJ). Notice that the y-axis can experience some
1871 variations between sites.
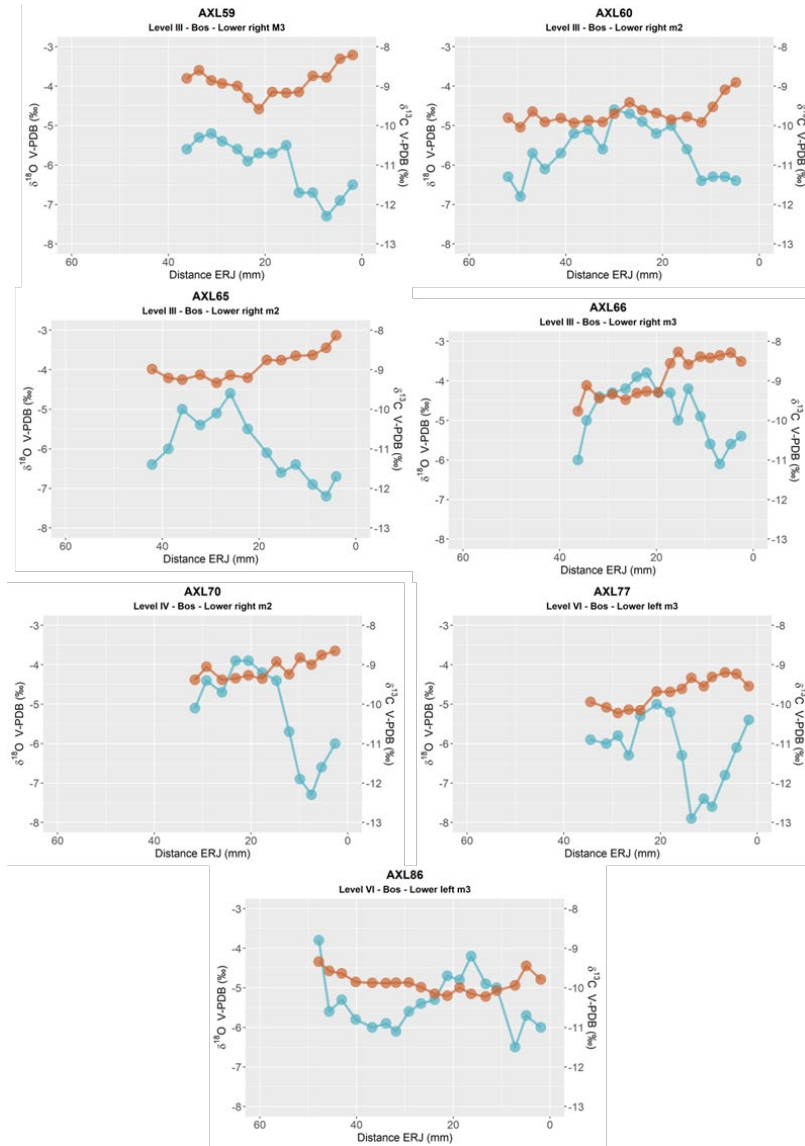
1872

1873 **Figure C1.** Intratooth plots of oxygen (δ¹⁸O) and carbon (δ¹³C) isotope composition from teeth from Axlor, considering distance
1874 from enamel root junction (ERC).

1875

1876
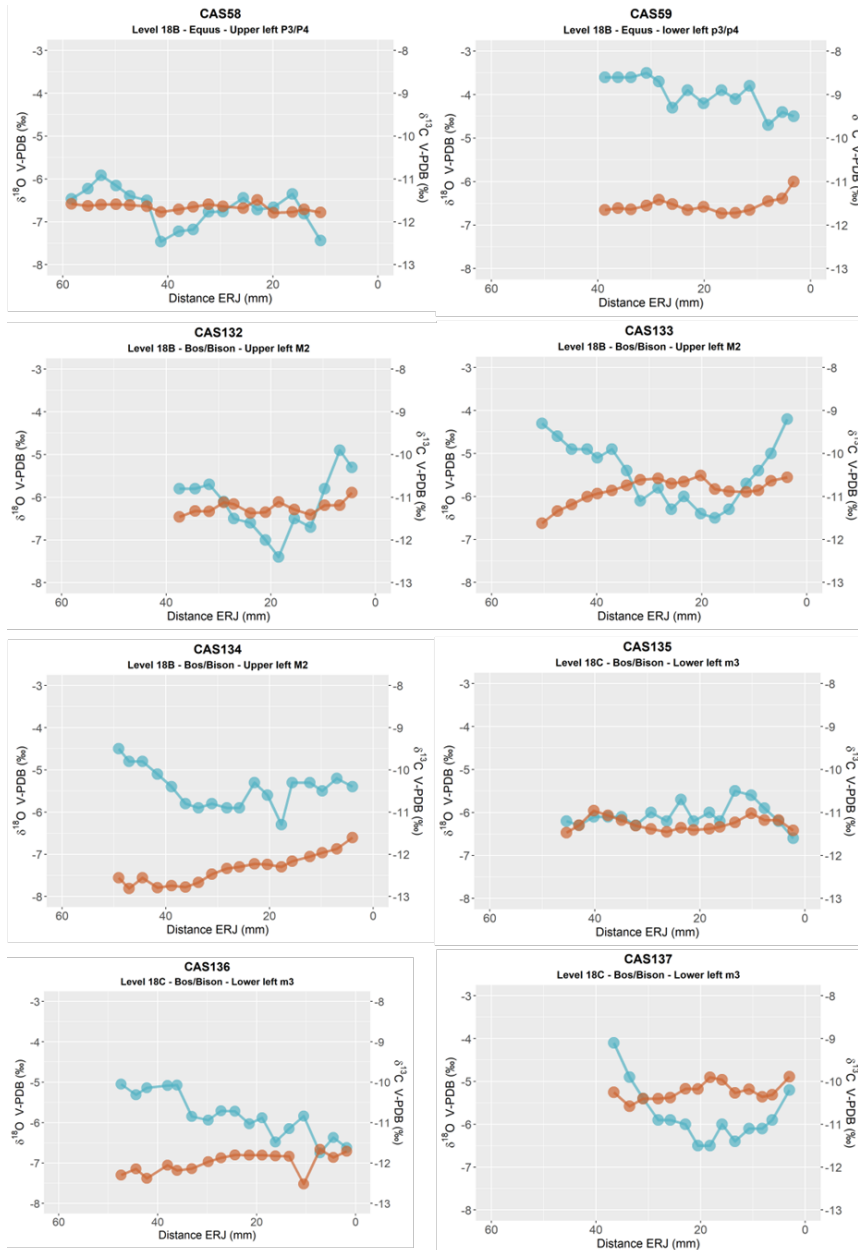
1877

Figure C2. Intratooth plots of oxygen (δ18O) and carbon (δ13C) isotope composition from teeth from El Castillo, considering the sample's distance from the enamel root junction (ERC).
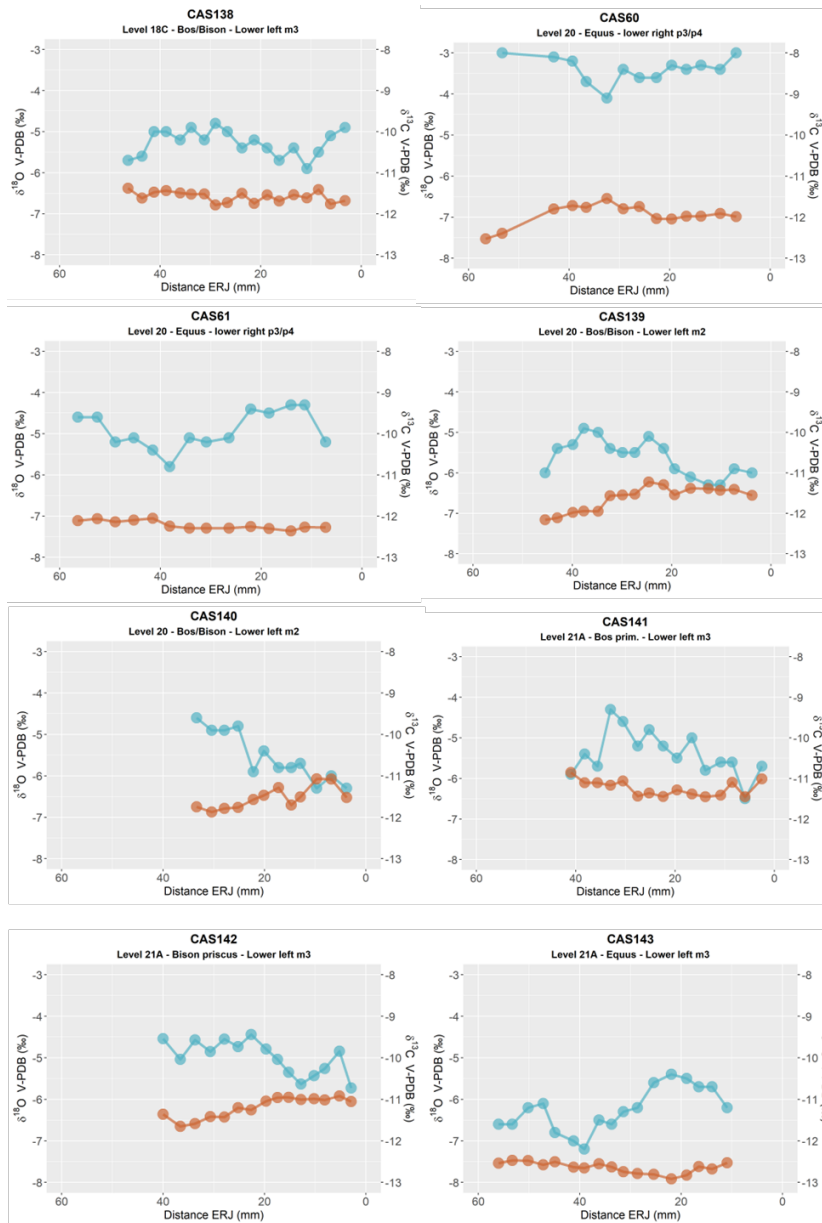
1880

Figure C3. Intratooth plots of oxygen (δ18O) and carbon (δ13C) isotope composition from teeth from El Castillo, considering the sample's distance from the enamel root junction (ERC).

1881
1882

1883

1884
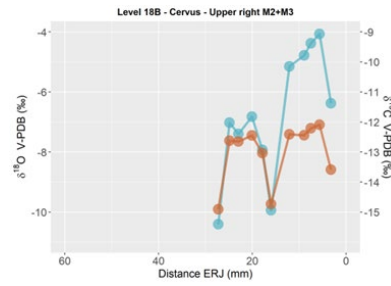
1885

1886 **Figure C4.** Intratooth plots of oxygen (δ18O) and carbon (δ13C) isotope composition from teeth from El Castillo, considering the
1887 sample's distance from the enamel root junction (ERC).

1888
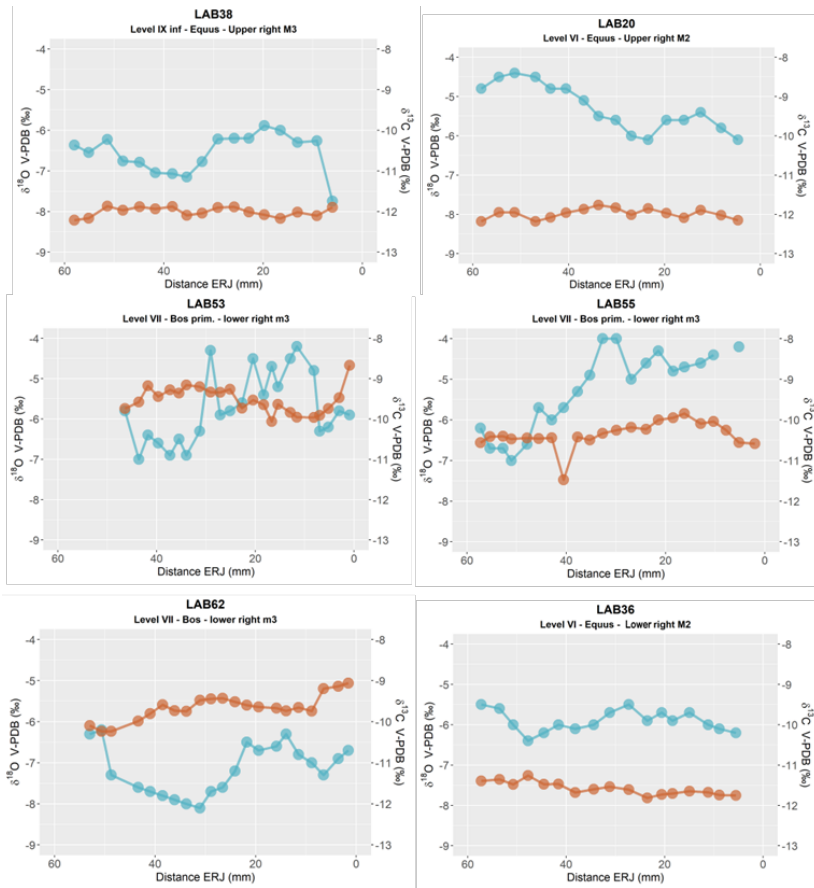
1889

1890 **Figure C5.** Intratooth plots of oxygen (δ18O) and carbon (δ13C) isotope composition from teeth from Labeko Koba, considering the
1891 sample's distance from the enamel root junction (ERC).
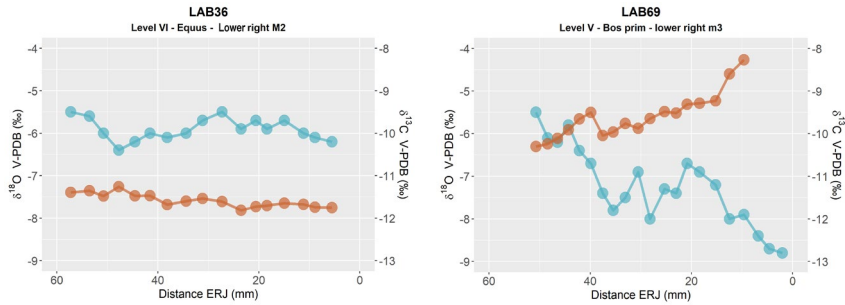
1892
1893
1894
1895
1896
1897
1898
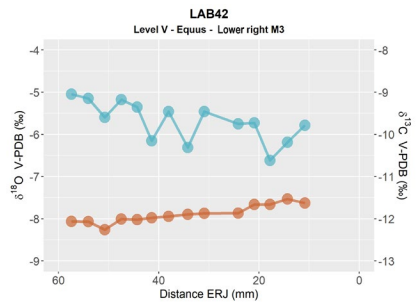
1899 **Figure C6.** Intratooth plots of oxygen (δ18O) and carbon (δ13C) isotope composition from teeth from Labeko Koba, considering the
1900 sample's distance from the enamel root junction (ERC).

1901

1902
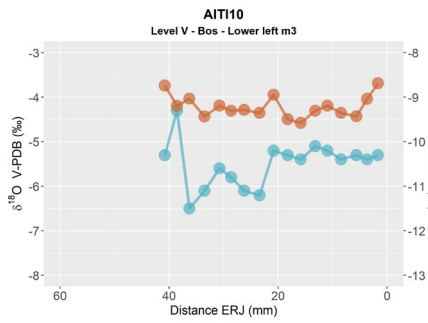
1903

1904 **Figure C7.** Intratooth plots of oxygen (δ18O) and carbon (δ13C) isotope composition from teeth from Aitzbitarte III interior,
1905 considering the sample's distance from the enamel root junction (ERC).
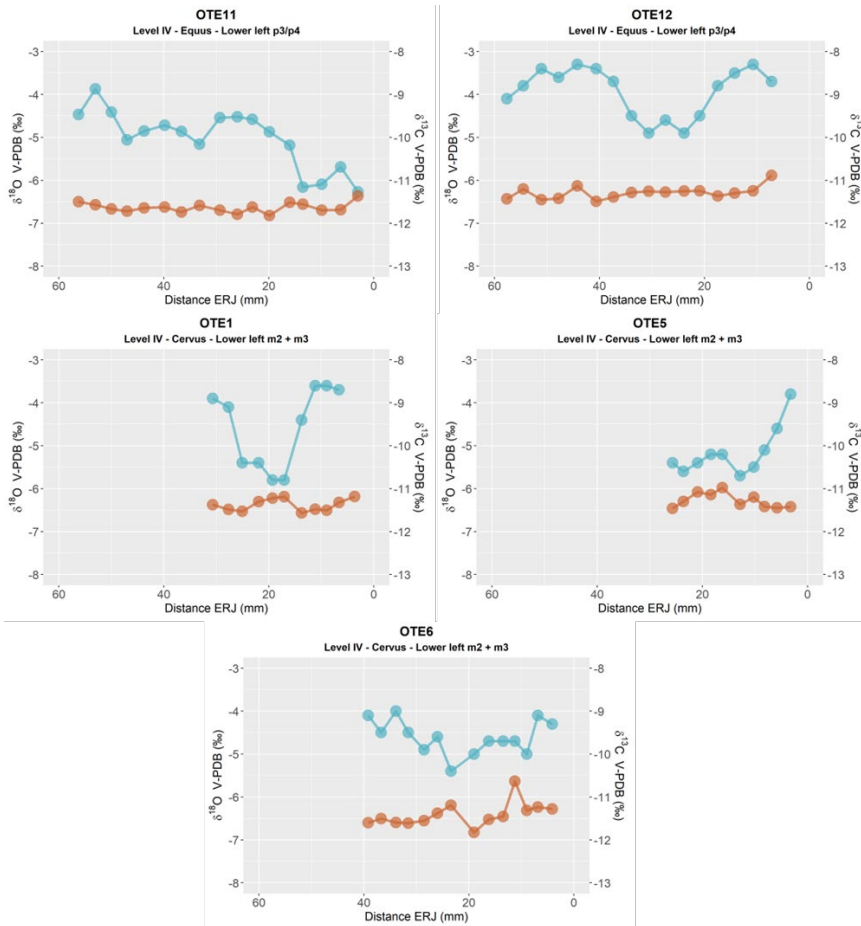
1906

Figure C8. Intratooth plots of oxygen (δ¹⁸O) and carbon (δ¹³C) isotope composition from teeth from El Otero, considering the sample's distance from the enamel root junction (ERC).
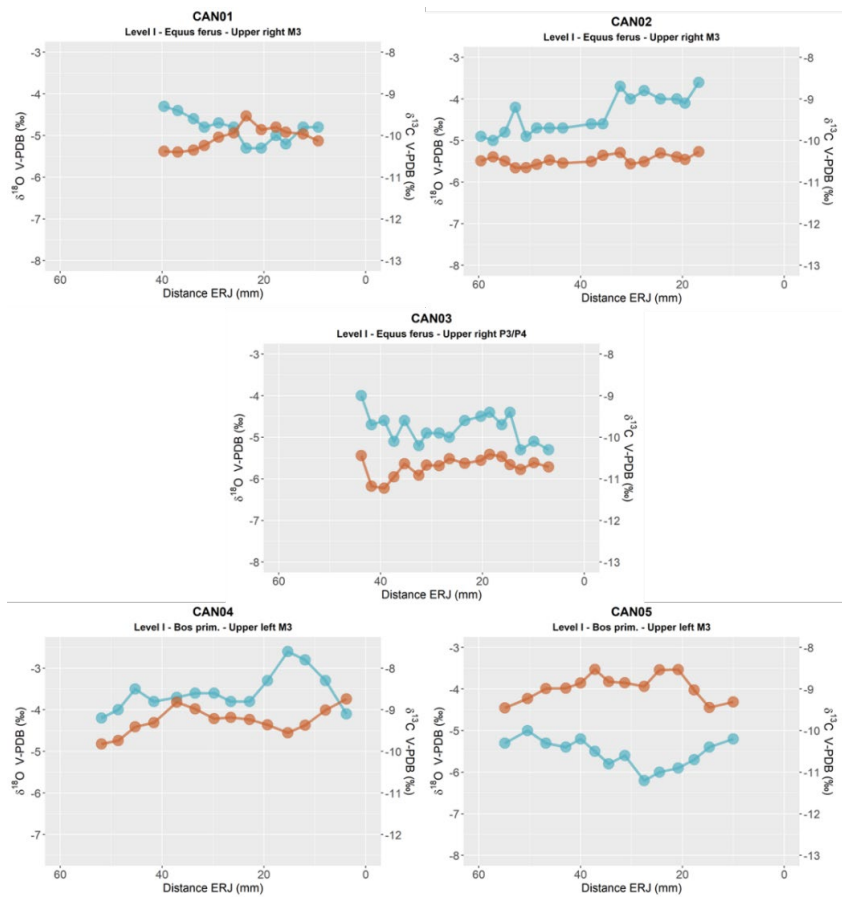
1909

Figure C9. Intratooth plots of oxygen (δ18O) and carbon (δ13C) isotope composition from teeth from Canyars considering the sample's distance from the enamel root junction (ERC).

Appendix D. Inverse Modelling: Methodological Details and Models

The intratooth $\delta^{18}O$ profiles presented in this study were obtained through the application of inverse modelling, using an adapted version of the code published in reference (Passey et al., 2005b). This modeling approach allowed for the correction of the damping effect and the reconstruction of the original $\delta^{18}O\delta18O$ input time series. The model reproduces the temporal delay between $\delta^{18}O$ changes in the animal's input and their manifestation in tooth enamel, exhibiting a consistent x-direction delay in the modelled $\delta^{18}O$ curve relative to the enamel $\delta^{18}O$ input time series. The model utilizes different species-specific parameters related to enamel formation, which vary between bovines and equids. These parameters have been established based on previous studies (Bendrey et al., 2015; Zazzo et al., 2012; Passey and Cerling, 2002; Kohn, 2004; Blumenthal et al., 2014). For *Bos/Bison* sp., the initial mineral content of enamel is fixed at 25%, the enamel appositional length is set at 1.5 mm, and the maturation length is 25 mm. For *Equus* sp., the initial mineral content of enamel is fixed at 22%, the enamel appositional length is set at 6 mm, and the maturation length is 28 mm.

In addition, the model requires other variables related to sampling geometry, as well as error estimates derived from mass spectrometer measurements. The distance between samples varies for each tooth, but as a general trend, the sampling depth on the tooth enamel surface in the samples of this study represents approximately 70% of the total enamel depth. The standard deviation of the measurements obtained from the mass spectrometer was typically set at 0.12%, taking into account the uncertainty associated with the standards. Finally, the models require a damping factor that determines the cumulative damping along the isotopic profile by adjusting the measured error (Emeas) to the prediction error (Epred). In the teeth analysed in this study, the damping factor ranged from 0.001 to 0.1.

The most likely model solutions were selected, and summer and winter values were extracted from the $\delta^{18}O$ profiles, considering the original peaks and troughs identified in the unmodelled $\delta^{18}O$ profile. This approach was adopted to prevent the introduction of artificial peaks that the model may produce, particularly in teeth without a distinct sinusoidal shape. Flat and less sinusoidal profile are less suitable for the application of the model, given its inherent assumption of an approximately sinusoidal form. Non-sinusoidal curves can lead to complex interpretations in the model outcomes. Consequently, this methodology was not applied to analysed intratooth $\delta^{13}C$ profiles, as the examined individuals did not exhibit appreciable seasonal change.
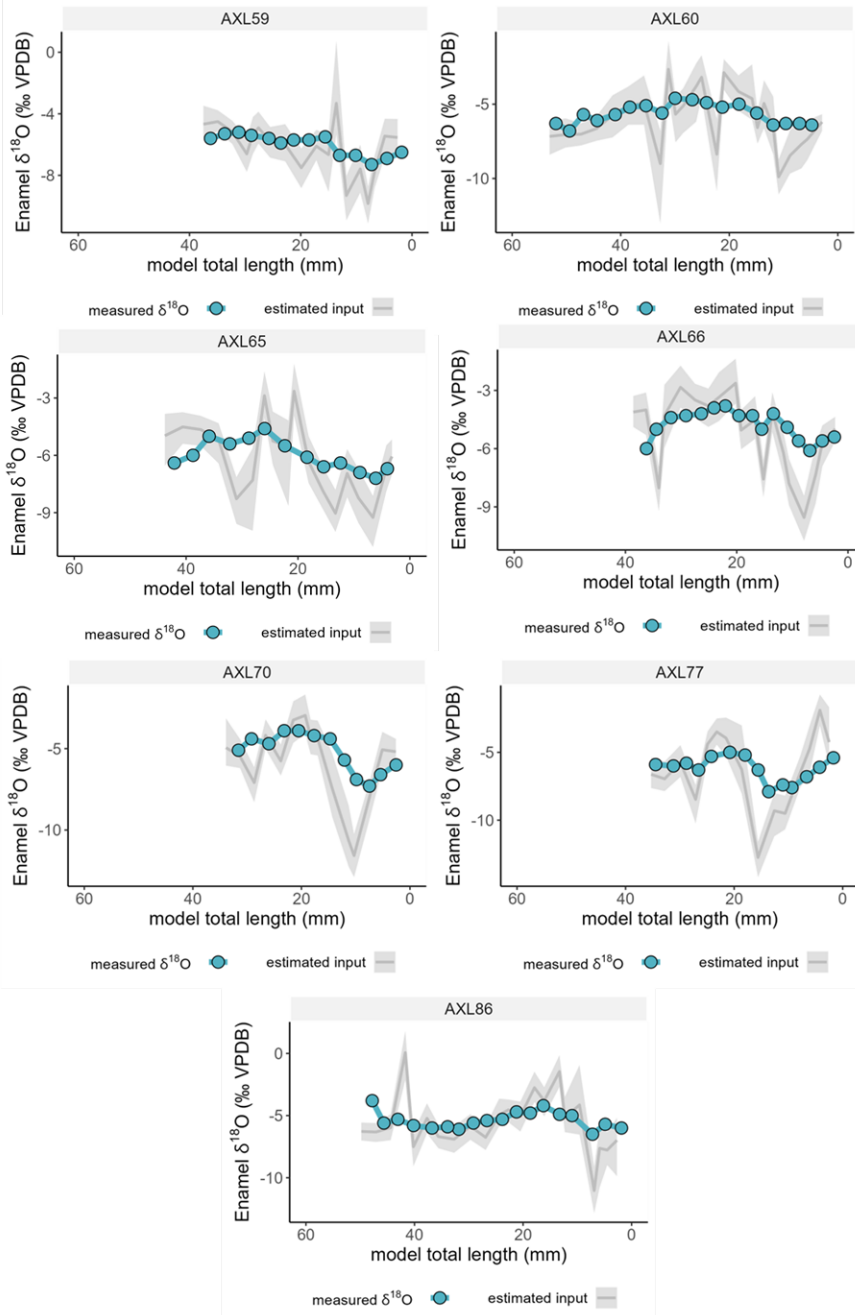
1942

Figure D1. Inverse models for oxygen isotope composition (δ^{18}O) from teeth from Axlor, considering distance from enamel root junction. The blue line and points correspond to original data and grey line the most likely model solution, with the 95% confidence interval shown in shaded areas.

1945
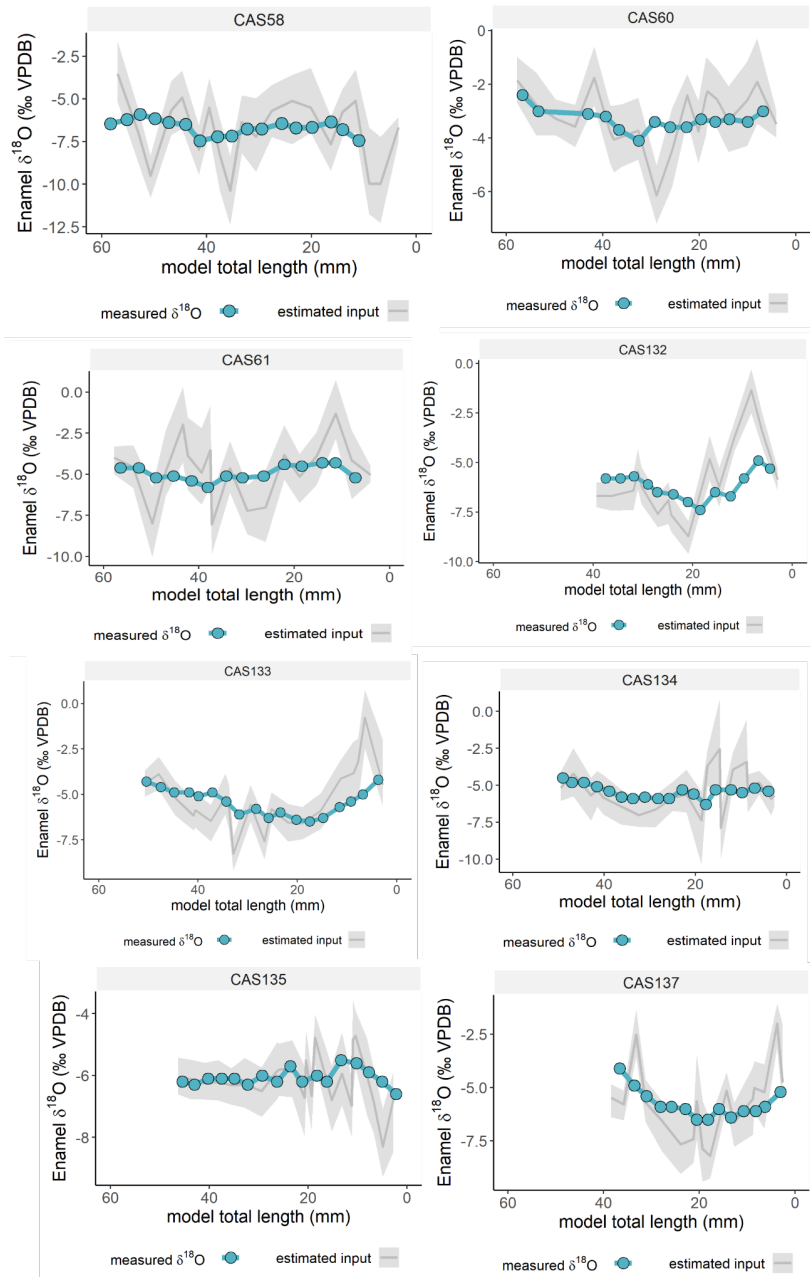
Figure D2. Inverse models for oxygen isotope composition (δ18O) from teeth from El Castillo, considering distance from enamel root junction. The blue line and points correspond to original data and grey line the most likely model solution, with the 95% confidence interval shown in shaded areas.

Figure D3. Inverse models for oxygen isotope composition ($\delta^{18}O$) from teeth from El Castillo, considering distance from enamel root junction. The blue line and points correspond to original data and grey line the most likely model solution, with the 95% confidence interval shown in shaded areas.
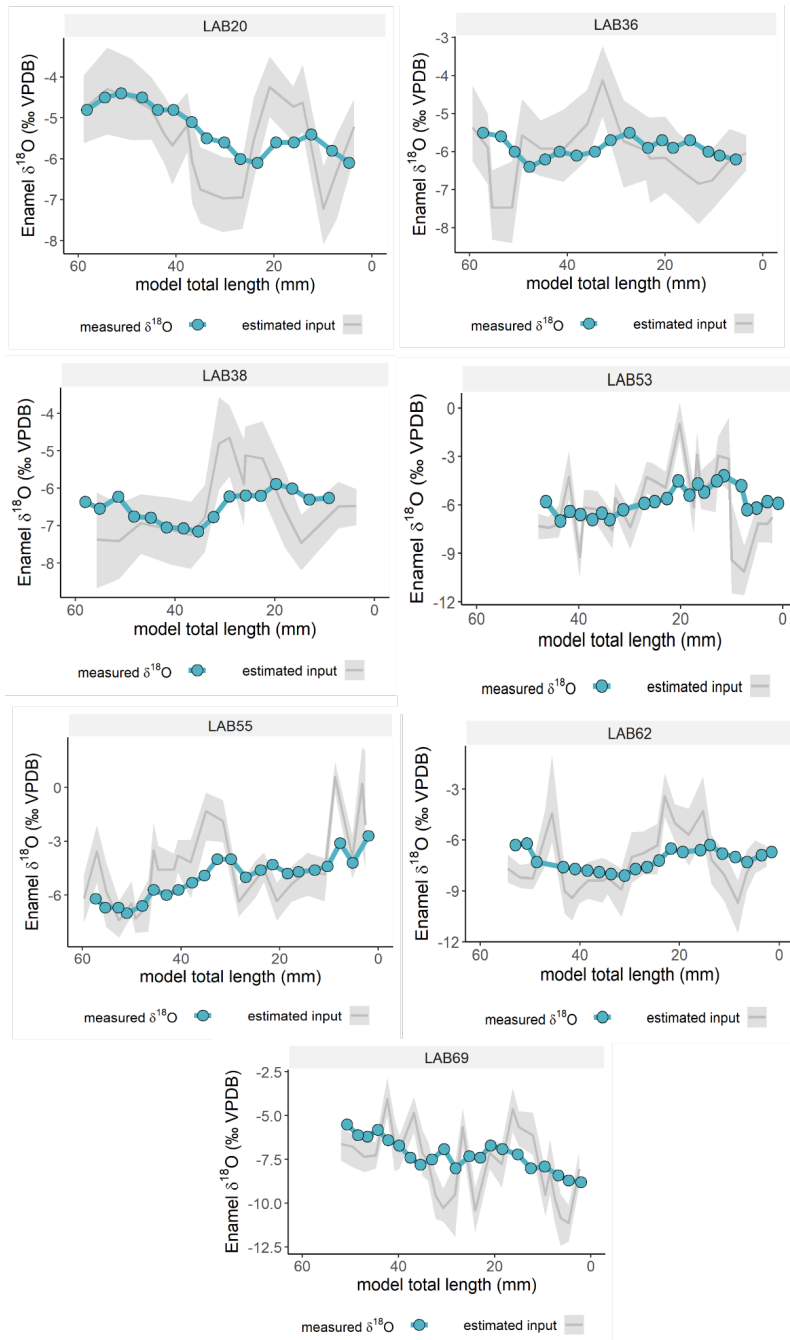
1957

Figure D4. Inverse models for oxygen isotope composition (δ18O) from teeth from Labeko Koba, considering distance from enamel root junction. The blue line and points correspond to original data and grey line the most likely model solution, with the 95% confidence interval shown in shaded areas.

1961
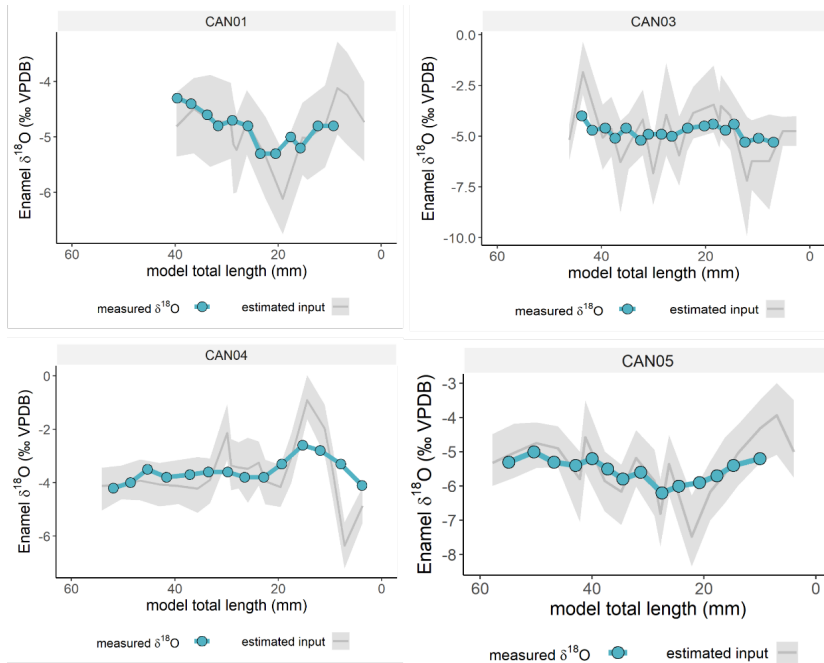
1962
1963 **Figure D5.** Inverse models for oxygen isotope composition (δ18O) from teeth from Canyars considering distance from enamel root junction. The
1964 blue line and points correspond to original data and grey line the most likely model solution, with the 95% confidence interval shown in shaded
1965 areas.
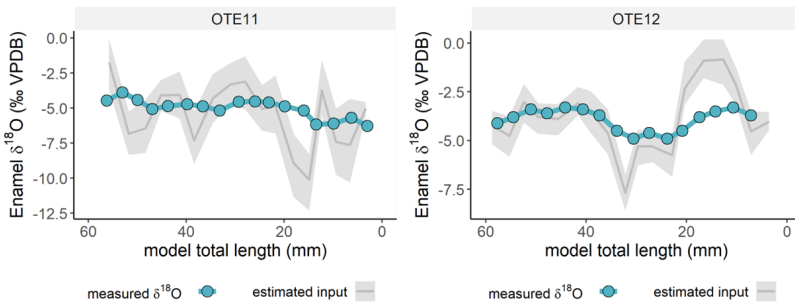
1966

1967 **Figure D6.** Inverse models for oxygen isotope composition (δ18O) from teeth from El Otero, considering distance from enamel root junction. The
1968 blue line and points correspond to original data and grey line the most likely model solution, with the 95% confidence interval shown in shaded
1969 areas.
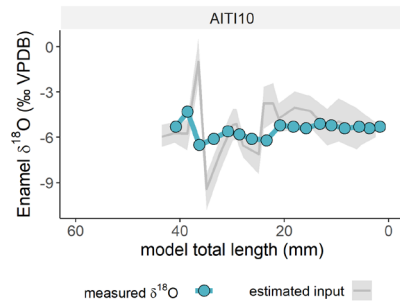
Figure D7. Inverse models for oxygen isotope composition (δ18O) from teeth from Aitzbitarte III interior, considering distance from enamel root junction. The blue line and points correspond to original data and grey line the most likely model solution, with the 95% confidence interval shown in shaded areas.

References Appendix D

Bendrey, R., Vella, D., Zazzo, A., Balasse, M., Lepetz, S., 2015. Exponentially decreasing tooth growth rate in horse teeth: implications for isotopic analyses. Archaeometry 57, 1104–1124. https://doi.org/10.1111/arcm.12151

Blumenthal, S.A., Cerling, T.E., Chritz, K.L., Bromage, T.G., Kozdon, R., Valley, J.W., 2014. Stable isotope time-series in mammalian teeth: In situ δ18O from the innermost enamel layer. Geochimica et Cosmochimica Acta 124, 223–236. https://doi.org/10.1016/j.gca.2013.09.032

Kohn, M.J., 2004. Comment: Tooth Enamel Mineralization in Ungulates: Implications for Recovering a Primary Isotopic Time-Series, by B. H. Passey and T. E. Cerling (2002). Geochimica et Cosmochimica Acta 68, 403–405. https://doi.org/10.1016/S0016-7037(03)00443-5

Passey, B.H., Cerling, T.E., 2002. Tooth enamel mineralization in ungulates: implications for recovering a primary isotopic time-series. Geochimica et Cosmochimica Acta 66, 3225–3234. https://doi.org/10.1016/S0016-7037(02)00933-X

Passey, B.H., Cerling, T.E., Schuster, G.T., Robinson, T.F., Roeder, B.L., Krueger, S.K., 2005. Inverse methods for estimating primary input signals from time-averaged isotope profiles. Geochimica et Cosmochimica Acta 69, 4101–4116. https://doi.org/10.1016/j.gca.2004.12.002

Passey, B.H., Robinson, T.F., Ayliffe, L.K., Cerling, T.E., Sponheimer, M., Dearing, M.D., Roeder, B.L., Ehleringer, J.R., 2005. Carbon isotope fractionation between diet, breath CO2, and bioapatite in different mammals. J. Archaeol. Sci. 32, 1459–1470. https://doi.org/10.1016/j.jas.2005.03.015

Zazzo, A., Bendrey, R., Vella, D., Moloney, A.P., Monahan, F.J., Schmidt, O., 2012. A refined sampling strategy for intra-tooth stable isotope analysis of mammalian enamel. Geochimica et Cosmochimica Acta 84, 1–13. https://doi.org/10.1016/j.gca.2012.01.012